Physiology and Development of Inner Retinal Photoreception

Timothy J. Sexton

A dissertation
submitted in partial fulfillment of the
requirements for the degree of

Doctor of Philosophy

University of Washington

2013

Reading Committee:

Russell Van Gelder, Chair

Peter Detwiler

Fred Rieke

Rachel Wong

Program Authorized to Offer Degree:

Neurobiology and Behavior

University of Washington

Abstract

Physiology and Development of Inner Retinal Photoreception

Timothy J. Sexton

Chair of the Supervisory Committee
Russell Van Gelder, M.D., Ph.D.
Department of Ophthalmology

Melanopsin is the photopigment in intrinsically photosensitive retina ganglion cells (ipRGCs). Melanopsin endows ipRGCs with a photo-response that can act independently or be summed directly with input from rods and cones, with ipRGCs acting as the conduit for all non-visual photic information. ipRGCs project primarily to the suprachiasmatic nuclei and the olivary pretectal nuclei, subserving circadian entrainment to lighting cycle and the pupillary light response respectively. Here I examined at 3 aspects of *in situ* melanopsin function in whole retina: 1) the melanopsin photocycle, 2) ipRGC recovery from light and 3) mechanisms of melanopsin adaptation. First, I found that melanopsin is resistant to bleaching by visible light. Conversely, ultraviolet light (UV) can substantially bleach melanopsin. Using UV bleaching and retinoid supplementation techniques, *cis*-retinal was determined to be the *in vivo* chromophore preference of apo-melanopsin. Neither all-*trans*-retinal nor the Müller glial photocycle product, *cis*-retinol, can restore ipRGC function after UV bleaching. Melanopsin is resistant to chemical

bleaching with hydroxylamine both in light and in darkness, a characteristic of bistable pigments. In sum, these experiments are consistent with the hypothesis that melanopsin is a bistable pigment requiring 11-*cis*-retinal to bind the apo-form to constitute a functional photopigment. Secondly, I found the ability of ipRGCs to recover from short and long light exposures decreases over the course of development from postnatal (P) day 8 to P30. A concurrent decrease in photosensitivity is observed over the same period as measured by on-latency, maximal firing rate, off-latency and total spike count during light exposure in response to a 1-min duration, 480 nm light stimulus. The age dependent decrease in recovery cannot be reversed with exogenous 9-*cis*-retinal supplementation but can partially be overcome with a 10-fold increase in light intensity, i.e., ipRGCs did not bleach but adapted to light. This observation suggests that adaptation mechanisms but not photocycle mechanisms change in ipRGCs over time. The most dramatic difference is found in the ability of P8 Type 1 ipRGCs to recover nearly completely from a 1-hr 480 nm light exposure within 20-min of incubation in the dark. At all ages studied, all other ipRGC subtypes recover to more modest levels of 60% or less of the pre-exposure levels over the course of a 1-hour dark incubation period. Finally, I found that the G-protein related kinase 2 (GRK2) plays a small role in melanopsin inactivation. I thus investigated whether the age dependent changes in adaptation were regulated by GRK2 by knocking out GRK2 specifically in melanopsin expressing cells. Previous in vitro work indicated GRK2 was responsible for melanopsin inactivation. However, in the mutant only small increases in the response decay constant and in the off-latencies were found, indicating that GRK2 is either not the primary, or not the only kinase responsible for melanopsin phosphorylation.

Table of Contents

Acknowledgements

I would like to thank Jack Saari for his help with retinol synthesis and who, even though he had no academic responsibility for me, found ample time for casual talks of all thing photocycle. I would also like to thank Peter Detwiler and the members of his lab, Greg Newkirk and Andrew Gartland, for teaching me the rudiments of patch clamping and two-photon microscopy and pep talks – patch clamping requires lots of pep talks. One last thank you to Rachel Wong and Horacio de la Iglesia who acted as sounding boards so often. Oh, and a humble thank you to Fred Rieke, who inspired me to conquer my anxiety over math and take two years of calculus and linear algebra so I could begin to understand what he was talking about; because as he said "you will never get a chance to do this again."

For a vast majority of the immunohistochemistry presented here, or done on a whim for projects that didn't make it, I wish to thank Jing Huang and Dan Possin for help with immunohistochemistry and imaging, respectively. I thank Leona Ding for introducing me to what many would consider rather esoteric statistical analyses when it was the only thing that would work.

Finally, I wish to thank Russell Van Gelder for always encouraging me be better, and the people in the Van Gelder Lab for support, encouragement, and general silliness over the last six years. In particular I would like to thank Angela Sandt for making that ship go every day.

In the interest of full disclosure and just in case the NIH begins to employ NSA-like tactics, I would like to thank the donors for their support This research was supported in part by NIH grants EY009339 and P30EY07031, unrestricted support from Research to Prevent Blindness, and the Burroughs-Welcome Translational Scientist Award

Dedications

I would like to thank all of my friends and family who continued to encourage me to fulfill, what really have always been, childhood dreams, a Ph.D. among them.

In particular, I dedicate this work to the memory of my undergraduate mentor

Stephen Arch.

After teaching and mentoring for forty years,
he recently retired, and unexpectedly passed away.

Preface

Melanopsin is the photopigment of the intrinsically photosensitive retinal ganglion cells (ipRGCs), the mammalian eye's third photoreceptor after rods and cones. ipRGCs control the pupillary light response (PLR) and entrain the body's master circadian clock to day length. A drug to modulate melanopsin function is an enticing goal. This idea was first proposed to me by my advisor Russell Van Gelder, with the description of "sunshine in a bottle." Coming from a background in the molecular and cellular biology of psychiatric disease, I understood such a drug's potential to help treat diseases including major depression, bipolar disorder, and in particular seasonal affective disorder (SAD). In nearly every psychiatric disease circadian rhythms and sleep are disturbed. While SAD is a unique form of depression in which routine anti-depressant treatment is largely ineffective, the idea of studying what seemed to be a direct biological underpinning for the disorder in the form of ipRGCs was intriguing. These cells respond best to the blue spectrum, the same wavelengths that most effectively treat SAD. The possibility of a clearer etiology was refreshing after a decade of working on the serotonin hypothesis of depression, which became ever more convoluted as we learned of serotonergic subsystems that had opposite effects in different parts of the brain using the same molecular and cellular machinery.

To find such a drug and understand the disease etiology it mitigates, many puzzles must be solved. We have known of melanopsin for only a little over a decade; and, while an enormous amount of work has been done, in that time much about melanopsin's function remain undefined. Questions about its most basic biochemical mechanisms such as its photocycle would need to be more clearly delimited to help develop something akin to "sunshine in a bottle." Chapter 2 aims

to help in our understanding of the melanopsin photocycle, starting with the basic question of what melanopsin's *in vivo* chromophore preference is. Heterologous expression systems have shown that the chromophore 11-*cis*-retinal is necessary for melanopsin's light response. They also showed that the retinaldehyde isomer all-*trans*-retinal could produce a comparatively small light response. These findings, along with melanopsin's phylogenetic position, suggested that melanopsin was a bistable pigment. Here I addressed the same questions for the first time for *in situ* melanopsin in intact retina.

The vast majority of work in the lab had been done with early post-natal P8-P10 mice. For purposes of direct comparison with past work, and because recordable ipRGCs are most abundant at those ages, in Chapter 2 I used P8-P10 animals for bleaching and supplementation experiments to determine melanopsin's chromophore preference. Bleaching ipRGCs with visible light (centered at melanopsin's maximal absorption peak of 480 nm) was ineffective in depleting activity in ipRGCs. Instead, UV light exposure centered at 365 nm was used to reduce firing to a minimum by directly activating melanopsin and breaking down endogenous retinoids that could be used as a source of new chromophore. In addition to testing the question of melanopsin's bistability *in situ*, I examined the ability ipRGCs to use the Müller glial cell based photocycle, which produces the alcohol 11-*cis*-retinol. This photocycle is used by the cones, and is the only other known photocycle in the retina. It also appeared to be a good candidate source of chromophore since Müller glial cells form synaptic-like connections with ipRGCs that allow synaptic jumping virus to move from ipRGCs to Müller cells. Such close approximation has not been observed between Müller cells and other retinal ganglion cells(Viney et al., 2007). While I found evidence for ipRGC's use of 9-*cis*-retinal, an analog of 11-*cis*-retinal, to reconstitute bleached activity, I could not demonstrate efficacy for retinol. As a complement to UV

bleaching, I also attempted bleaching *in situ* melanopsin with the chemical hydroxylamine, both in the dark and in the light to simulate conditions under which cone opsin and rhodopsin can be bleached respectively. Hydroxylamine does not bleach ipRGCs, which is a characteristic of rhabdomeric photoreceptors and their bistable opsins, suggesting that melanopsin is a bistable pigment, but one requiring 11-*cis*-retinal for initial chromophore binding.

Following up on the bleaching and supplementation studies of Chapter 2, I attempted to repeat the studies in isolated ipRGCs whose activity would be monitored via patch clamping. Finding a faithful marker for ipRGCs for *in vitro* isolation proved frustrating. To learn patch clamping while searching for a suitable marker, my first "assignment" was to look at ipRGC light pulse integration time in intact retina. Defining integration over very short intervals would help in understanding more about the kinetics of melanopsin activation and inactivation. From this information, molecular mechanisms of could be postulated and tested. However, leaky genetic markers available for melanopsin expression made these experiments impractical. Concurrently, I looked at integration times using MEA recording as I had done for the earlier bleaching and supplementation work. Primarily these experiments investigated the possibility of very long integration times for sub-threshold light to produce cell firing in both young and older animals. Unfortunately, others published those results before I was able to complete my analysis. From my data, however, I found distinct difference in ipRGC light responses in older and younger animals. At the same time, studies were published demonstrating melanopsin's involvement in post-natal retinal development, including the time period in which I saw light response differences. The experiments in Chapter 3 aim to describe the developmental changes of ipRGC responses. Understanding changes over time and defining adaptation times more clearly would also help when isolated ipRGCs could be obtained technically. It would provide a

benchmark against which isolated cell responses could be measured. To that end I not only characterized changes in light response dynamics at different ages but also recovery from short and long light exposures.

I demonstrated that developmental differences in ipRGCs ability to recover from light exposure appeared to be a function of age-dependent changes in adaptation and not in the photocycle. As recovery changes with time, this gives means for understanding mechanisms. Adaptation changes could be at any of the steps downstream of melanopsin activation and probably at many. I began at the most proximal point of GPCR inactivation mechanisms, phosphorylation. Data from *in vitro* studies suggested GRK2 controlled melanopsin inactivation via phosphorylation. I used a GRK2 knockout animal to look at the inactivation kinetics of melanopsin mediated firing in ipRGCs. However, only modest changes to firing inactivation were observed, suggesting GRK2 plays only a small role or that compensatory changes occurred in the knockout to normalize cell function. These studies are described in Chapter 4.

Chapter 1: Introduction: Melanopsin and mechanisms of non-visual ocular photoreception

This chapter was published previously

Sexton, T., Buhr, E., & van Gelder, R. N. (2012). Melanopsin and Mechanisms of Non-visual Ocular Photoreception. *Journal of Biological Chemistry*, *287*(3), 1649–1656.

Summary

In addition to rods and cones, the mammalian eye contains a third class of photoreceptor, the intrinsically photosensitive retinal ganglion cell (ipRGC). ipRGCs are heterogeneous irradiance-encoding neurons that primarily project to non-visual areas of the brain. Characteristics of ipRGC light responses differ significantly from rod and cone responses, including depolarization to light, slow on- and off-latencies, and relatively low light sensitivity. All ipRGCs use melanopsin (*Opn4*) as their photopigment. Melanopsin resembles invertebrate rhabdomeric photopigments more than vertebrate ciliary pigments, and uses a G_q signaling pathway in contrast to the G_t pathway used by rods and cones. ipRGCs can recycle chromophore in the absence of retinal pigment epithelium, and are highly resistant to vitamin A depletion. This suggests melanopsin employs a bistable sequential photon absorption mechanism typical of rhabdomeric opsins.

ipRGCs discovery

In 1927, Clyde Keeler noted that the blind *rodless* mouse retained pupillary light responses (PLR) despite apparent degradation of all rod and cone photoreceptors (Keeler, 1927). Over 50 years later, Ebihara and colleagues similarly noted that mice with the same outer retinal degeneration mutation (now called *rd1*) continue to synchronize their circadian rhythms to light-dark cycles despite apparent visual blindness (Ebihara and Tsuji, 1980). Extensive experiments by Foster and colleagues in the 1990s demonstrated that preservation of light entrainment of the circadian clock was not a unique phenomenon to the *rd1* mutation, but was observed after the introduction of synthetic outer retinal degeneration gene constructs (Freedman et al., 1999). However, circadian entrainment to light was lost in both anophthalmic mice lacking eyes (Laemle and Ottenweller, 1998) as well as those blind from optic nerve hypoplasia (*Math5-/-)* (Wee et al., 2002). These results demonstrated that a photoreceptive cell must be preserved in eyes of animals with complete outer retinal degeneration.

In 2002, Berson and colleagues used a retrograde tracing technique to identify retinal ganglion cells projecting specifically to the master circadian pacemaker, the suprachiasmatic nucleus (SCN) of the hypothalamus (Berson et al., 2002). Patch clamp recording of these cells revealed they were intrinsically photosensitive; these cells have subsequently been called intrinsically photosensitive retinal ganglion cells (ipRGC) or alternately photosensitive retinal ganglion cells (pRGC) (we will use the former term in this review). ipRGCs constitute 2-3% of retinal ganglion cells, and project in the mouse brain primarily to non-visual centers including the SCN, the olivary pretectal nucleus (OPN, locus of the PLR), and the intergeniculate leaflets of the geniculate nuclei (IGL) (Hattar et al., 2002; Hattar et al., 2006).

The identity of the photopigment subserving the ipRGC became a critical question. Two candidates were postulated: melanopsin and cryptochrome. Melanopsin (*Opn4*) was discovered in 1998 by Provencio and Rollag, who identified this novel opsin from the dermal melanophores of *Xenopus* (Provencio et al., 1998). The mammalian homologue was found to be expressed in a small subset of retinal ganglion cells (Provencio et al., 2000; Provencio et al., 2002). Cryptochrome is a flavin-based photopigment which subserves circadian entrainment in *Arabidopsis* and *Drosophila* (Oztürk et al., 2007). There are two mammalian *cryptochrome* homologues (*Cry1* and *Cry2*), which are also expressed in the inner retina (Thompson et al., 2004). Interestingly, knockouts of either *Opn4* or *Cry1;Cry2* in mice do not prevent circadian or diurnal entrainment to light-dark cycles, nor eliminate the pupillary light response (Panda et al., 2002; Ruby et al., 2002; Lucas et al., 2003). However, when *Opn4* knockout mice are combined with homozygous *rd1* mutation (Panda et al., 2003) (or equivalently compounded with *Gnat1* and *Cng3a* mutations to eliminate outer retinal photoreceptive function (Hattar et al., 2003)), mice lose all circadian entrainment and pupillary light response, while these phenomena are at least partially preserved in *Cryptochrome* null mice with retinal degeneration (Van Gelder, 2003). These results demonstrated that melanopsin is necessary and sufficient for inner retinal photoreception.

Subtypes of ipRGCs and neural connections

Subsequent work has confirmed that the ipRGC population and the melanopsin-expressing cell population are identical (Gooley et al., 2001; Hattar et al., 2002). Initially, the melanopsin containing ganglion cells were believed to be a homogenous cell population carrying photic

information to the SCN, OPN, and IGL. However, further analysis of anatomic and functional properties of genetically labeled ipRGCs has revealed deeper complexity, with the identification of distinct subtypes of ipRGCs (Figure 1) (Tu et al., 2005; Baver et al., 2008). The SCN receives input primarily from "M1" ipRGCs, which are characterized anatomically by dendritic arborization in the outer sublamina of the inner plexiform layer of the retina (IPL) (Baver et al., 2008). The OPN receives innervation from both M1 cells and "M2" cells, whose dendritic fields are found in the inner sublamina of the IPL (Baver et al., 2008). M1 cells primarily utilize melanopsin-dependent intrinsic photosensitivity, while M2 cells appear to rely more on conveyance of light information from upstream rods and cones (Schmidt and Kofuji, 2009).

More sophisticated, genetically-based anatomic tracing tools have recently uncovered a more diverse assortment of ipRGC subtypes. By combining mice expressing Cre recombinase under the control of the *Opn4* promoter and Cre-activated reporters such as GFP or alkaline phosphatase, Ecker and colleagues were able to identify cells which express melanopsin at low levels or transiently (both of which are undetectable by immunostain or β-galactosidase) (Ecker et al., 2010). This revealed approximately 2000 melanopsin labeled cells in each mouse retina compared to the roughly 600-800 M1 cells detected by analysis of β-galactosidase in $Opn4^{tau\text{-}LacZ}$ mice (Hattar et al., 2002; Ecker et al., 2010). The family of ipRGCs has now been expanded to include the previously described M1 and M2 cells, as well as bistratified M3 cells which are functionally similar to M2 cells (Berson et al., 2010; Schmidt and Kofuji, 2011) and M4 cells which are characterized by their large soma size and dendritic field (Ecker et al., 2010) (as well as perhaps a rare M5 classification). Using this distinction, Ecker, *et al.* showed that M2-4 cells send processes to diverse brain regions including areas involved in visual processing such as the dorsal and ventral subregions of the lateral geniculate nucleus (in addition to the aforementioned

IGL) and the superior colliculus (Ecker et al., 2010). Intriguingly, these melanopsin RGCs function in visual circuits and cause cellular activity in the visual cortex of two different types of "melanopsin only" mice lacking conventional photoreceptors (Brown et al., 2010; Ecker et al., 2010). M2-M5 cells show much weaker intrinsic photoresponses than M1 cells, and may function *in vivo* primarily as conduits for outer retinal-derived light signals (see below) (Ecker et al., 2010).

Using additional molecular genetic labeling tools, Chen, *et al.* (Chen et al., 2011) found a further subdivision in projections among M1 cells. *Brn3b* is a marker for retinal ganglion cells, but is not expressed in all ipRGCs (Badea et al., 2009; Chen et al., 2011). *Brn3b*-positive M1 ipRGCs cells make up the majority of projections to the OPN whereas *Brn3b*-negative M1 cells project mainly to the SCN. In keeping with this anatomical distinction, mice in which *Brn3b* positive ipRGCs have been ablated using a targeted diphtheria toxin show severely reduced PLR but normal photo-entrainment and masking in light:dark cycles (Chen et al., 2011). The full diversity of ipRGC types continues to expand (Figure 1).

Redundant and unique ipRGC photoreceptor functions in behavior and physiology

As noted above, mice lacking melanopsin continue to show PLRs and circadian entrainment, as do mice lacking rods and cones (Panda et al., 2002; Ruby et al., 2002; Lucas et al., 2003). Two models could explain this redundancy. First, ipRGCs could receive outer retinal input from rod- and cone-based pathways and pass this signaling on to downstream brain nuclei, such as the SCN and OPN, signaling in series. Alternatively, non-ipRGC ganglion cells could transduce outer retinal signals to these brain regions in parallel with ipRGCs. Analysis of mice in which

ipRGCs were ablated using diphtheria toxin (Güler et al., 2008; Hatori et al., 2008) or using toxic antibodies (Göz et al., 2008) showed complete loss of circadian entrainment and PLR, consistent with the serial model in which all non-visual signaling is transduced by ipRGCs. Because rods and cones provide input to ipRGCs, the contributions of these outer photoreceptors and the intrinsic photosensitivity of melanopsin can sum under normal conditions to affect behavior. Mice carrying null alleles of melanopsin still entrain to light:dark cycles, but show reduced behavioral phase shifts in response to brief light pulses and reduced circadian period lengthening in response to constant light (Panda et al., 2002). Conversely, mice with melanopsin as their only photoreceptors entrain to light:dark cycles and phase shift to bright light pulses indistinguishably from wild-types (Freedman et al., 1999; Panda et al., 2003). Melanopsin appears to exert its unique influence on behavior at bright light intensities or exposures of long duration. For example, the PLR response of mice without melanopsin appears normal at low light intensities and for short durations; however, at high light intensities the response is reduced and at long durations of high intensity the pupil begins to escape constriction (Lucas et al., 2003; Zhu et al., 2007). Similarly, negative masking, or the suppression of behavioral activity by light exposure, is also lost over several-hour-long light durations in *Opn4*$^{-/-}$ mice (Mrosovsky and Hattar, 2003). Being nocturnal, mice and rats naturally confine the majority of their sleep during the light portion of a light:dark cycle. However, short bouts of sleep are induced during the night if light is presented at an inappropriate phase (Benca et al., 1998). In mice lacking melanopsin, this acute light-mediated sleep induction is lost (Altimus et al., 2008; Lupi et al., 2008; Tsai et al., 2009). These effects on circadian entrainment and sleep in melanopsin deficient animals may give insight into the higher incidence of seasonal affective disorder (SAD) among humans who carry a particular allele of the melanopsin gene (Roecklein et al., 2009).

Although a lack of melanopsin is associated with the deficiencies discussed above, the influence of rod and cone photoreception on ipRGCs should not be understated. Photo-entrainment, PLRs, and other non-visual light-mediated behaviors function normally at low light intensities without melanopsin (Hattar et al., 2003; Panda et al., 2003; Güler et al., 2008). Distinct responses from outer photoreceptors and melanopsin can be observed at the level of the SCN (Brown et al., 2011). At scotopic light intensities rods alone are sufficient for photo-entrainment, and even at photopic light levels at which rods cannot support pattern vision they signal through cones to support entrainment (Altimus et al., 2010). Cones can also mediate circadian phase shifting, but with short light exposures. Mice lacking cones sensitive to middle wavelength light exhibit reduced phase shifting in response to pulses of green light for 15-min or shorter, but behave similarly to wild-type animals when exposed to light of shorter wavelength or longer pulses of middle wavelength light (Dollet et al., 2010). To spectrally separate cone input from other photoreceptors, Lall *et al.* utilized mice in which the mouse middle wavelength cones were replaced with human long wavelength sensitive cones (Lall et al., 2010). In these mice long durations of long wavelength light yields weak phase shifts, but the same number of photons delivered as discontinuous 15-min pulses produces phase shifts similar in magnitude to those observed in response to melanopsin/rod stimulating wavelengths of light. It is likely that in an animal with functional rods, cones, and melanopsin all three photoreceptors play a role in photic entrainment, PLR, and masking, but exert their strongest influence at specific wavelengths, intensities, and stimulus durations.

Role of melanopsin during retinal development

Melanopsin is expressed early in retinal development, at about embryonic day 10 (E10). Melanopsin-containing ganglion cells are light responsive from birth (Tarttelin et al., 2003; Fahrenkrug et al., 2004; Sekaran et al., 2005; Tu et al., 2005), making them the first light-sensitive cells functional in the newborn retina. At birth the projections from the ipRGCs sit poised at the ventral surface of the SCN and begin sending projections into the SCN between postnatal day 1 (P1) and P4 (Muñoz Llamosas et al., 2000; Sekaran et al., 2005; McNeill et al., 2011). Additionally, the number of melanopsin-containing ganglion cells decreases dramatically between P0 and P19 (Tu et al., 2005).

Rod and cone circuitry to RGCs is not functional until at least P10 in mice (Ratto et al., 1991; Bakall et al., 2003; Tian and Copenhagen, 2003). Might the early expression of melanopsin in ipRGCs have functional significance during development? Negative phototaxis, or an avoidance of bright light is observed in mouse pups as early as P6 and is dependent on the presence of melanopsin (Johnson et al., 2010). Melanopsin also contributes to the light-mediated segregation of ipsi- and contralateral retinogeniculate projections during visual development (Renna et al., 2011). This contribution to segregation of retinal efferents coincides with a melanopsin-dependent enhancement of waves of retinal activity observed in early postnatal development (Renna et al., 2011).

Physiology of ipRGC photosensitivity

Currently, two melanopsin gene families are recognized (Bellingham et al., 2006). The originally identified gene from *Xenopus* represents one family found in all vertebrates except mammals, and is designated *Opn4x*. The second gene family, *Opn4m*, occurs in all vertebrates surveyed but is the only melanopsin gene found in mammals. Comparison of the phylogenetic position of the two families indicates that they split at a very early point in vertebrate evolution. Both melanopsin families share greater sequence similarity to the opsins found in invertebrate rhabdomeric photoreceptors than vertebrate ciliary photoreceptors, displaying 39% and 30% sequence similarity, respectively (Provencio et al., 1998) (Figure 2A). Specific similarities to rhabdomeric opsins include the presence of an aromatic *versus* acidic counter ion, balancing the charge of the Schiff base linkage between the opsin and retinal, and the insertion of a rhabdomeric-like sequence in a portion of the third cytoplasmic loop associated with G-protein specificity (Figure 2B) (Provencio et al., 1998).

As the phylogenetic position suggests, melanopsin and ipRGC function is different from cilliary photoreceptor function. Whereas light causes a graded hyperpolarization in rods and cones, light leads to depolarization and the production of action potentials in ipRGCs. The exact mechanism by which this is accomplished is still not well understood, but likely resembles the steps occurring in rhabdomeric photoreceptors, where opsins, such as those found in *Drosophila* photoreceptors, are coupled to a G_q/phospholipase C (PLC) second messenger cascade that induces depolarizing currents in the cell by activation of transient receptor potential (TRP) and TRP–like channels (Hardie and Raghu, 2001; Hardie, 2011). This contrasts with the mechanism of ciliary opsin, such as in mammalian rhodopsin, which couple to a $G_{transducin,}$/phosphodiesterase (PDE) cascade that leads to hyperpolarizing currents via a cyclic-nucleotide-gated ion channel

(Palczewski, 2006).

The definitive second messenger cascade of melanopsin has not been established but does appear to utilize G_q family signaling. When melanopsin is expressed in heterologous expression systems, general disruption of G-protein signaling interferes with melanopsin-dependent light responses (Melyan et al., 2005; Qiu et al., 2005). Additionally, G_q inhibitors and antibodies as well as PLC inhibitors reduce light responses (Panda et al., 2005; Qiu et al., 2005) but $G_{i/o}$ inhibitors do not (Melyan et al., 2005). In ipRGCs, the light response has been shown to occur in isolated ipRGC membranes, where G_q and PLC inhibitors but not other G-protein inhibitors alter the light response (Graham et al., 2008) suggesting that melanopsin uses a G_q family ($G_{q/11/14}$) pathway.

The channel(s) activated to produce the membrane depolarization remain to be determined. TRP channels have been suggested as the effector channels, as they are the mammalian homologue of invertebrate TRP channels activated by rhabdomeric opsins (Hardie and Postma, 2008). In particular TRPC 6 and 7 are of interest as they are localized to ipRGCs (Warren et al., 2006; Hartwick et al., 2007). However, light-dependent ipRGC activity is preserved in mice lacking either TRPC3, 6, or 7 (Perez-Leighton et al., 2011). It is only when both TRPC6 and TRPC7 are knockout that the ipRGC light response is dramatically reduced but not absolutely abolished(Xue et al., 2011).

Compared with rhodopsin, melanopsin appears to be expressed at low levels in ipRGCs, estimated to be 1/10,000 rhodopsin density (Do et al., 2009). The sum effect of the low pigment density, long-lasting meta-state, and G_q/PLC signaling are light responses that, compared with rods and cones, are very slow in onset, relatively insensitive, and very slow to inactivate (Tu et

al., 2005). Latencies from lights-on to ipRGC firing can be several seconds, while off-latencies can be up to tens of seconds from lights-off. Latency is directly related to the light intensity, as are the cells' maximal and steady state firing rates, with high intensity lights leading to shorter on-times, longer off-times and higher firing rates (Berson, 2003; Tu et al., 2005). Irradiance response relationships recorded with multi-electrode array techniques show threshold sensitivities of 1×10^{11} to 1×10^{13} photons/cm^2/s for individual ipRGCs, with peak sensitivity at 480 nm and an action spectrum consistent with the Dartnell nomogram for opsin photoreception (Tu et al., 2005). The proportionality of response times and firing rates to light intensity is consistent with the concept that ipRGCs are irradiance detectors rather than photoreceptors subserving vision.

Mechanisms of melanopsin pigment regeneration

Ciliary opsins require regeneration of chromophore in a second cell type (Figure 3A). The dominant retinal recycling mechanism in the mammalian retina is located in the retinal pigment epithelium (RPE). There, all-*trans*-retinal is converted back to 11-*cis*-retinal by a series of enzymes including lecithin:retinol acyltransferase (LRAT) and the rate-limiting enzyme, RPE65 (Kiser et al., 2011). The 11-*cis*-retinal is then returned to photoreceptors. Initial reports indicated that ipRGC function was dependent upon the retinal epithelium (RPE)-based photocycle (Fu et al., 2005; Doyle et al., 2006). Knock-outs of the genes for those two critical enzymes in the RPE photocycle mentioned, *Rpe65* and *Lrat*, yields a 100-fold less sensitive PLR compared with wild-type. However, ipRGC sensitivity, measured in isolated retina on multielectrode arrays is unchanged in *Rpe65* and *Lrat* knockout mice (Tu et al., 2006). In

addition, acute poisoning of the RPE photocycle with all-*trans*-retinylamine does not alter PLR sensitivity in mice in which ipRGCs are the only functioning photoreceptor (Tu et al., 2006). Retinoid depleted outer retina seems to inhibit inner retina activity but the RPE photocycle itself is not necessary for ipRGC function.

A major biochemical difference between ciliary and rhapdomeric opsins is the mechanism of chromophore regeneration. After a ciliary opsin absorbs a photon of light, 11-*cis*-retinal is isomerized into all-*trans*-retinal and released from the opsin protein (Palczewski, 2006). Regeneration of the chromophore then requires its transport to a second cell type with the enzymatic machinery to re-isomerize the *trans*- to 11-*cis*-retinal (Figure 3A) (Kiser et al., 2011). In rhabdomeric opsins, all-*trans*-retinal is not released from the opsin. Instead, the opsin absorbs a second photon at a specific reversing wavelength and re-isomerizes all-*trans*- to 11-*cis*-retinal (Figure 3B). These opsins are thus 'bistable' and feature an activated form, or meta-state, of the opsin that is thermally stable for seconds to minutes (whereas the meta-state of vertebrate ciliary opsins is extremely labile, lasting only milliseconds (Hillman et al., 1983; Hardie and Raghu, 2001)). Bistable pigments may have a secondary method of chromophore regeneration that relies upon other isomerases that are light dependent (Seki, 1984; Robles et al., 1995) and located with in the cell or light independent and take place in a second cell type (Wang et al., 2010) (Figure 3B). If melanopsin is indeed rhapdomeric-like, such a bistable mechanism could help explain the remarkable resistance of ipRGC function to systemic vitamin A depletion (Thompson et al., 2001). The question of melanopsin bistability has been most thoroughly investigated in heterologous cellular expression systems. In these systems, light responses are dependent upon the addition of retinoid, with 11-*cis* and 9-*cis*-retinal producing the most robust responses. Use of all-*trans*-retinal produces a response one-tenth to one-quarter that found with

cis-retinal, but this response increases with long exposure to high levels of light at wavelengths greater than 540 nm, or with the co-expression of arrestin with melanopsin and the use of white light (Melyan et al., 2005; Panda et al., 2005). However it is unclear if light exposure is directly isomerizing all-*trans*-retinal bound to melanopsin or is photoconverting all-*trans*-retinal free in solution into *cis*-conformations that then bind to apo-melanopsin. Attempts to demonstrate long-wavelength photoreversal *in vivo* have had mixed and conflicting results. Mure *et al.* (Mure et al., 2007) demonstrated that pre-exposure of mice to long-wavelength light (630 nm) potentiated cell firing responses in the SCN in response to blue light (480 nm), suggesting *in vivo* photoreversal. Presumably this was through increased ipRGC activity, as no potentiation in SCN activity in melanopsin null animals was observed. However, attempts to replicate this result studying ipRGC firing in isolated retina by MEA and an identical light protocol found no changes in ipRGC activity (Mawad and Van Gelder, 2008).

However, even a mechanism of bistability does not fully explain the behavior of melanopsin. Routinely, after a 1-min 480 nm light exposure *in vitro*, full ipRGC activity is seen after 5-min of dark incubation (Tu et al., 2005). Restoration of activity in the dark is not consistent with a purely bistable pigment, and requires a mechanism whereby all-*trans*-retinal in the dark is converted back to 11-*cis*-retinal. Such a mechanism is suggested by the work of Terakita *et al.,* (Terakita et al., 2008). Using purified, recombinant Amphioxus melanopsin, this group showed restoration of the activated melanopsin absorption spectrum towards the pre-exposure spectrum after a 5-min dark incubation. With a subsequent exposure to orange light, the absorbance spectrum fully returned to its pre-exposure appearance. Therefore multiple mechanisms of chromophore regeneration are possible (Figure 4A)

A second retinal photocycle has been described for cone photopigment recycling.

Characterized initially in the cone-dominant chicken retina and localized to the Müller glial cells, this cycle has been found recently in mouse and primate retina (Wang et al., 2009; Wang and Kefalov, 2009). This pathway works in parallel to the RPE photocycle to supply cones with chromophore. This mechanism provides cones with the alcohol 11-*cis*-retinol, which cones (but not rods) are capable of converting to 11-*cis*-retinal (Wang and Kefalov, 2011). Müller glial cells have closer contacts with ipRGCs than with other RGCs (Viney et al., 2007). Therefore it is possible that ipRGCs make use of the Müller glial photocycle, although this has not been demonstrated to date (Figure 4B).

Melanopsin purification

A major impediment to the study of mammalian melanopsin has been its scarcity. While Amphioxus melanopsin has been purified and studied *in vitro* (Koyanagi and Terakita, 2008; Terakita et al., 2008; Gomez et al., 2009), the paucity of melanopsin-expressing cells in the mammal (i.e. 2000 cells in the murine retina) makes purification from *in vivo* sources unfeasible. Heterologous expression systems for opsins are fraught with issues of proper protein folding and secondary modifications that could alter characteristics such as absorption spectra (Newman et al., 2003; Melyan et al., 2005). For example, heterologously-expressed and purified mammalian melanopsin in one study had a peak absorption spectrum between 420 nm and 440 nm, approximately 50 nm blue-shifted compared with *in vivo* sensitivity (Newman et al., 2003). Only one study, Walker *et al.*, (Walker et al., 2008) has been able to partially characterize native mammalian melanopsin *in situ* by a process of immuno-magnetic enrichment of ipRGCs from multiple retinas. HPLC analysis of the melanopsin purified from dark-adapted retinas showed

only 11-*cis*-retinal present, while ipRGCs exposed to a brief flash of 480 nm light contained predominately all-*trans*-retinal with small amounts of 11-*cis*-retinal. In addition this group found some evidence for the production of two photoproducts in the difference spectrum of illuminated, solubilized melanopsin and the subsequent acid-trapping of the illuminated pigment. However changes in the difference spectrum were very small, presumably because of limited starting material and the scarcity of ipRGCs.

Frontiers of melanopsin research

Understanding the molecular mechanisms of non-visual ocular photoreception assumes increased importance as melanopsin begins to be used as a means to confer light sensitivity on cells. Lin *et al.* were able to confer widespread photosensitivity to blind retinas by virally-mediated transduction of melanopsin (Lin et al., 2008), restoring some visual function to blind mice with this process. Ye *et al.* have recently utilized melanopsin to create an opto-genetic system capable of secreting glucagon-like peptide 1 in response to light in synthetic implants for the treatment of diabetes (Ye et al., 2011).

Given that ipRGCs were definitively identified less than 10 years ago, tremendous progress has occurred in understanding this important pathway in a relatively short time. Several important questions, however, await answer in the years ahead. The functional redundancy of rod/cone 'through-signaling' and intrinsic photosensitivity still remains incompletely characterized. What selective pressures have retained melanopsin in this system when its function can be largely subsumed by outer retinal photoreceptors? The exact signal transduction mechanism for melanopsin also remains unclear, in particular the identities of effector cation

channels in ipRGCs. The photocycle of melanopsin remains poorly characterized. It is clearly independent of retinal pigment epithelial function, but whether it is cell autonomous (as heterologous expression experiments would suggest) or relies on a second cell type for chromophore recycling remains to be determined. And of course, ultimate understanding of mechanisms of melanopsin-based photoreception await purification of the pigment and determination of its three-dimensional structure and native chromophore dynamics, which awaits development of scalable heterologous expression systems that faithfully produce functional pigment.

Figure 1

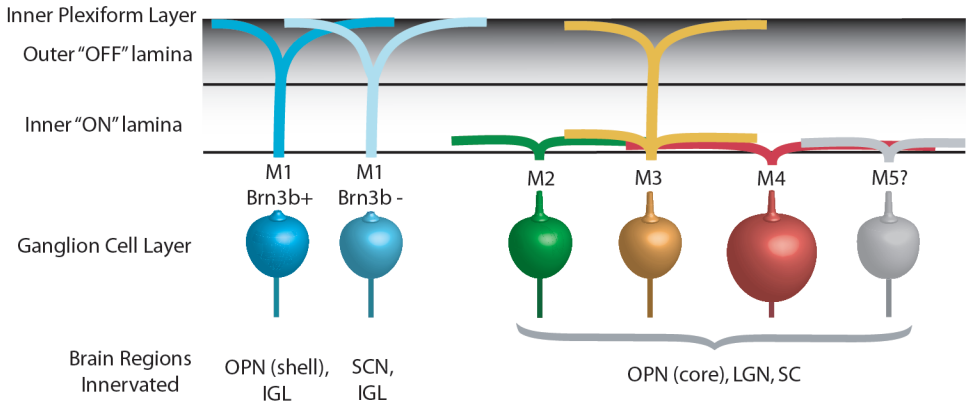

Figure 1. ipRGC subtypes. An illustration of the morphologic and molecularly defined subtypes of ipRGCs (M1-M5, and M1 Brn3b transcription factor positive and negative) with neural projections including the suprachiasmatic nucleus (SCN), olivary pretectal nucleus (OPN), lateral geniculate nucleus (LGN), and the intergeniculate leaflet (IGL) of the geniculate nucleus

Figure 2

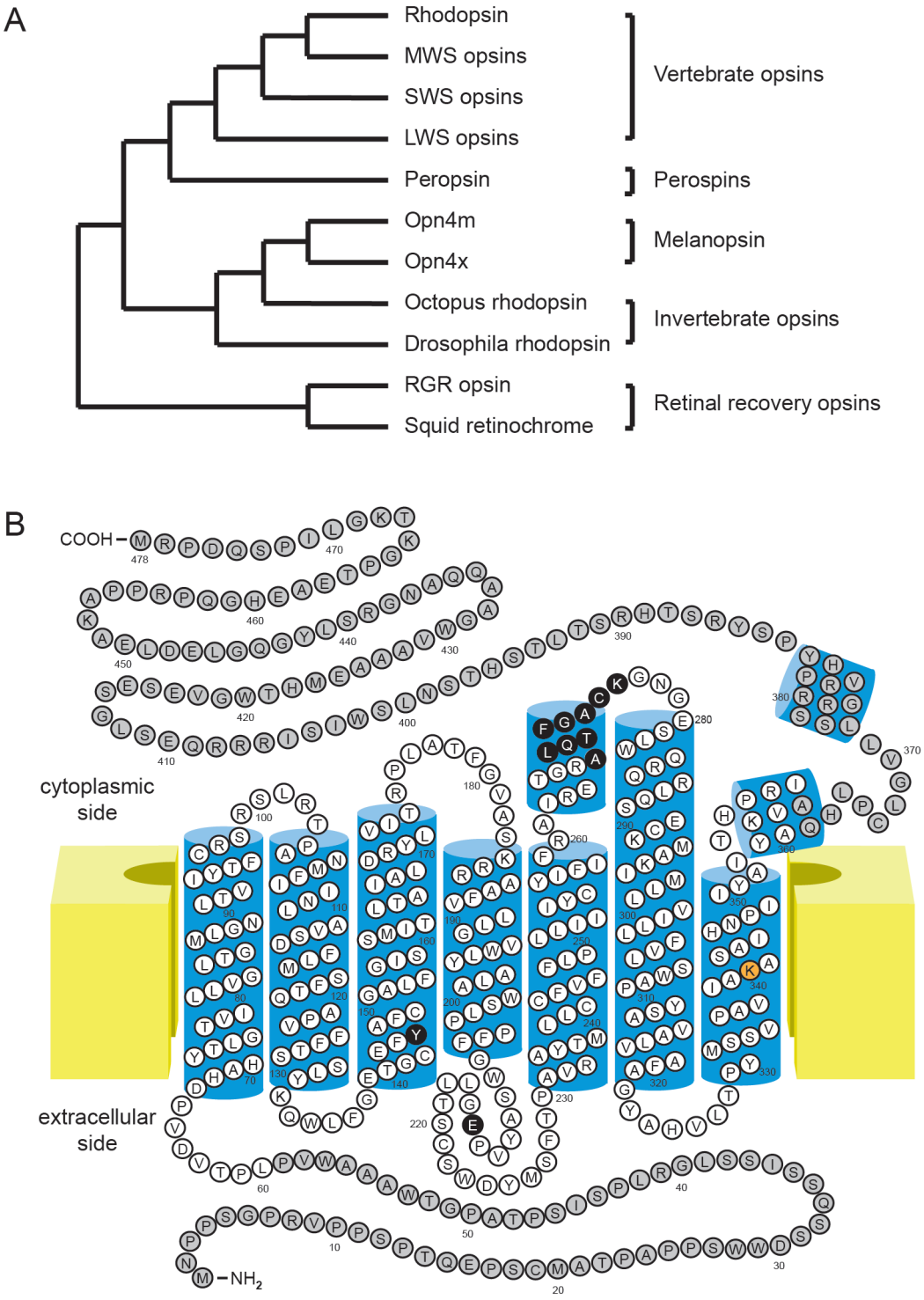
A
Rhodopsin
MWS opsins
SWS opsins
LWS opsins
Vertebrate opsins
Peropsin
Perospins
Opn4m
Opn4x
Melanopsin
Octopus rhodopsin
Drosophila rhodopsin
Invertebrate opsins
RGR opsin
Squid retinochrome
Retinal recovery opsins
B
COOH
NH2
cytoplasmic side
extracellular side

Figure 2. Melanopsin's structural relationship to other opsins. A) Dendrogram of melanopsin's relatedness (Opn4m and Opn4x) to other members of the opsin family demonstrating melanopsin's close relationship to rhapdomeric opsins. B) 2-D diagram of human melanopsin based on the structures of bovine rhodopsin (Hargrave and McDowell, 1992; Palczewski et al., 2000) and squid rhodopsin (Murakami and Kouyama, 2008). Amino acids in white are commonly used in sequence comparisons within and between species. Highlighted amino acids include the retinal attachment site in orange, K300, the two proposed Schiff base counterions in black, Y106 and E175 and a rhabdomeric-like G-protein specificity sequence in black, A268-K276. C-terminal and N-terminal structures of rhodpsins are not understood as well as the core transmembrane domain.

Figure 3

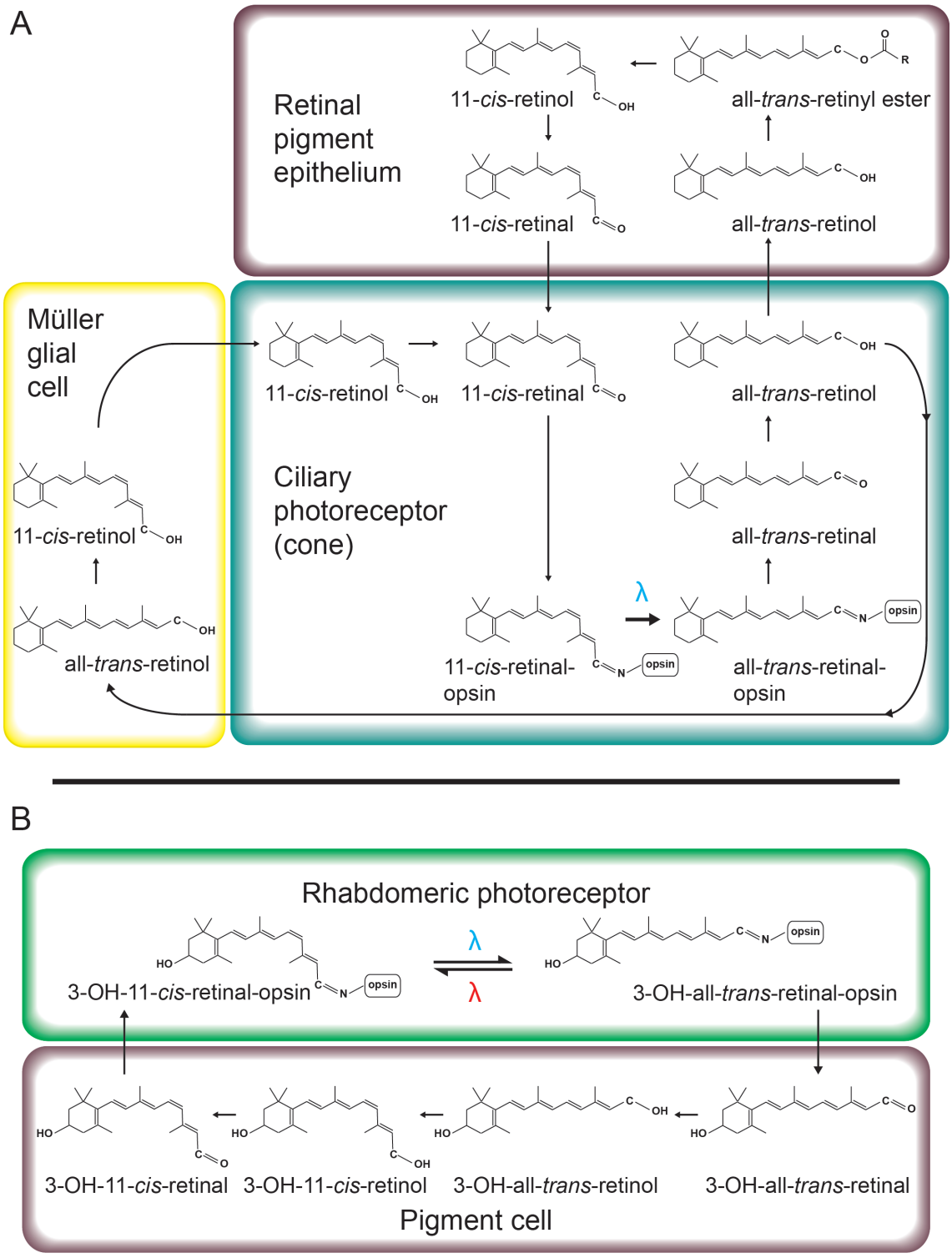
A
Retinal pigment epithelium
11-cis-retinol
all-trans-retinyl ester
11-cis-retinal
all-trans-retinol
Müller glial cell
11-cis-retinol
11-cis-retinal
all-trans-retinol
Ciliary photoreceptor (cone)
all-trans-retinal
λ
opsin
11-cis-retinal-opsin
all-trans-retinal-opsin
11-cis-retinol
all-trans-retinol
B
Rhabdomeric photoreceptor
3-OH-11-cis-retinal-opsin
λ
λ
3-OH-all-trans-retinal-opsin
3-OH-11-cis-retinal
3-OH-11-cis-retinol
3-OH-all-trans-retinol
3-OH-all-trans-retinal
Pigment cell

Figure 3. A summary of chromophore recycling steps. Illustrated are steps for A) ciliary and B) rhabdomeric photoreceptor photocycles. Difference between a sequential bistable mechanism of chromophore regeneration seen in rhabdomeric photoreceptors and the thermally unstable activation of opsins in ciliary photoreceptors are illustrated. A blue lambda indicates light activation of opsin from ground- to meta-state and conversion of the retinoid from the *cis* to *trans* conformation. A red lambda indicates the sequential absorption of a photon at a second wavelength that converts the meta-state to the ground-state and reisomerizes the retinoid back to the *cis* conformation. Note, rhabdomeric photoreceptors often use alternate retinoids such as 11-*cis*-3-hydroxy-retinal (3-OH-11-*cis*-retinal) in Drosophila used in the example above.

Figure 4

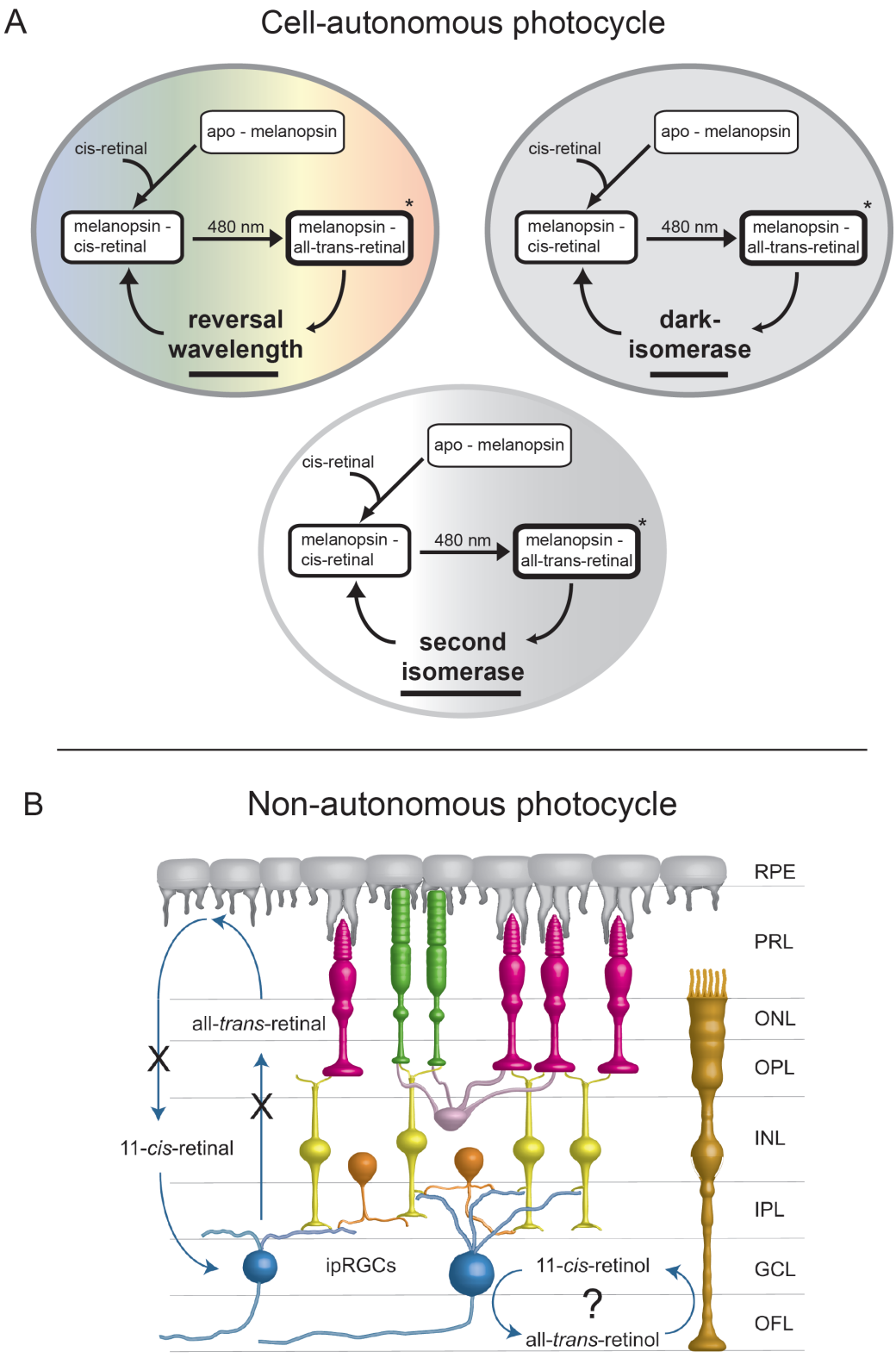
A
Cell-autonomous photocycle
cis-retinal
apo - melanopsin
melanopsin - cis-retinal
480 nm
melanopsin - all-trans-retinal
*
reversal wavelength
dark- isomerase
second isomerase
B
Non-autonomous photocycle
RPE
PRL
ONL
OPL
INL
IPL
GCL
OFL
all-trans-retinal
11-cis-retinal
ipRGCs
11-cis-retinol
?
all-trans-retinol

Figure 4. Potential models for cell-autonomous and non-autonomous melanopsin chromophore recycling. A) Three potential models for cell-autonomous chromophore recycling, including photo-reversal, intrinsic dark isomerase, and second isomerase mechanisms. These mechanisms are not mutually exclusive. B) Model for non-autonomous pigment recycling using Müller glial-based recycling. X indicates block to LRAT or RPE65, neither of which disrupt ipRGC function. Anatomic structures shown include the retinal pigment epithelium (RPE), photoreceptor layer (PRL), outer nuclear layer (ONL), outer plexiform layer (OPL), inner nuclear layer (INL), inner plexiform layer (IPL), ganglion cell layer (GCL), and the optic fiber layer (OFL).

Chapter 2: Resistance of melanopsin to light and chemical bleaching *in vivo*

This chapter was published previously

Sexton, T. J., Golczak, M., Palczewski, K., & van Gelder, R. N. (2012). Melanopsin is highly resistant to light and chemical bleaching in vivo. *Journal of Biological Chemistry*, *287*(25), 20888–20897.

Abstract

Melanopsin is the photopigment of mammalian intrinsically photosensitive retinal ganglion cells (ipRGCs), where it contributes to light entrainment of circadian rhythms, and to the pupillary light response. Previous work has shown the melanopsin photocycle is independent of that used by rhodopsin (Tu et al., 2006). Here we determined the ability of apo-melanopsin, formed by *ex vivo* ultraviolet (UV) light bleaching, to use selected chromophores. We found that 9-*cis*-retinal, but not all-*trans*-retinal or 9-*cis*-retinol, is able to restore light-dependent ipRGC activity after bleaching. Melanopsin was highly resistant to both visible-spectrum photic bleaching and chemical bleaching with hydroxylamine under conditions that fully bleach rod and cone photoreceptor cells. These results suggest that the melanopsin photocycle can function independently of both rod and cone photocycles, and that apo-melanopsin has a strong preference for binding *cis*-retinal to generate functional pigment. The data support a model in which retinal is continuously covalently bound to melanopsin and may function through a reversible, bistable mechanism.

Introduction

In addition to rods and cones, mammalian retinas contain a population of intrinsically photosensitive retinal ganglion cells (ipRGCs) (Peirson and Foster, 2006; Guler et al., 2007; Do and Yau, 2010). These photoreceptive cells are found in a small subpopulation of ganglion cell neurons that primarily project to areas of the brain involved in circadian rhythm orchestration and pupillary light responses (Chen et al., 2011). Unlike rods and cones, which employ rhodopsin and cone pigments for phototransduction, ipRGCs use melanopsin (Hattar et al., 2003; Panda et al., 2003; Tu et al., 2005). All opsins utilize *cis* to *trans* isomerization of the retinaldehyde chromophore as the primary photoreceptive event, and must regenerate the *cis* chromophore to regain photosensitivity. Although photocycles for chromophore regeneration of rhodopsin and, to a lesser extent, cone opsins, are well understood (Kuksa et al., 2003), the mechanisms of melanopsin pigment regeneration are less well studied (Fu et al., 2005; Nickle and Robinson, 2007; Walker et al., 2008). Previous work demonstrated that melanopsin can function independent of the retinal pigmented epithelium-based photocycle that forms the basis for all rod and most cone pigment regeneration (Tu et al., 2006). The bleaching characteristics of melanopsin *in situ* have not been systematically studied to date

Methods

Tissue preparation

C57Bl/6 mice (Jackson Laboratories, Bar Harbor, ME) were used as the wildtype strain. Melanopsin knockout mice (*Opn4*$^{-/-}$) were bred in a mixed 129/C57/Bl6 background (Panda et al., 2002). For analysis of ipRGC responses, multi-electrode array recordings were obtained from wildtype animals at ages P8-P10 or P13-16 (Tu et al., 2005). Opn4$^{-/-}$ P13-16 mice were used to record rod- on cone-driven responses. Mice were maintained in a 12:12 hr light-dark cycle. All experiments were performed in accordance with Association for Research in Vision and Ophthalmology guidelines for animal studies, under an approved animal study protocol at the University of Washington.

All procedures were performed under dim red light illumination. Mice were euthanized by CO_2 narcosis and cervical dislocation. Isolated mouse retinas were cut into squares and positioned with the vitreal face in contact with a multielectrode array (MEA) (Multi Channel Systems, Reutlingen, Germany) and superperfused (2 ml/min) with a bicarbonate-buffered physiologic solution (125 mM NaCl, 2.5 mM KCl, 1 mM $MgCl_2$, 1.25 mM NaH_2PO_4, 20 mM glucose, 26 mM $NaHCO_3$, 2 mM $CaCl_2$, 500 μM glutamine) oxygenated with 95% O_2/5% CO_2 to obtain a pH of 7.4. The temperature of both perfusate and tissue chamber was maintained at 33.0^{o}C. For ipRGC recordings from wildtype P8-10 mouse retinas, spontaneous retinal waves (Wong et al., 2000) (as well as any input from rod and cone photoreceptors), were suppressed by using glutamatergic [50 μM d(2)-2-amino-5-phosphonopentanoic acid (d-AP5); 20 μM d(-)-2-amino-4-phosphonobutyric acid (d-AP4), 10 μM CNQX] and cholinergic (5 nM epibatidine)

inhibitors (Tocris Biosciences, Ellisville, MO). For ipRGC recordings from wildtype P13-16 mouse retinas only glutamatergic blockade was used [100 μM d(2)-2-amino-5-phosphonopentanoic acid (d-AP5); 50 μM d(-)-2-amino-4-phosphonobutyric acid (d-AP4), 40 μM CNQX]. Signals from *Opn4*$^{-/-}$ mouse retinas were recorded without pharmacological intervention.

Multi-electrode recordings

Electrophysiologic recordings were performed using planar arrays of 60 electrodes (30 μm diameter, 200 μm inter-electrode spacing; Multi Channel Systems, Reutlingen, Germany). Raw electrical signals were amplified, filtered, and digitized through an A/D card (National Instruments, Austin, TX), written to disk and analyzed off-line, as described previously (Holy et al., 2000).

Retinas were stimulated with a Xenon light source (Sutter Instruments, Novato, CA) fed through a liquid light guide and diffusing filter (Thorlabs Inc., Newton, NJ). Intensities and wavelengths of light were adjusted via neutral density and narrow band-pass 480 nm interference filters (full width, half max, 10 nm)(Thorlabs, Inc., Newton, NJ) and calibrated with a radiometer (Advanced Photonics International, Fairfield, CT). Light stimuli were delivered and monitored by a computer-controlled shutter (Vincent Associates, Rochester, NY). UV light was provided by an Optimax 365 UV flashlight (Spectronics Corporation) mounted 10 cm above the tissue. The Optimax contains a single high-output UV LED with a narrow spectrum centered at 365 nm. At 10 cm, the device delivered 9.19×10^{15} photons cm^{-2} s^{-1} (IR 16) as measured by radiometry.

Retinoids

Both 9-*cis*-retinal and all-*trans*-retinal were purchased from Sigma (St. Louis, MO). Retinals were dissolved in acetonitrile, aliquoted and dried under argon. 9-*cis*-Retinol was generated by reduction of 9-*cis*-retinal (Garwin and Saari, 2000). Briefly 2 mg of 9-*cis*-retinal was suspended in acetonitrile and incubated with 20 mg sodium borohydride for 15 min. Reaction products were extracted and analyzed by UV spectrophotometry and HPLC and dried under argon. All retinoids were resuspended in ethanol for determinations of concentration and experimental use.

UV retinal depletion and retinoid treatment

Irradiance response curves were determined for each wildtype P8-10 mouse retina by using 480 nm light at IR 13.6, 12.6, and 11.6 ($4.0x10^{13}$, $4.0x10^{12}$, $4.0x10^{11}$ photons cm^{-2} s^{-1} respectively). Retinas were exposed to 365 nm UV light for 15 min, allowed to recover for 10 min, and then tested regularly at IR 13.6 over 2 hours post-UV light treatment. Retinas with responses recorded immediately after irradiation that were not at or below 2% of pre-UV treatment were excluded from analysis. Retinas used for retinoid replenishing experiments were treated in the same manner up to the 10-min post-UV light test. Thereafter, retinas were superperfused for 30 min with a mixture of the test retinoid in a non-carbogenated HEPES/bicarbonate-buffered physiologic solution (10 mM HEPES, pH 7.4, 125 mM NaCl, 2.5 mM KCl, 1 mM $MgCl_2$, 1.25 mM NaH_2PO_4, 12

mM glucose, 26 mM $NaHCO_3$, 2 mM $CaCl_2$, 500 μM glutamine) with 1% ethanol as a carrier mixed with carbogen bubbled bicarbonate-buffered physiologic solution at a 1:1 ratio just prior to tissue delivery. Retinas were returned to the bicarbonate-buffered physiologic solution and tested for light evoked activity (480 nm light at IR 13.6) 60 min and 90 min post-UV light treatment. Results were analyzed by two-way ANOVA for time and retinoid treatment and corrected for multiple comparisons with the Bonferonni method.

HPLC analysis of retinoids

To validate the UV depletion protocol, 8 whole retinas from p8-10 wildtype mice were treated with UV light and snap-frozen on dry ice. Whole control retinas from the other eye of the same animals were removed and immediately frozen on dry ice. Samples were suspended in 1 ml of 12 mM phosphate buffer, 137 mM NaCl, 2.7 mM KCl, 20 mM NH_2OH, 50% methanol (v/v) and homogenized in a glass-glass Dounce homogenizer. After 20 min incubation in room temperature, homogenates were extracted with 4 ml of hexane. Organic phases were collected, dried down by vacuum centrifugation and redissolved in 0.2 ml of hexane. Retinoids were separated on a normal phase HPLC column (5-μm ZORBAX SIL, 4.6 × 250 mm, Agilent Technology) by a step gradient of ethyl acetate in hexane (0.5% for 15 min and 6% from 15 to 60 min at 1.4 ml/min flow rate). Retinoids were detected at 325 and 360 nm by using a diode array detector and identified based on their elution times and characteristic UV/Vis spectra. Retinylaldehydes and retinol were quantified based on standard curves that correlated

integrated peak areas calculated from chromatograms with known amounts of synthetic standards injected onto the column.

Hydroxylamine treatments

Hydroxylamine, obtained from Sigma (St. Loius, MO), was dissolved in a bicarbonate-buffered physiologic solution and neutralized with Tris-base to pH 7.4. Retinas were superperfused with neutralized hydroxylamine bubbled with carbogen with or without 480 nm light exposure (IR 13.6). Concentrations for hydroxylamine-only treatments were 10 mM and 30 mM whereas those for hydroxylamine-light co-treatment were 10 mM, 30 mM and 60 mM. Retinas were returned to bicarbonate-buffered physiologic solution and tested with IR 13.6 at 10 and 60 min post-hydroxylamine treatment.

Results

Melanopsin is resistant to long-term bleaching by visible light

To determine whether melanopsin can be photobleached by visible light *in situ,* we exposed retinas from P8-10 wildtype mice, under glutamatergic and cholinergic blockade, to saturating light (480 nm, IR 13.6) for 1 hour. Retinal ganglion cell activity was measured by multi-electrode array recording (Tu et al., 2005). As rod and cone signaling is not established by P10, only melanopsin-dependent ipRGC cell firing is observed

under these conditions (Tu et al., 2005). During dissection, the retinal pigmented epithelium remains firmly attached to the sclera and is therefore absent from the retinal preparation. As controls, retinas from slightly older P13-16 melanopsin-deficient mice (*Opn4*$^{-/-}$), which demonstrate only rod and cone-dependent retinal ganglion cell firing, were exposed to the identical lighting regimen. Following the one-hour light exposure, light-dependent ipRGC firing activity was still present, but had decreased to 7% of its initial activity (Figures 1A and 1B). In *Opn4*$^{-/-}$ retina, all light-dependent ganglion cell firing activity was abolished at the end of the one-hour light exposure. Following a ten minute dark recovery period, 65% of baseline light-dependent ipRGC activity was restored in P8-10 wildtype retinas, whereas no activity was detected in rod- and cone-driven ganglion cells of *Opn4*$^{-/-}$ retina (Figure 1B). This result demonstrates that melanopsin chromophore is substantially regenerated under conditions that fully bleached rod and cone chromophore.

Melanopsin is bleached for extended periods by intense 365 nm UV light

As bright visible light did not bleach melanopsin, we used intense UV light at 365 nm instead to degrade endogenous retinoids (Tu et al., 2004). Treatment of retinas with 15 min of UV light reduced light-dependent ipRGC firing to <2% of maximal pre-UV light evoked spiking 10 min after exposure. This was followed by recovery to a stable level of ~25% of maximal pre-UV light-induced activity over the course of one hour in the dark. Non-ipRGC activity from *Opn4*$^{-/-}$ retinas exposed to the same UV treatment did not show any significant recovery (Figure 2A). HPLC analysis of retinoid composition extracted

from 8 whole, untreated retinas revealed the presence of 80 pmols of 11-*cis*-retinal per retina (~5 pmol retinoids per mg of protein) whereas immediately after UV treatment, retinoid levels were below the HPLC-detectible limit of ~2 pmols per retina (Figures 3A and 3B). Retinoids could not be detected at the 90-min recovery time point (Figure 3C). This does not exclude the presence of trace amounts of retinoid still available to form minute amounts of functional pigment, as is suggested by the small, transient RGC response in UV treated *Opn4*$^{-/-}$ animals. This activity also may be uncorrelated spontaneous firing that cannot be suppressed as *Opn4*$^{-/-}$ retinas are not recorded under synaptic blockade.

UV-bleached melanopsin reconstitutes with cis-retinal but not all-*trans*-retinal

To test the *in situ* preference of bleached melanopsin for *cis*-retinal vs. all-*trans*-retinal, we UV-bleached retinas using the method described above, followed by treatment with *cis* or *trans*-retinaldehyde. Treatment of UV-light exposed retinas with 100 μM 9-*cis*-retinal reconstituted retinal light-induced spiking activity to 110% of pre-UV levels (Figure 2B) (ANOVA $P<0.005$, Bonferroni corrected) whereas 20 μM 9-*cis*-retinal failed to reconstitute light-dependent signaling over levels observed with the vehicle control (Figure S1A). Treatment with 100 μM all-*trans*-retinal failed to increase activity above control levels (Figure 2B) as did both higher (200 μM) and lower (20 μM) concentrations (Figure S1B). Indeed, 200 μM all-*trans*-retinal treatment decreased activity levels under what we view as toxic effects as is suggested by evidence for oxidative phosphorylation decoupling and other toxic effects with high retinoid concentrations in cell culture.

Exposure of all-*trans*-retinal-supplemented retinas to high intensity white light (to facilitate possible photoconversion of *trans* to *cis*-retinal) also failed to reconstitute subsequent photosensitivity above levels achieved by vehicle alone (data not shown).

Figure 2C shows the distribution of rescued individual cell firing activity in response to light 90 min post-UV light exposure following treatment with vehicle and 100 μM retinoids. These histograms demonstrate that only 9-*cis*-retinal shifted the distribution of cell responses away from the depleted post-UV state (seen with vehicle treatment), back towards the baseline "pre-UV" distribution centered near a 100% response. Interestingly, a few cells in the 9-*cis*-retinal treatment had a dramatically increased response to light compared with pre-bleach levels, as was noted in patch clamp study of ipRGC by Do *et. al* (Do et al., 2009).

HPLC analysis of retinoid-treated retinas showed adequate penetration of exogenously applied retinoids (Figure 3D, 3E) reaching or exceeding pre-treatment levels at ~44 pmol mg^{-1} retina (n=4 retinas) for 9-*cis*-retinal treatment and ~10 pmol retinoid mg^{-1} retina for all-*trans*-retinal (n=7 retinas). Binding with 200 μM all-*trans*-retinal treatment was ~6 pmol mg^{-1} (n=3 retinas). No retinoids were detected after the 20 μM *cis*- or *trans*-retinoid treatments.

ipRGCs are unable to utilize 9-*cis*-retinol in their photoresponse

A second photocycle present in the retina is found in Müller glial cells, which produce 11-*cis*-retinol. Cones, but not rods, can use the *cis*-retinol product of this

photocycle (Wang and Kefalov, 2011). To test if ipRGCs can utilize this photocycle, UV-bleached retinas were treated with several concentrations of 9-*cis*-retinol. Photosensitivity was not reconstituted following 100 μM or several lower concentrations of this retinoid (Figure 2B and Supp. Figure 1C). Moreover, 100 μM 9-*cis*-retinol treatment also appeared to decrease significantly the ability of cells to respond to light below that of cells treated with vehicle only (Figure 2C), whereas lower concentrations of 9-*cis*-retinol lessened this effect (Figure S1C). In contrast to *cis*- and *trans*-retinaldehyde, uptake of 9-*cis*-retinol was not detected by HPLC analysis (data not shown).

Melanopsin in situ resists hydroxylamine bleach

Hydroxylamine is used to chemically bleach opsins (Wald et al., 1955). This small molecule interferes with formation of the protonated Schiff-base between retinaldehyde and the lysine side chain of the opsin binding site, by substituting for the lysine side chain. The products of this reaction are apo-opsin and retinyloxime. Cone opsins are bleached by exposure to hydroxylamine in the dark, presumably because the chromophore is exposed to the external milieu in the opsin ground-state (Wald et al., 1955; Abrahamson et al., 1974). In the case of rhodopsin in rods, light is required for activation to metarhodopsin II before hydroxylamine accesses and attacks the Schiff base, as 11-*cis*-retinal is protected from the local environment by the rhodopsin molecule ground-state (Dartnall, 1968; Brin and Ripps, 1977; Leibrock and Lamb, 1997). Hydroxylamine can also prevent regeneration of the opsin-retinal molecule by sequestering *cis*-retinal and all-*trans*-retinal as retinal oximes after light bleaching (Wald and Brown, 1950). Compared

to rod and cone opsins, bistable pigments of invertebrate rhabdomeric photoreceptors are highly resistant to hydroxylamine bleaching, even after light exposure (Hubbard and St George, 1958).

To test if melanopsin is susceptible to hydroxylamine bleaching in the dark, wildtype P13-16 retinas under glutamatergic blockade (i.e., ipRGCs only) were treated for 15 min with hydroxylamine concentrations previously used to bleach cones (Bowmaker and Loew, 1976; Nemargut and Wang, 2009) without light exposure. For direct comparison with cone opsin-based activity, P13-16 *Opn4*$^{-/-}$ retinas (i.e., with RGC firing from rods and cones only) were treated identically but without glutamatergic blockade. Following 10 mM hydroxylamine treatment, non-ipRGC spiking activity in *Opn4*$^{-/-}$ retinas was transiently abolished at 10 min post-treatment but recovered by 60 min, whereas ipRGC activity was unaltered at both time points (Figure 4A). With 30 mM hydroxylamine treatment, activity in *Opn4*$^{-/-}$ retinas was abolished at 60 min whereas ipRGC activity in wildtype retinas was reduced only to ~50% of pre-treatment levels (Figure 4B).

To test if melanopsin susceptibility to hydroxylamine is increased by light exposure, wild-type P8-10 retinas under glutamatergic blockade were treated for 15 min with hydroxylamine, at similar concentrations as those used previously, along with concurrent 480 nm light, at a level that saturates ipRGC firing (IR 13.6). For comparison, similar retinas were treated with hydroxylamine in the dark. At 60 min following 10 mM /light co-treatment, ipRGC activity decreased only mildly, as also occurred in the dark (Figure 4C). But following 30 mM/light co-treatment, activity again decreased slightly but less than in darkness alone. Similar moderate levels of activity were seen following 60 mM hydroxylamine treatment in either light or dark. These results suggest that light increases

the apparent susceptibility of melanopsin to hydroxylamine only slightly if at all. Of note, 10 min following 30 and 60 mM hydroxylamine treatment with or without light, the ability of all ganglion cells to fire in response to elevated KCl was reduced or eliminated. However, firing ability recovered to normal levels by 60 min (data not shown) with a concurrent return of light-induced activity in ipRGCs. This indicates that hydroxylamine exerts some non-specific effects. Despite this caveat, our data indicate that melanopsin chromophore is substantially reconstituted under several conditions that lead to bleaching of rod- and cone pigments.

Discussion

Melanopsin shares greater sequence similarity to opsins commonly found in invertebrate rhabdomeric photoreceptors than to vertebrate ciliary opsins, displaying only 30% sequence similarity with other mammalian ciliary (rod and cone) opsins but about 40% sequence similarity with rhabdomeric cephalopod rhodopsin (Provencio et al., 1998; Bellingham et al., 2002). This suggests that melanopsin functions more like rhabdomeric opsins, which have long-lasting meta states and regenerate chromophore via sequential photon absorption. When ciliary opsins absorb a photon of light, 11-*cis*-retinal is isomerized into all-*trans*-retinal and released from the opsin protein (Palczewski, 2006). A separate isomerase then reconverts esterified *trans*-retinal to *cis*-retinol (Palczewski, 2006; Kiser et al., 2011). In rhabdomeric opsins, all-*trans*-retinal is not released from the opsin, but instead absorbs a second photon and is re-isomerized to 11-*cis*-retinal. This is possible because rhabdomeric pigments have stable meta-states that last for seconds to

minutes, whereas vertebrate meta-states last only milliseconds (Hillman et al., 1983; Hardie and Postma, 2007). Rhabdomeric opsins are thus considered bistable molecules.

Suggestions of melanopsin bistability have been supported by heterologous expression experiments. Panda *et al.* (Panda et al., 2005) found that expressing mouse melanopsin in *Xenopus* oocytes conferred white light sensitivity that was dependent upon the addition of 9-*cis*-retinal to these cells. Addition of all-*trans*-retinal had only 10% the effect of 9-*cis*-retinal, suggesting that melanopsin has a preference for the *cis*-chromophore. Co-expressing arrestin with melanopsin increased the latter's activity by 12-fold after 9-*cis*-retinal incubation. Depending upon the arrestin co-expressed, melanopsin's all-*trans*-retinal-dependent light activity increased 10 to 30-fold, approaching that conferred by 9-*cis*-retinal, perhaps through arrestin's stabilizing the meta-states. Melyan *et al*. (Melyan et al., 2005) found that human melanopsin expressed in Neuro2A cells also conferred an intensity-dependent light response to these cells. Again, this response required pre-incubation with 9-*cis*-retinal. Incubation with all-*trans*-retinal produced a response about 25% of the magnitude observed with 9-*cis*-retinal. When cells were incubated with all-*trans*-retinal and illuminated with 540 nm light for 10 min, the photoresponse increased 3-fold over that following all-*trans*-retinal incubation alone. Taken together, these results suggest melanopsin is capable of bistable functioning.

Melanopsin photosensitivity is reconstituted by cis-retinal chromophore after UV bleaching in situ

In the current studies, prolonged 480 nm light exposure reduced light-activated ipRGC activity. This could result from either adaptation of melanopsin signaling (Wong et al., 2005) or bleaching of pigment. However, light-driven ipRGC activity recovered substantially within minutes (Figure 1), suggesting either rapid chromophore regeneration or reversal of adaptation. To obtain a more definitive bleaching paradigm, high intensity UV light was employed to bleach melanopsin by degrading endogenous retinoids. UV light exposure for 15 min lowered ipRGC firing to a stable 25% of maximal pre-bleach activity and reduced endogenous retinoids to below our HPLC detectable limits of 0.1 pmol (Stecher and Palczewski, 2000). Exposure to more than 15 min of UV light led to substantial tissue mortality (data not shown). Residual ipRGC activity found after treatment likely represents a very small quantity of *cis*-retinal resistant to destruction by UV light, suggesting either that melanopsin has very high affinity for trace amounts of the remaining intact chromophore, or may itself help to shield some *cis*-*c*hromophore from UV-mediated destruction. It is remarkable that any activity remained with such low retinoid levels as all rod and cone activity was abolished under the same bleaching conditions (Figure 2).

Following bleaching, reconstitution of ipRGC activity by addition of exogenous retinoid was successful only with 100 μM 9-*cis*-retinal. No restoration of light-dependent activity above baseline was seen following any tested concentration of all-*trans*-retinal. HPLC-measured levels of post-reconstitution retinoids were higher following 9-*cis*-retinal rescue than after all-*trans*-retinal, likely because of *cis*-specific

binding mechanisms in rod and cone photoreceptors. Despite this lower level of all-*trans*-retinal, the amount found in retinas after exogenous supplementation was equivalent to pre-bleached levels of total endogenous retinoids. Therefore adequate penetration of the retina by passive diffusion of retinoids was likely achieved, suggesting that melanopsin in ipRGCs *in situ* has a functional preference for the *cis* over the *trans* conformation of retinal. This preference presumably extends from 9-*cis*-retinal to 11-*cis*-retinal. (9-*cis*-retinal was used in these experiments because of the large quantities needed and its stability during long periods of constant perfusion of retinas with multielectrode arrays (MEAs) that made use of 11-*cis*-retinal practically unfeasible).

ipRGCs function independently of the Müller glial based photocycle

Melanopsin has previously been shown to function independently of the retinal pigment epithelium-based photocycle (Tu et al., 2006). The only other known photocycle present in the retina is found in Müller glial cells. But instead of producing 11-*cis*-retinal, the Müller glial cell-based photocycle converts all-*trans*-retinol produced by photoreceptors into 11-*cis*-retinol that is then transported to cones, which have the capacity to oxidize the alcohol to the 11-*cis*-retinal required to bind cone opsin (for review see (Wang and Kefalov, 2011)). As we were unable to restore light activated activity to ipRGCs after the exogenous addition of 9-*cis*-retinol at several concentrations (Fig S1C), we conclude that ipRGC function is independent of this cone-specific photocycle. Thus, there would appear to be at least three functional photocycles in the

murine retina. Neither the RPE-based rod/cone nor the Müller-based cone photocycle is needed to regenerate chromophore in ipRGC.

Melanopsin displays bistable-like pigment behavior in response to in situ hydroxylamine treatment

Hydroxylamine treatment constitutes a classic method for photospectrometric analysis of opsins. Here we used it in live tissue to chemically bleach native photopigments *in situ* (Brin and Ripps, 1977; Leibrock and Lamb, 1997). We observed only minimal to moderate bleaching of melanopsin by low concentrations hydroxylamine, either in the dark or with concurrent light exposure. This contrasts with the complete transient or sustained rod and cone opsin bleaching following hydroxylamine treatment under the same conditions. Although 60 mM hydroxylamine treatment led to a consistently moderate to large loss of light-sensitivity in ipRGCs, and 30 mM hydroxylamine showed inconsistently sized losses, we believe these changes were mostly due to off-target effects as they coincided with decreased RGC firing in response to high K^+ concentrations. Above 50 mM, hydroxylamine has been shown to cause significant disruptions in G-protein coupled receptor phosphorylation and $G_q \alpha$ palmitoylation-mediated membrane localization (Pepperberg, 1992; Pepperberg et al., 1995). These and potentially other non-specific effects of hydroxylamine could lead to the apparent loss of light-sensitivity seen here as well as the inability of all ganglion cells to fire in response to an increased KCl concentration.

Our results suggest that melanopsin's chromophore is protected from the external milieu and not readily available for hydroxylamine binding in either its ground state or its signaling meta-state. This is a characteristic of bistable pigments, which do not easily release chromophore, (i.e. octopus rhodopsin (Hubbard and St George, 1958)). This finding may also explain the remarkable preservation of ipRGC signaling in animals that have been severely depleted of Vitamin A (Thompson et al., 2004)

All bistable pigments have been shown to 'photoreverse' at a different wavelength (usually red shifted) from the activation wavelength. This reversal re-isomerizes all-*trans*-retinal to 11-*cis*-retinal. *In vitro* work by Melyan *et al.* (Melyan et al., 2005) showed that melanopsin expressed in cell culture appeared to convert exogenously added all-*trans* to 11-*cis*-retinal after prolonged exposure to bright light above 540 nm (Melyan et al., 2005). This reversal was assessed by an increase in the light evoked current above what could be evoked with all-*trans*-retinal in the dark. Similarly, Mure *et al.* (Mure et al., 2007) showed that animals pre-exposed to 630 nm light had potentiated firing of suprachiasmatic neurons *in vivo* in response to 480 nm light, presumably through increased ipRGC activity. However, Mawad and Van Gelder (Mawad and Van Gelder, 2008) found no potentiation of ipRGCs in whole retina studied *ex vivo* by using multi-electrode array recording under the identical lighting protocol, suggesting the potentiation seen by Mure *et al.* relied on non-ipRGC- or non-melanopsin-based mechanisms (Mawad and Van Gelder, 2008). Thus it is unclear whether ipRGCs *in situ* have a distinct red-shifted photoreversal mechanism.

Heterologously expressed melanopsin from the protochordate *Amphioxus* does appear to have a red-shifted photoreversal mechanism (Koyanagi et al., 2005; Terakita et al.,

2008). Difference spectra of recombinant *Amphioxus* melanopsin purified from HEK293 cells and exposed to alternating blue and orange light, indicate a reversal wavelength near 515 nm. This constitutes a red shift of 30 nm from the forward activation wavelength. Red shift magnitudes vary greatly among rhabdomeric opsins from different species, ranging from 7 nm in squid to 100 nm in fly (Hubbard and St George, 1958; Vought et al., 2000). Even opsins from quite closely related species such as squid and octopus do not have similar red shift magnitudes, (i.e. 7 nm and 35 nm, respectively (Hubbard and St George, 1958; Koutalos et al., 1989)). It is possible that murine melanopsin may function as a bistable pigment but with a reversal wavelength spectrum that overlaps so closely with the forward activation spectrum that the two cannot be functionally separated (Figure 5).

Photoreversal, even if operative, does not fully explain the behavior of melanopsin, however. As shown in Figure 1, melanopsin photosensitivity is reconstituted substantially in the dark. Thus, a mechanism must exist whereby all-*trans*-retinal in the dark is converted back to *cis*-retinal. Restoration of activity in the dark is not consistent with a purely bistable pigment that does not release its chromophore. Such a mechanism is suggested by the work of Terakita *et al.* (Terakita et al., 2008). Using purified, recombinant *Amphioxus* melanopsin, this group showed a blue shift of the activated melanopsin spectrum towards the pre-exposure spectrum after a 5-min dark incubation. It is possible that melanopsin acts as a dark isomerase itself, by using stored energy in this protein to convert the *trans*- to *cis*-chromophore. Such thermal relaxation has been established as a second, but slower, mechanism of chromophore regeneration to photoreversal in bacterial and archeabacterial opsins (Chow et al., 2011). Alternatively,

the melanopsin photocycle could mirror the cephalopod photocycle in which a second photoisomerase, similar to retinochrome (Ozaki et al., 1983), recycles all-*trans* back into 11-*cis*-retinal in a light-dependent manner.

Conclusions

Our results suggest: 1) melanopsin is remarkably resistant to bleaching by light, UV radiation and hydroxylamine, 2) apo-melanopsin has a preference for *cis* over *trans*-retinal, and 3) melanopsin does not appear to release chromophore easily to allow bleaching by hydroxylamine. Definitive photocycle assessment will require single cell measurements *in vivo* and purified melanopsin. Closest to achieving this objective is Walker *et al.* (Walker et al., 2008) who determined that immunopanned ipRGCs maintained in the dark contained only 11-*cis*-retinal whereas cells exposed to light after panning predominantly contained all-*trans*-retinal. This is consistent with the requirement for the *cis* confirmation of retinal for the light response found here. In addition we found that melanopsin is not readily bleached by hydroxylamine, which suggests that it does not easily release its chromophore after light activation and its isomerization to all-*trans*-retinal. The latter is a characteristic of bistable pigments. If melanopsin is a bistable pigment, it is possible that the *in vivo* apo-form may require the *cis* conformation for chromophore binding.

Figure 1

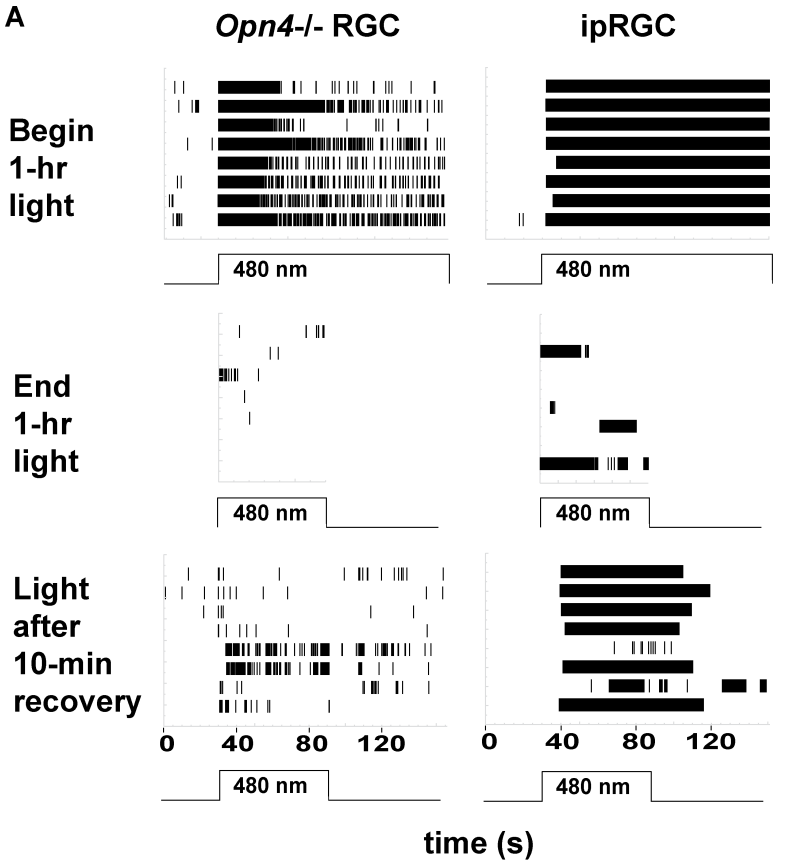
A
Opn4-/- RGC
ipRGC
Begin 1-hr light
End 1-hr light
Light after 10-min recovery
480 nm
0 40 80 120
time (s)
B
Pre-exposure activity (%)
100 80 60 40 20 0
0 10 20 30 40 50 60
Light exposure duration (min)
ipRGC
Opn4-/- RGCs
C
Pre-exposure activity (%)
100 80 60 40 20 0
Begin 1-hr
End 1-hr
10-min recovery
ipRGCs
Opn4-/- RGCs

Figure 1: ipRGC activity is resistant to light bleaching. A) Raster plots of light induced firing activity in 8 RGCs from 2 Opn4-/- retinas and 8 ipRGCs from one wildtype retina at the beginning and end of a 1 hour 480 nm light exposure (IR 13.6) followed by a one minute light test of all cells after a 10 minute dark recovery period immediately following the hour of light. B) Percent light-induced activity (defined as percent initial activity) from cones (n=8 cells from 2 retinas) and ipRGC (n= 16 cells from 2 retinas) during 1 minute recording periods taken at various times over the course of 1-hr with a continuous, 480 nm light stimulus at IR 13.6. Error bars are SEM. C) A bar graph of firing activity from Figure B at the beginning and end of the 1-hr of light exposure followed by a 1-min 480 nm test stimulus (IR 13.6) administered ten minutes after the end of the 1-hr exposure. Error bars are SEM. * Statistically significant difference in firing rate between ipRGCs and opn4-/- RGCs (repeated measures one-way ANOVA, $P<0.001$, Bonferroni corrected). † Not significantly different from zero statistically, paired-student's t-test.

Figure 2

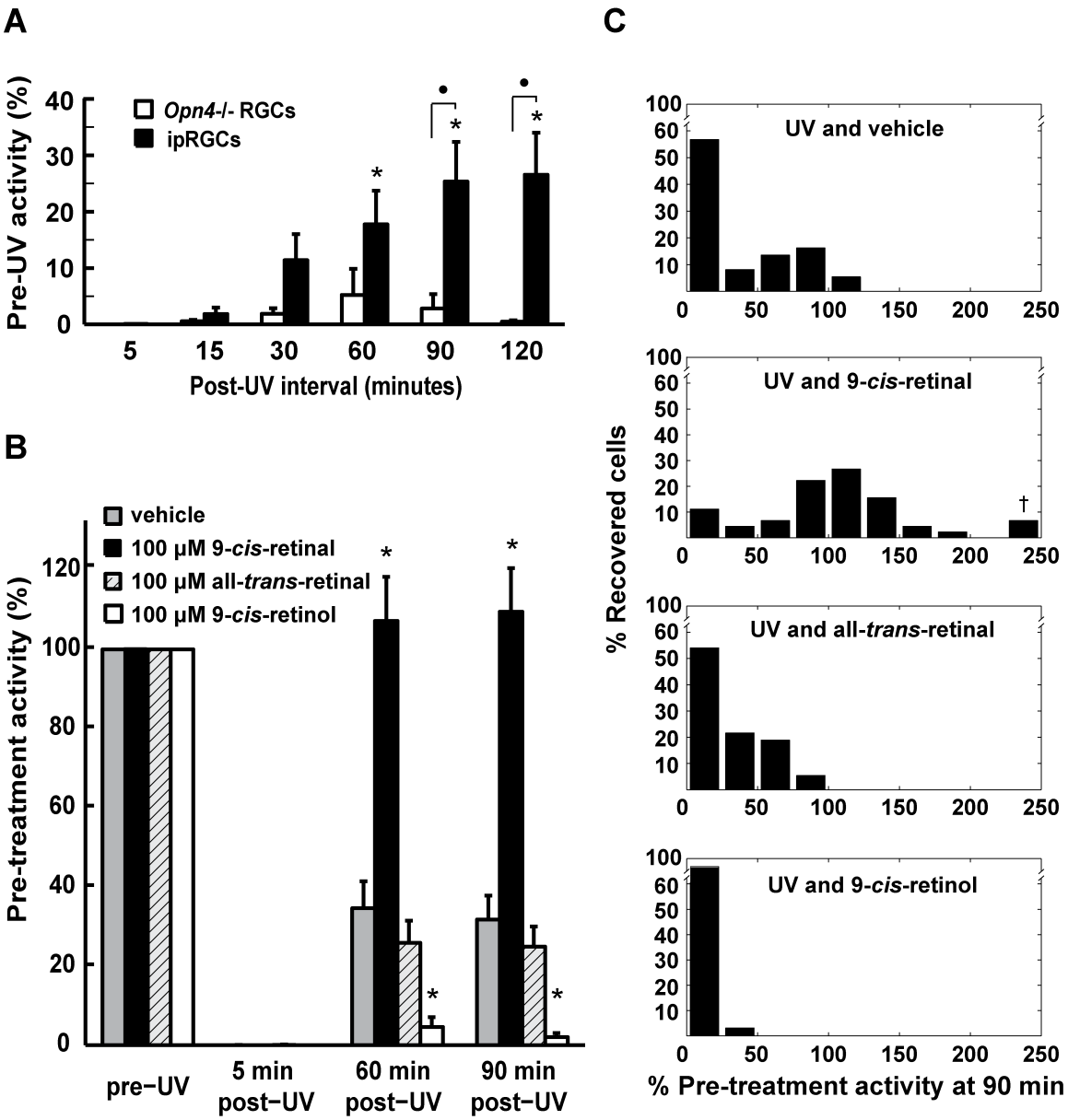
A
Pre-UV activity (%)
Opn4-/- RGCs
ipRGCs
Post-UV interval (minutes)
B
Pre-treatment activity (%)
vehicle
100 µM 9-cis-retinal
100 µM all-trans-retinal
100 µM 9-cis-retinol
pre−UV
5 min post−UV
60 min post−UV
90 min post−UV
C
% Recovered cells
UV and vehicle
UV and 9-cis-retinal
UV and all-trans-retinal
UV and 9-cis-retinol
% Pre-treatment activity at 90 min

Figure 2: 9-*cis*-retinal restores ipRGC activity after UV depletion. A) Retinas were treated for 15 min with UV to deplete endogenous retinoids. Rod and cone (*Opn4*$^{-/-}$) (n=10 cells from 4 retinas) and ipRGC (wildtype)(n=23 cells from 4 retinas) activity in response to a periodic 1 min 480 nm test light at IR 13.6 was monitored over 2 h after UV-treatment. Error bars are SEM. * Statistically significant difference in firing rate between ipRGCs and opn4-/- RGCs, P<0.005; • ipRGC firing rate significantly different from zero statistically, P<0.05 (repeated measures one-way ANOVA, Bonferroni corrected). Error bars are SEM. B) ipRGC activity is restored after 15 min of UV treatment by the addition of 100 μM 9-*cis*-retinal (n=45 cells from 5 retinas). No activity exceeding that of vehicle control (n=37 cells from 5 retinas) is seen with the addition of 100 μM all-*trans*-retinal (n=37 cells from 6 retinas) or 100 μM 9-*cis*-retinol (n=32 cells from 4 retinas). * 9-*cis*-retinal treatment results significantly different statistically from all other retinoid treatment, P<0.005 (repeated measures two-way ANOVA, Bonferonni corrected). Error bars are SEM. C) Normalized histrograms of ipRGC activity level at the 90-min time point from graph B demonstrates that only 9-*cis*-retinal increases the activity of most cells above vehicle only. The y-axis is the percentage of treated cells responding at the percent of their pre-UV-light induced activity level. † Three cells with activity of 234%, 330%, and 403 % respectively.

Figure 3

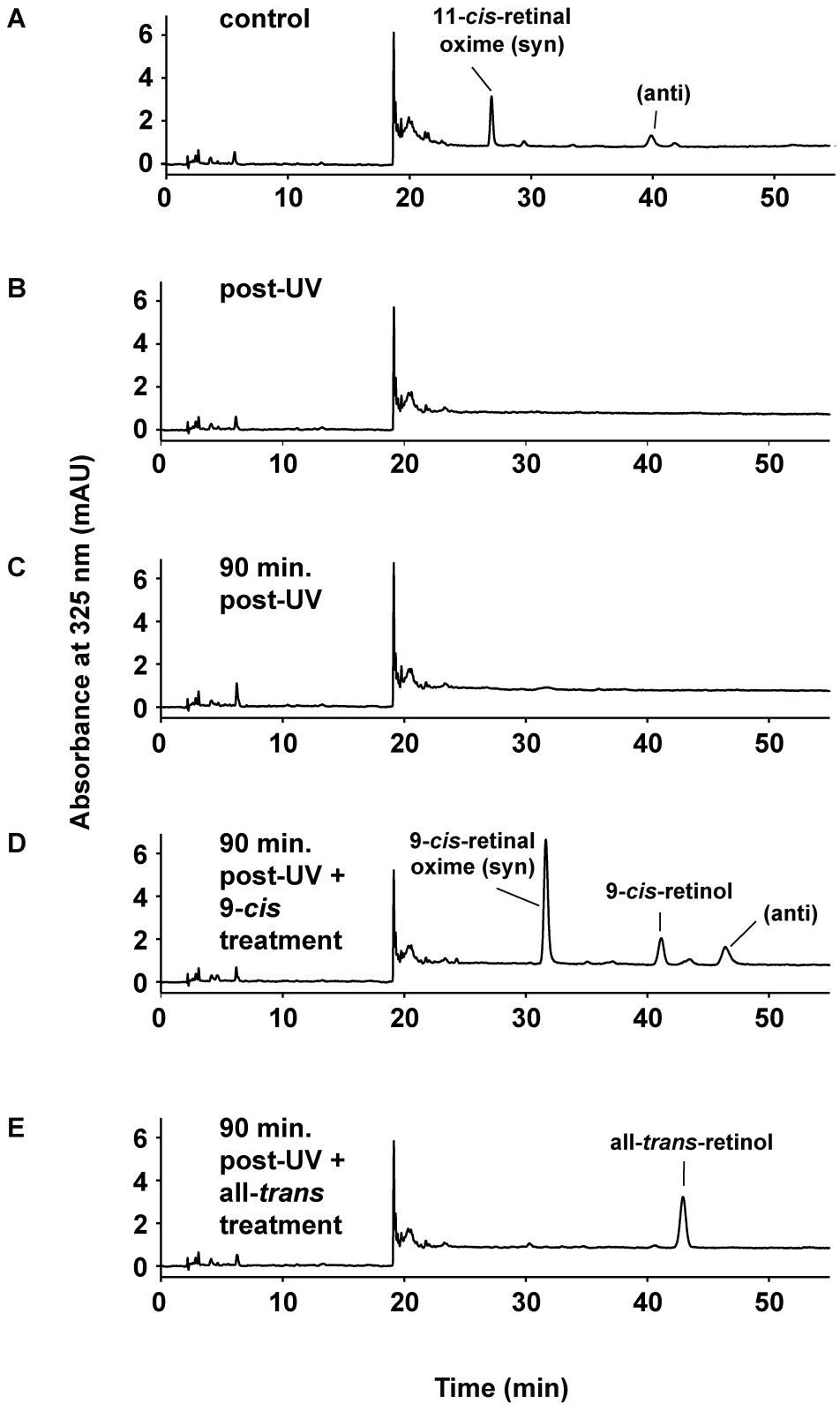
A
control
11-*cis*-retinal
oxime (syn)
(anti)
B
post-UV
C
90 min.
post-UV
D
90 min.
post-UV +
9-*cis*
treatment
9-*cis*-retinal
oxime (syn)
9-*cis*-retinol
(anti)
E
90 min.
post-UV +
all-*trans*
treatment
all-*trans*-retinol
Absorbance at 325 nm (mAU)
Time (min)

Figure 3: UV treatment decreases endogenous retinoids to below HPLC-detectable levels while exogenous retinoids are confirmed to penetrate tissue. A) One retina was taken from each of 8 P8-P10 animals, frozen and later assayed by HPLC for endogenous retinoids levels. B) The contra-lateral retina from each animal in A was exposed to 15 min of UV light, frozen and assayed by HPLC. No retinoids were detected after UV treatment. The remaining chromatograms show retinoid levels from retinas taken after UV exposure and subsequent treatment with C) vehicle (n=3), D) 100 μM 9-*cis*-retinal (n=4), and E) 100 μM all-*trans*-retinal (n=7).

Figure 4

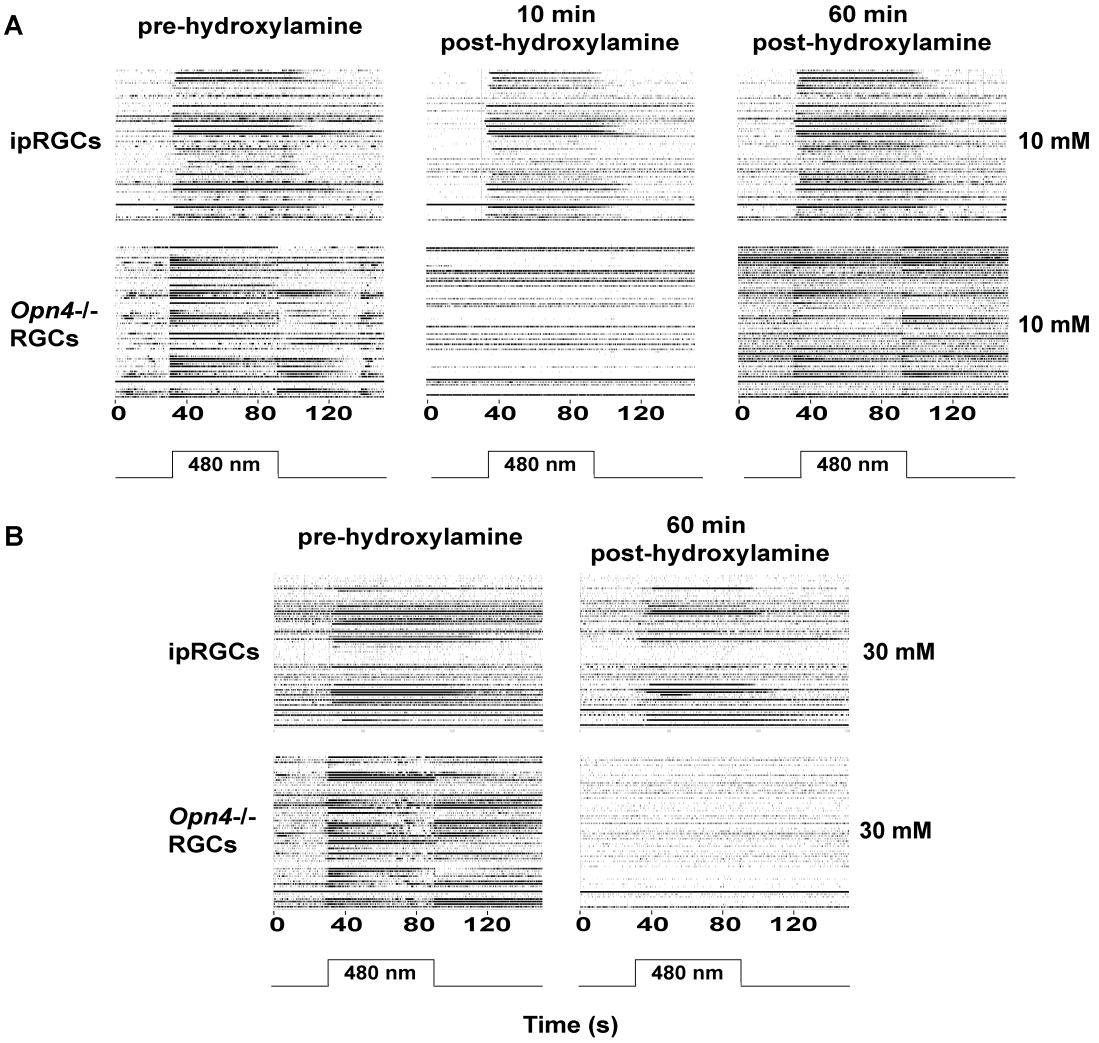
A
pre-hydroxylamine
10 min post-hydroxylamine
60 min post-hydroxylamine
ipRGCs
10 mM
Opn4-/- RGCs
10 mM
0 40 80 120
480 nm
B
pre-hydroxylamine
60 min post-hydroxylamine
ipRGCs
30 mM
Opn4-/- RGCs
30 mM
0 40 80 120
480 nm
Time (s)

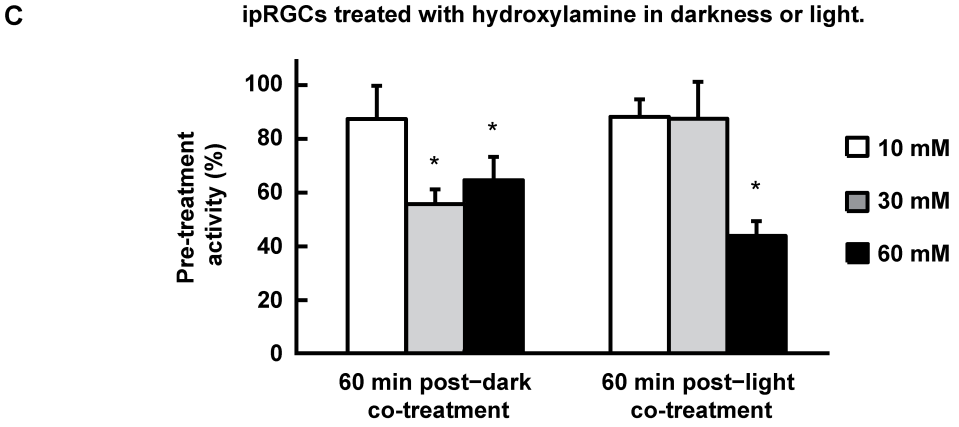
C
ipRGCs treated with hydroxylamine in darkness or light.
Pre-treatment activity (%)
100
80
60
40
20
0
*
*
*
10 mM
30 mM
60 mM
60 min post−dark co-treatment
60 min post−light co-treatment

Figure 4: ipRGCs are resistant to hydroxylamine bleaching. Raw data rasters of retinas (one retina per row) from P13-16 wildtype mice, under glutamatergic blockade to record ipRGCs, and *Opn4*$^{-/-}$ mice, to record rods and cones, treated for 15 min with hydroxylamine in the perfusate at A) 10 mM or B) 30 mM and then tested with a 1 min 480 nm light stimulus (IR 13.6) 60 min post-treatment. ipRGCs were resistant to hydroxylamine at concentrations that bleach cones. C) Cells from P8-10 wildtype mouse retinas treated with 10 mM, 30 mM and 60 mM hydroxylamine in either darkness or under 480 nm light at IR 13.6 were resistant to hydroxylamine bleaching under all sets of conditions. Error bars are SEM. Cell numbers for the treatments were 36 cells from 4 retinas for 10 mM/dark, 33 cells from 3 retinas for 10 mM/light, 35 cells from 4 retinas for 30 mM/dark, 50 cells from 3 retinas for 30 mM/light, 48 cells from 6 retinas for 60 mM/dark and 62 cells from 6 retinas for 60 mM/light. * Significantly different from pretreatment, $P<0.05$, Student's t-test, uncorrected for multiple comparisons; mean's 95% confidence interval do not include 100% activity.

Figure 5

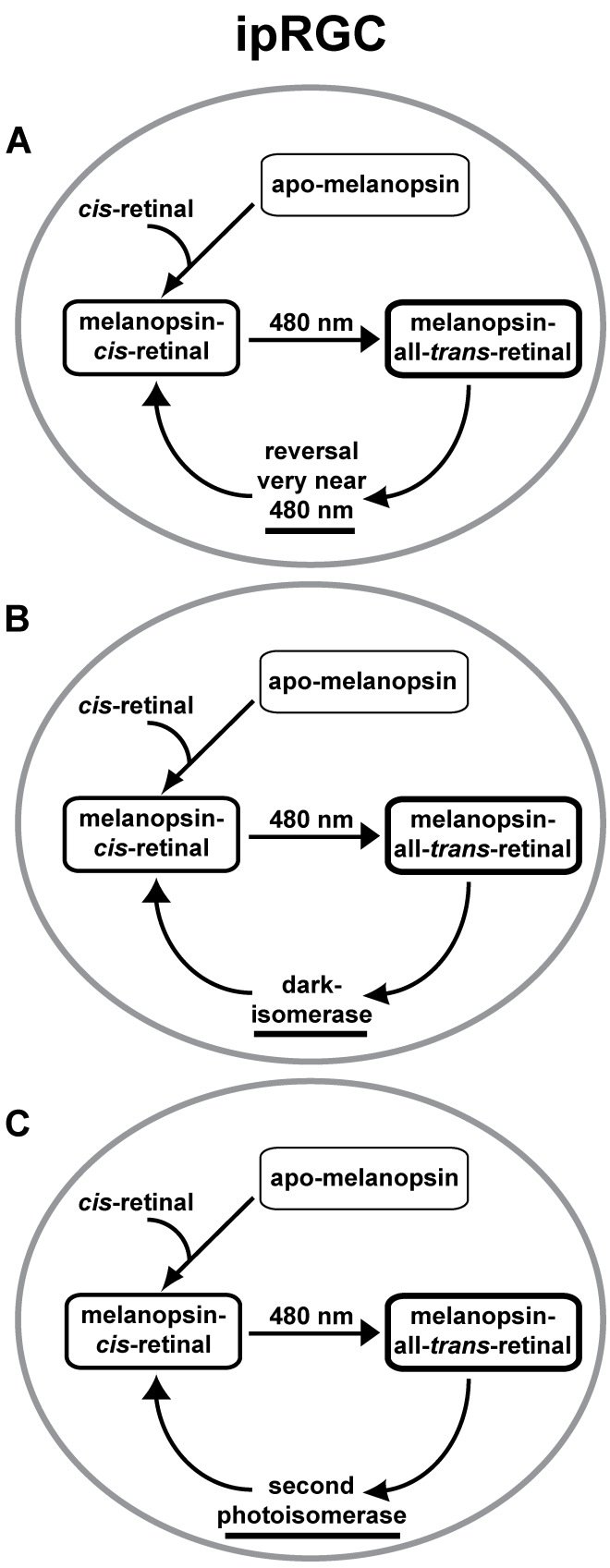
ipRGC
A
apo-melanopsin
cis-retinal
melanopsin-cis-retinal
480 nm
melanopsin-all-trans-retinal
reversal very near 480 nm
B
apo-melanopsin
cis-retinal
melanopsin-cis-retinal
480 nm
melanopsin-all-trans-retinal
dark-isomerase
C
apo-melanopsin
cis-retinal
melanopsin-cis-retinal
480 nm
melanopsin-all-trans-retinal
second photoisomerase

Figure 5: Three models for the ipRGC photocycle. In all models of the ipRGC photocycle above, apo-melanopsin can only bind the *cis* conformation of retinal but recycling of all-*trans*-retinal differs. The models are not mutually exclusive. A) After binding, melanopsin may have a bistable photocycle with a reversal wavelength so close to the forward wavelength that the two are nearly indistinguishable under normal circumstances. B) Melanopsin may also possess dark-isomerase activity that fully resets melanopsin activity to dark adapted levels. C) There may still be a photoisomerase that reisomerizes all-*trans*-retinal into 11-*cis*-retinal similar to the retinochrome in the squid.

Figure 1S

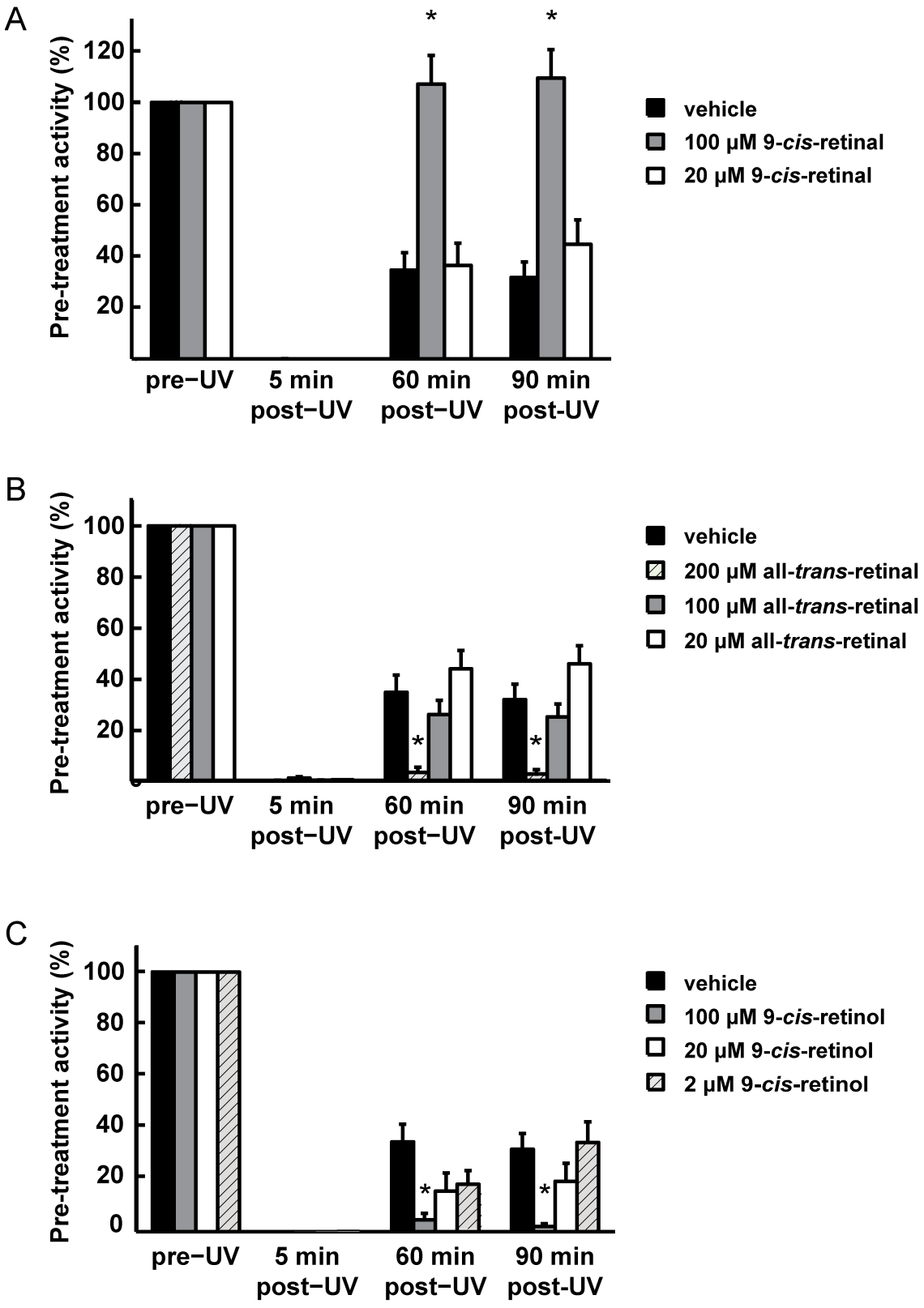
A
Pre-treatment activity (%)
120
100
80
60
40
20
*
*
pre−UV
5 min post−UV
60 min post−UV
90 min post-UV
vehicle
100 μM 9-cis-retinal
20 μM 9-cis-retinal
B
Pre-treatment activity (%)
100
80
60
40
20
*
*
pre−UV
5 min post−UV
60 min post−UV
90 min post-UV
vehicle
200 μM all-trans-retinal
100 μM all-trans-retinal
20 μM all-trans-retinal
C
Pre-treatment activity (%)
100
80
60
40
20
0
*
*
pre−UV
5 min post−UV
60 min post−UV
90 min post-UV
vehicle
100 μM 9-cis-retinol
20 μM 9-cis-retinol
2 μM 9-cis-retinol

Supplemental Figure 1: Only 100 μM 9-cis retinal restores light induced ipRGC activity. Retinas were treated with UV and either A) 9-cis-retinal, B) all-trans-retinal, or C) 9-cis retinol. Number of cells: vehicle, n=37 from 6 retinas; 100 μM 9-*cis*-retinal, n=45 from 5 retinas; 20 μM 9-*cis*-retinal, 17 channels from 3 retinas; 200 μM all-*trans*-retinal, n=18 from 3 retinas; 100 μM all-*trans*-retinal, n=37 from 7 retinas; 20 μM all-*trans*=retinal, n=19 from 3 retinas; 100 μM 9-*cis*-retinol, n=32 from 5 retinas; 20 μM 9-*cis*-retinol, n=11 from 4 retinas; 2 μM 9-*cis*-retinol, n=12 from 3 retinas.

Chapter 3: Developmental changes of the ipRGC photoresponse by age and cell subtype

This chapter is a manuscript in preparation for publication

Developmental changes of the ipRGC photoresponse by age and cell subtype.

Timothy J. Sexton[1,4], and Russell N. Van Gelder[1,2,3,4]

Departments of [1]Ophthalmology, [2] Biological Structure and [3]Pathology, and [3]Program for Neurobiology and Behavior, University of Washington, Seattle, WA 98195; and

Abstract

In adult mice intrinsically photosensitive retinal ganglion cells (ipRGCs) mediate entrainment to light and the pupillary light response, but may function in different roles in retinal and behavioral development (Johnson et al., 2010; Rao et al., 2013). There are documented changes to ipRGC photosensitivity between post-natal development and adulthood (Tu et al., 2005; Schmidt et al., 2008). Photosensitivity changes may correlate with changing roles of ipRGCs with age. Here we measure several parameters of ipRGC function between post-natal and adult wildtype mice. Melanopsin-positive cell density decreased by 40% between P8 and P15 but is unchanged thereafter. We find decreases in ipRGC maximal firing rate and off-latencies and increases in on-latencies with age. Following a 1-min light pulse and a 1-min dark period, total spiking activity recovers to 65-70% of initial activity in both P15 and P30 with full recovery taking 10-min, whereas recovery in P8 cells at the same point is 90% of initial activity with full recovery after 6-min. Similarly, ipRGCs at P15 and P30 recover only 30-40% of initial activity over the 60-min following a 1-hr light stimulus, while P8 animals recovered to 100% over the hour. P8 ipRGCs recovery is attributable mostly to Type 1 cells, with recovery reaching over 100%. Type 2 cells show a slight increased ability to recover with age whereas Type 3 cells show a decrease in recovery. Both types recover to levels lower than P8 Type 1. The difference in Type 1 suggests a unique role for this cell during early post-natal development

Introduction

Mammalian retinas contain three types of photoreceptors that currently account for all visual and non-visual photoreception (Hattar et al., 2003). These are rods, cones and melanopsin expressing intrinsically photosensitive retinal ganglion cells (ipRGCs). Rods and cones form active synapses and convey light responses to bipolar and consequently ganglion cells in mouse starting around post-natal day 10 (P10) (Fisher, 1979; Sernagor et al., 2001). In contrast, ipRGCs produce light responses at the time of birth, making them the earliest functional photoreceptors in mammals (Fahrenkrug et al., 2004; Sekaran et al., 2005; Tu et al., 2005). Recent work has suggested new roles for ipRGCs in development. Anatomically, melanopsin dependent photoreception influences the development of retinal vasculature (Rao et al., 2013), and the segregation of retinogeniculate projections (Renna et al., 2011). The later is thought to be a consequence of ipRGC involvement in retinal wave modulation (Renna et al., 2011; Kirkby and Feller, 2013). Behaviorally, knocking out melanopsin has shown that melanopsin mediates negative phototaxis (Johnson et al., 2010) and its accompanying vocalizations (Delwig et al., 2012), the earliest document light responses in mice, occurring between post-natal days 6 and 9 (P6-P9). These functions are different from those known to be subserved by ipRGCs during adulthood, namely circadian entrainment and the pupillary light reflex (PLR) controlled by the suprachiasmatic nucleus (SCN) and the olivary pretectal nucleus (OPN), respectively (Panda et al., 2002; Hattar et al., 2003; Panda et al., 2003). These newly described functions occur during a developmental period in which projections to the SCN and OPN are either not measurable or minimal (McNeill et al., 2011).

Differences in photosensitivity between post-natal and adult ipRGCs have been reported previously (Tu et al., 2005; Schmidt et al., 2008), but have not been systematically studied. Here we follow several measurements of ipRGC light responses over the course of post-natal development and find a general decrease in photosensitivity and the ability to recover from both short and long exposures of light with increasing age. Following long light exposures, ipRGC subtypes of both post-natal and adult mice display differences in the ability to recover responses.

Methods

Tissue preparation

For analysis of ipRGC responses, multi-electrode array recordings were obtained from retinas of C57BL/6 mice (Jackson Laboratories, Bar Harbor, ME) at ages P8-P10 (P8) or P15-20 (P15) and P30-P35 (P30). Animals were maintained in a 12:12-hr light-dark cycle. All experiments were performed in accordance with Association for Research in Vision and Ophthalmology guidelines for animal studies, under an approved animal study protocol at the University of Washington.

All procedures were performed under dim red light illumination. Mice were euthanized by CO_2 narcosis and cervical dislocation. Isolated mouse retinas were cut in half, positioned with the vitreal face in contact with a multielectrode array (MEA) (Multi Channel Systems, Reutlingen, Germany) and superperfused (2-3 ml/min) with a bicarbonate-buffered physiologic solution (125 mM NaCl, 2.5 mM KCl, 1 mM $MgCl_2$, 1.25 mM NaH_2PO_4, 20 mM glucose, 26 mM $NaHCO_3$, 2 mM $CaCl_2$, 500 μM glutamine) oxygenated with 95% O_2/5% CO_2 to obtain a pH of 7.4. The temperature of both perfusate and tissue chamber was maintained at 33.0^{o}C. For ipRGC recordings from P8-10 mouse retinas, spontaneous retinal waves (Wong et al., 2000)(as well as any possible input from rod and cone photoreceptors), were suppressed by using glutamatergic [50 μM d(2)-2-amino-5-phosphonopentanoic acid (d-AP5); 20 μM d(-)-2-amino-4-phosphonobutyric acid (d-AP4), 10 μM CNQX] and cholinergic (5 nM epibatidine) inhibitors (Tocris Biosciences, Ellisville, MO). For ipRGC recordings from P15-35

mouse retinas, only glutamatergic blockade was used (200 μM d-AP5, 100 μM d-AP4 and 80 μM CNQX).

Multi-electrode recordings

Electrophysiological recordings were performed using planar arrays of 60 electrodes (30 μm diameter, 200 μm inter-electrode spacing; Multi Channel Systems, Reutlingen, Germany). Raw electrical signals were amplified, filtered, and digitized through an A/D card (National Instruments, Austin, TX), written to disk and analyzed off-line, as described previously (Holy et al., 2000). Retinas were stimulated with a Xenon light source (Sutter Instruments, Novato, CA) fed through a liquid light guide and diffusing filter (Thorlabs Inc., Newton, NJ). Intensities and wavelengths of light were adjusted via neutral density and narrow band-pass 480 nm interference filters (Thorlabs, Inc., Newton, NJ) and calibrated with a radiometer (Advanced Photonics International, Fairfield, CT). Light stimuli were delivered by a computer-controlled shutter (Vincent Associates, Rochester, NY).

Light Stimulation Protocols

For short-term bleaching/adaptation experiments, retinas were exposed to a 1-min, 480 nm light stimulus at 3.98 x 10^{13} photon cm^{-2} s^{-1} (IR 13.6) followed by recovery intervals of 1 to 10-min and then a second 1-min light test. Age specific response dynamics were assessed from the first light exposure of each retina in the 1-min

experiment. For long-term bleaching/adaptation experiments, retinas were exposed to a 1-hr, continuous 480 nm light stimulus IR 13.6 and allowed to recover in darkness for 1-hr. Activity over the 1-hr exposure was monitored continuously but analyzed in 1-min blocks taken every 5-min. Beginning 10-min into the recovery period and every 10-min thereafter, a 1-min test stimulus of the same light was administered to access recovery.

For experiments involving retinoid supplementation, 9-*cis*-retinal (Sigma,St. Louis, MO) was dissolved in acetonitrile, aliquoted and dried under argon for storage at -70 °C. For each experiment 9-*cis*-retinal was freshly resuspended in ethanol. Perfusion of retinas was performed as described previously (Sexton et al., 2012b). Briefly, retinas were superperfused for 25 to 30-min with 9-cis-retinal in a non-carbogenated HEPES/bicarbonate-buffered physiologic solution (10 mM HEPES, pH 7.4, 125 mM NaCl, 2.5 mM KCl, 1 mM $MgCl_2$, 1.25 mM NaH_2PO_4, 12 mM glucose, 26 mM $NaHCO_3$, 2 mM $CaCl_2$, 500 μM glutamine) with 1% ethanol as a carrier, mixed with carbogen bubbled bicarbonate-buffered physiologic solution at a 1:1 ratio, just prior to tissue delivery. Retinas were then returned to purely bicarbonate-buffered physiologic solution for 10 minutes and tested for light evoked activity

Immunohistochemistry

Retinas for melanopsin immuno-staining were fixed overnight in 4% paraformaldehyde and blocked overnight in 5% donkey serum, 2mg/ml BSA, 0.3% Tx-100 in PBS. The retinas were incubated with primary antibody for 3 nights at 4° C, using a custom made polyclonal rabbit anti-mouse melanopsin antibody targeting the N-

terminus. Secondary antibody incubation was overnight at 4° C with a 568 Alexa secondary antibody (Invitrogen). Immuno-positive cells were counted using a microscope with a 20X objective and epi-fluorescence. The field of view was measured with a micrometer. A region (area=0.96 mm^2) was sampled from each of the four quadrants of the retinas, with each region centered 1 mm from the optic disc. Cell densities were averaged across 5 retinas of each age (P8, P15, and P30). Retinas used for Brn3a immunolabeling were fixed for 1-hr in 4% paraformaldehyde and blocked overnight. Retinas were then labeled using a Brn3a primary antibody (SC-31984, Santa Cruz Biotechnology, Santa Cruz, CA) as for melanopsin labeling. For each of 5 retinas, four images of 0.58 mm^2 were taken with a Hamamatsu digital camera (Hamamatsu Photonics K.K., Hamamatsu City, Japan) using Metamorph software (Molecular Devices, San Diego, CA). Cell counts were done by hand using the Cell Counter plug-in of Image J (NIH)

Analysis

Data processing and analysis was done using custom MATLAB scripts (Mathworks, Natick, MA). Statistical analysis of 1-min and 1-hr recovery data was done with SPSS (IBM, Armonk NY) using a linear mixed model (LMM) instead of traditional univariate/multivariate repeated measures ANOVA for longitudinal/time sequence datasets. LMM incorporates a combination of a fixed variable, a random variable, and random error to each group to derive a linear model. Parameters for the fixed and random variables are derived from maximum likelihood estimates based on the data.

Group models are then compared for differences in parameters. A LMM was used in the 1-min recovery experiment because of missing data in repeated measures assessment, which violates ANOVA data structure requirements. Data for individual cells in the P15 and P30 ages did not cover all intervals tested because of the limited ability of adult ipRGCs to recover fully after multiple closely spaced light exposures. Recovery levels to the same recovery interval could drop several tens of percent if performed after 3 or 4 trials. For the 1-min analysis fixed effects were age, time, and the age by time interactions, while random effects were time and intercepts subjects. A LMM was used for 1-hr recovery data because of non-normality caused by driving cells to zero output and allowing cells to recover. Traditional non-parametric multivariate analysis requires balanced sample size, which is not the case in our data because of the large proportion of Type 1 cells in P8 animals. In analyzing recovery data by age only fixed effects were age, time, and the age by time interactions, while random effects were intercepts for subject and covariance. When analysis was done by age and cell subtype, two types of analyses were done. In the first, age was held constant, in which case the fixed effects were subtype, time, and the subtype by time interactions, while random effects were intercepts for subjects. In the second, subtype was held constant, in which case the fixed effects were age, time, and the age by time interactions, while random effects were intercepts for subjects. Alpha levels for multiple comparisons were adjusted using Bonferronni corrections in the LMM and when making more than 3 comparisons elsewhere. Non-normal data are plotted in boxplots (whisker plots) with outliers plotted individually if they are greater than 2.7 standard deviations from the mean, assuming a normal distribution. Data were not interpreted as being from a normal distribution.

Categorizing ipRGC subtypes was done as previously described (Tu et al., 2005) with modifications to reduce light exposure prior to recovery experiments. Subtyping measurements were made at the beginning of experiments. P8 cells were first divided into cells with on-latencies (time from light on to time of maximal firing) less than 12-sec (Type 3 cells) and greater than 12-sec (Type 1 cells) in response to a 1-min, 480 nm light at 1.0×10^{12} photon cm^{-2} s^{-1} (IR 12). Those cells with a light response at IR 13.6 but no light response at IR 12 were categorized as Type 2 cells. In older animals, cells with on-latencies of less than 12-sec in response to a 1-min, 480 nm light at 1.0×10^{13} photon cm^{-2} s^{-1} (IR 13) were designated Type 3 cells and while those with on-latencies greater than 12-sec were Type 2 cells (Table 1).

Table 1. ipRGC functional subtype categorization.

	Type 1	**Type 2**	**Type 3**
P8	On-latency > 12-sec at IR 12.6 Light response at IR 12.6	Light response at IR 13.6 but not 12.6	On-latency < 12-sec at IR 12.6
P15 and P30 (Adult)	Not present	On-latency > 12-sec at IR 13	On-latency < 12-sec at IR 13

Results

ipRGC Density

The number of ipRGCs measured by melanopsin immunopositivity decreased by ~40% between P8 and P15 (means 90 ± 5 cells cm^{-2} and 54 ± 3 cells cm^{-2} respectively, n=20 each ; P<0.005, One-way ANOVA) but remained stable between P15 and P30 (means 54 ± 3 cells cm^{-2} and 50 ± 3 cells cm^{-2} respectively, n=20 each)(Figure 1B). This decrease in melanopsin cell density is consistent with those seen previously (Sekaran et al., 2005) and with other melanopsin cell density estimates (Ruggiero et al., 2009; Hughes et al., 2013). To determine if this change could be explained by age dependent retinal growth, a Brn3a antibody was used to quantify a large subset of RGC (Badea et al., 2009; Shi et al., 2013) at the three ages studied. Cell density means were 4005 ± 95 cells cm^{-2} for P8, 3824 ± 93 cells cm^{-2} for P15, 3168 ± 67 cells cm^{-2} for P30 (n=20 each). Between P8 and P15 a statistically significant decrease of 12% was seen in staining (P<0.005, One-way ANOVA). By P30, the decrease from P8 was 27%, or a 17% decrease from P15 (Figure 1B)(P<0.005, One-way ANOVA). When cell density numbers are multiplied by retinal area measurements (P8 area~11.5 mm^2, P15 area~13 mm^2, P30 area~15 mm^2 (Coombs et al., 2007)), total cell numbers are 49,497; 51,124; and 49,964 for the three ages or roughly 90% of total RGCs estimates (Williams et al., 1998). Density decreases in ipRGCs was thus much greater and occurred earlier than would be expected from retinal growth. If the same calculations are made for melanopsin-positive cell densities, the numbers are 1035, 742, and 775 for P8, P15 and P30 respectively, or a is a 28% decrease from P8 to P15, indicating that only a quarter of the 40% decrease in melanopsin cell density is attributable to age-related growth.

Light Response Dynamics

As animals aged from early post-natal to adult stages, changes occurred to many measures of the response to a 1-min 480 nm light stimulus at 3.98 x 10^{13} photon cm^{-2} s^{-1} (IR 13.6). Statistically significant changes occurred in the on-latency (time from lights on to maximal firing), maximal firing, off-latency (time from lights off until cells stopped firing for 5-sec) (Figure 2A) and the total spike number elicited from the light exposure. No significant changes with age were found in total spike number elicited during the light stimulus, initial spikes (first 30-sec of the 1-min stimulus), steady-state spikes (last 30-sec of the 1-min stimulus) although the parameters showed a trend of decreasing values with increasing age.

On-latency medians increased from 6-sec at P8 to 9.5-sec at P15 and 9.0-sec at P30 animals. Off-latency medians decreased from 67-sec in P8 to 17.5-sec at P15 and 15.5-sec at P30 (Figure 2). For both of these parameters P8 vs. P15 differences and P8 vs. P30 differences were significant ($P>0.05$, Kruskal-Wallace) but P15 vs. P30 differences were not. Median maximal firing was 18 Hz, 16 Hz, and 11.5 Hz for P8, P15 and P30, respectively. Only the difference between P8 and P30 was significant ($P>0.05$, Kruskal-Wallace). As suggested by the change in off-latencies and maximal firing, the total number of spikes elicited by the 1-min stimulus differed with age. Medians were 966, 630 and 410 spikes for P8, P15 and P30, respectively. All differences were significant ($P>0.05$, Kruskal-Wallace,). At all ages this leads to a significant difference in the number of total spike number occurring only during the light stimulus as a percentage of

total spikes elicited by the light stimulus (P8 median = 67%, range 15-100%; P15 median=89.5%, range 65-100%; P30 median = 94.8%, range 80-100%; P>0.05, Kruskal-Wallace)

Recovery from 1-min bright light exposure

Melanopsin cell responses decrease in response to short bright light exposures but recover over several minutes, with lower recovery levels and longer recovery times with increasing age. However, recovery time increased with age. Cells from P8 animals recovered 90% of total spikes elicited during the initial 1-min light exposure after a one minute recovery period and recovered completely by 6-min. Cells from P15 and P30 animals recovered only 60-70% of total spiking by 1-min recovery and required 6-10 minutes to recover fully (Figure 3B). Differences between P8 and P15 and P30 were statistically significant up to the 5-min recovery point. Changes in maximal firing and off-latencies mirrored those of total spiking. On-latencies for P8 cells remained close to 100% for all intervals while P15 and P30 cells decreased from a mean of 150% (longer latencies) to 100% by 10-min (data not shown). During 1-min recovery experiments, ipRGCs from older animals recovered to much lower levels after 3 to 4 recovery intervals, recovery dropping by several tens of percent. This was true even with a 15-min dark "rest" time between interval tests. Such a decrease was never observed in P8 cells. Because of this, cell responses at P15 and P30 were discarded after 4 recovery intervals. As a consequence sample sizes for each recovery time points were not the same.

Recovery from 1-hr bright light exposure

Melanopsin cell responses decrease in response to long bright light exposures and recover quickly in young animals but very slowly in older animals. Similar to the differences seen in recovery from short light exposures, changes were seen in recovery measurements after a 1-hr light exposure between P8 and P15 and P30 (Figure 4A, 4B and 4C). At all ages a slow decrease in total spiking was seen over the first 20-min of the 1-hr exposure. By 30-min, most cells ceased firing. A small number of cells continued to fire throughout the hour in all ages as is expected given that some ipRGCs can fire continuously to a 10-hrs light stimulus (Wong, 2012). Recovery was monitored for 1-hr with 1-min test stimuli of the same light every 10-min. After 10-min recovery P8 ipRGCs recover to a median of 80% of the total spiking in the first minute of the 1-hr exposure (starting spikes) and plateaued at a median of 100% of baseline for the remainder of the hour. In contrast, ipRGCs from P15 and P30 animals did not recovery significantly after 10-min. In P15 animals, recovery plateaued to a median of 30% of starting spikes while the median in P30 animals remained at zero with the 75% quartile of the distribution reaching 40% recovery of starting spikes over the 1-hr recovery. Maximal firing rate (Figure 5B), initial spikes and steady-state spikes (Figure 6A and 6B) all significantly decreased in their fractional recovery (percent recovery) of values from the beginning of the 1-hr light exposure between P8 and P15 but not between P15 and P30. However values continued to decrease in P30 animals. On-latencies were significantly longer in P15 and P30 than in P8 ipRGCs at all time points (Figure 5A), with an increase over initial values of up to 3-fold at P8 but 4 to 5-fold in P15/P30 ipRGCs. Off-latencies decreased substantially in P8 animals from a median of 67-sec to

only 20-sec after the 1-hr exposure (Figure 5C). A similar decrease is seen in P15 and P30, with many values becoming negative, indicating cells stopped firing before the light stimulus ceased or did not fire at all during the second stimulus.

Bleaching vs. Adaptation

In Chapter 2, P8 ipRGC pigment was shown to be difficult to bleach. However, changes in chromophore availability and thus susceptibility to bleaching may change over development. This was of concern in light of the many changes in ipRGC responses seen with age. To test whether the differences in recovery between age groups was attributable to changes in bleaching susceptibility or to changes in light/dark adaptation, ipRGCs from P30 animals were exposed to either 9-*cis*-retinal to reverse bleaching (Sexton et al., 2012b), or a ten-fold increase in light intensity to test for sensory adaptation during the 1-hr recovery period. Treatment with 9-*cis*-retinal did not increase recovery levels above vehicle control (1% ethanol in AMES) or untreated cells at the 60-min recovery point (Figure 4D and 4F). Increasing light intensity at 40, 50 and 60-min increased percent recovery over control at all three times points. The 60-min comparison point was significantly higher than control ($P<0.05$, Mann-Whitney rank sum). The falling recovery levels at 50 and 60-min suggests that cells were undergoing additional light adaptation in response to the increased light intensity. Taken together, these results suggest that changes in cell firing, following bright light exposure, was due to adaptation rather than bleaching.

Recovery of ipRGC subtypes from bright light exposure

When cells were categorized into subtypes according to on-latency and photosensitivity levels (see methods), differences were seen in the responses and recovery of individual ipRGC subtypes. In P8 animals the majority of Type 1 cells (n=45), with long on-latency and high photosensitivity, stopped firing by 20-min light exposure but a subset continued firing either throughout the 1-hr exposure non-stop (9%) or throughout with intermittent pauses (11%) (Figure 7A). Over the hour of recovery, Type 1 cells regained a median value of 100% of starting spikes, with a few cells reaching up to 175%. Type 2 cells (n=8), with long on-latency and low photosensitivity, generally stopped firing by 10-min of light exposure (Figure 7B). Median recovery of Type 2 cells remained at zero throughout the hour with 2 cells recovery a few percentage points by 50 and 60-min recovery. The one exception was one cell that recovered a moderate 30-40% over the 1-hr recovery time. The majority of type 3 (n=7), short on-latency and high photosensitivity, cells stopped firing by 20-min exposure (one out of 7 cells continued to fire throughout the hour) and recovered to a median of 50-70% over the hour monitored (Figure 7C).

On-latency recovery (Figure 8A) approached pre-exposure levels in Type 1 and Type 3 cells, although Type 3 cells had a broader distribution than Type 1. Type 2 cells had very long on-latencies that did not begin to recover until the end of the hour (non-firing cells were assigned on-latency values of 75-sec, well beyond any possible light induced response). Maximal firing levels during recovery were nearly indistinguishable in Type 1 and 3 cells, reaching 50-60% of pre-exposure levels (Figure 8B). Type 2 cells had only marginal recovery. Off-latencies of Type 1 and 3 cells were again indistinguishable over

recovery with median values of 20-sec. Type 2 cells displayed mostly negative values, indicating the cells stopped firing before the light ended (Figure 8C).

Despite the fact that maximal firing levels were the same in Type 1 and 3 cells, Type 1 cells were able to recover a much higher degree of pre-exposure spiking. This is explained by analyzing the initial spike recovery and steady-state spike recovery (Figure 9A and 9B) in which Type 1 cells recovered 90% of initial spikes and 140% of steady-state recovery. For all recovery measurements, only Type 2 cells had significantly different responses. Even with the high total spikes recovery in Type 1 cells, the sample size of Type 3 cells (n=7 or 13% of total P8 cells) may have been below levels that could produce a detectable a significant difference between types 1 and 3.

For the purpose of analysis, subtypes from P15 and P30 retina were combined to obtain adequate sample sizes of n=13 for Type 2 and n=12 for Type 3. This combination was suggested by the lack of statistically significant differences in all measures obtained between cells at P15 and P30 as described earlier. Post eye-opening Type 2 and 3 cells were similar to each other in all recovery measurements. Most cells stopped firing after 20-min light exposure but a subset continued firing either throughout the 1-hr exposure non-stop (Type 2 = 23%, Type 3=16%) or throughout with intermittent pauses (Type 2 = 23%, Type 3=15%). Median recovery of total spikes, initial spikes and steady-state spikes showed a trend toward lower values in Type 2 than in Type 3 cells but were not statistically significant. Within the same subtype, differences were found with age. Type 3 cells showed a significant decrease in recovery in maximal firing, off-latency (Figure 8), total spikes, initial spikes and steady-state spikes (Figure 9). This suggests an increase in adaptation with age. Type 2 cells only differed significantly with age in on-latency, but in

all other measurements there was a trend toward higher recovery levels. The small sample size of P8 Type 2 cells (n=8, or 13% of total P8 ipRGCs) mostly likely reduced the ability of the linear mixed model analysis to detect smaller differences (see methods). Despite this, all changes in Type 2 cells taken together, suggest a small increase in sensitivity between post-natal and adult ages. A small increase in sensitivity was also seen in the irradiance response curves of P8 versus P30 Type 2 cells in the work of Tu et al., (2005). Off-latency recover appeared to be an exception to the trend of decreased sensitivity with age. Median off-latencies in P15/P30 ipRGCs are 15 to 17-sec. During the 1-hr recovery, adult Type 2 and Type 3 cells recover to those values within 30 to 40 minutes. Median P8 off-latency is 67.5-sec. After 1-hr recovery, P8 Types 1 and 3 cells never recovered to medians greater than 20-sec. P8 Type 2 cells stop firing before the light stimulus ends.

Discussion

Several lines of evidence here indicate a general decrease in ipRGC number and photosensitivity with age, primarily between P8 and P15. Additionally, over this same period, changes in light and dark adaptation were observed that were specific to ipRGC functional subtype as well as age.

ipRGC density changes

Melanopsin immuno-positive cell density decreased by approximately 40% over the ages studied. Densities for P15/P30 correspond very closely to values found previously (Sekaran et al., 2005). In that study, an approximately 70% decrease was seen in melanopsin immuno-positive cells from P4 to P14. They did not measure general RGC changes over time, but noted the decrease corresponds well with the decrease in all RGCs over that period found in other studies (Strom and Williams, 1998). More recently Chen et al. (Chen et al., 2013) showed a more modest 50% decrease in the number of genetically labeled ipRGC between P3 and P9. They also found no difference in genetically marked ipRGC numbers between P9 and adulthood.

The decrease in cell number seen here could be the result of continued apoptosis at P8, even though Brn3a data suggests apoptosis has ended by P8. Since ipRGCs do not express Brn3a (Quina et al., 2005; González-Menéndez et al., 2011; Shi et al., 2013), apoptosis cannot be ruled out. However, apoptosis is inconsistent with MEA data. No decrease in the number of recordable cells is observed over the P8 to P10 ages, which includes ages in which ipRGC specific apoptosis is absent (Chen et al., 2013). Decreases seen here could be explained by decreased melanopsin expression. Expression levels are dynamic in response to lighting conditions, leading to changes in the number of detectable melanopsin immuno–positive cells (González-Menéndez et al., 2010).

Currently, 5 anatomically defined ipRGC subtypes have been described (Sexton et al., 2012a; Hu et al., 2013). It is also known that adult M4 and M5 ipRGC subtypes do not express melanopsin levels high enough to be detected by standard immunochemistry

(Ecker et al., 2010). Our data may reflect a decrease in melanopsin expression in M4 and M5 cells from higher P8 levels to adult sub-detection levels. However, the nearly 10-fold fewer ipRGCs recordable at P15/30 (~2-3 ipRGCs per retina) vs. P8 (~20 ipRGCs per retina) is not fully explained by decreases in ipRGCs seen here. The relatively small changes in absolute numbers seen here may alter ipRGC spacing to be less compatible with standard MEA electrode placement and separation distance. A more thorough study of cell numbers over these ages would be needed to answer this question. Other antibodies and more sensitive ICH techniques may be helpful as our numbers reflect only half of the number of adult melanopsin cells found in recent studies (Ecker et al., 2010; Hughes et al., 2013).

Age specific ipRGC light response recovery

Changes in on-latency, maximal firing rate, off-latency, and total spikes, correspond to increasingly lower sensitivity levels, consistent with the results of Tu et al. (2006). In response to 1-min light exposures, cell firing is more depressed and requires longer to recovery with increasing age. Upon long, 1-hr exposures most cells stop firing by 20-min but a few remain active throughout the hour regardless of age and subtype. Upon dark recovery, P8 cells recover more quickly and more fully compared to P15 and P30 cells. In particular, P8 Type 1 cells recover to above original levels of firing, suggesting sensitization.

Accompanying decreases in light sensitivity indicated by changes in on-latency, maximal firing and off-latency, changes occurred in the ability of ipRGCs to recover

responses following light exposure. After 1-min exposures, cells from older animals had lower initial percent spike recovery and longer times to full recovery than cells from younger animals. Similar recovery times for older animals were seen by Do and Yau (Do and Yau, 2013). It is unlikely that the age dependent decreases in light responses reflects bleaching of melanopsin as mounting evidence confirms melanopsin is a bistable pigment (Matsuyama et al., 2012) and highly resistant to bleaching (Sexton et al., 2012b). An increased light adaptation in older animals is more likely given that 9-*cis*-retinal supplementation does not increase recovery at the 1-hr light exposure where bleaching is much more likely. Additionally, adult ipRGCs are less able to recover from 1-min light exposures spaced less than 10-min apart. Therefore, some element of recovery not directly related to spike number recovery continues to function over much longer times.

Changes in the responses following a 1-hr light exposures are more dramatic. P8 cells recovered to 100% of initial activity after only 20-min while P15 and P30 cells recovered to only 30-40% by the end of the full 1-hr recovery period. As the melanopsin photocycle is centered upon a bistable mechanism (Matsuyama et al., 2012), the differences observed in recovery in this study raised the possibility that chromophore recycle and availability changed with age, possibly as a consequence of fully functioning rods and cones acting as sinks for available 11-*cis*-retinal in older animals. An absence of additional recovery after 9-*cis*-retinal supplementation argues against such changes. Instead, a difference in long acting adaptation mechanisms is likely to explain the change with age, as suggested by increased recovery in older animals upon exposure to 10-fold brighter light. Such a long period of recovery is consistent with the work of Wong et al.,

(Wong et al., 2005) who showed that ipRGCs can take 3-hrs to dark adapt after brief light exposures.

Subtype specific ipRGC light response recovery

When cells were functionally categorized as done previously by Tu et al., (2005)(Tu et al., 2005), the majority of age specific changes was attributable to P8 Type 1 cells. These cells had high levels of spike recovery, with initial spikes (spikes during the first 30-sec of the 1-min stimulus) reaching 90% and steady-state spikes (spikes during the last 30-sec of the 1-min stimulus) reaching 140% and higher, suggesting sensitization. This suggests adaptation in Type 1 cells differs from that in other subtypes.

The only measure in which ipRGCs recovered more poorly in P8 animals than in adults was in off-latency times. P8 cells never recover to full pre-exposure off-latency times while older cells do. With age, a difference in the mechanism controlling only the off-latency appears to change, as opposed to mechanisms controlling a decrease from maximal firing during light exposure. These mechanisms can be differentiated from one another since their outcomes upon recovery move in different directions in P8 cells. That is, steady-state spike number increased over pre-exposure levels while off-latency times never recovered to pre-exposure levels. Nearly the opposite was seen in older animals.

Schmidt et al.(Schmidt and Kofuji, 2009) postulate that the anatomically defined M1 and M2 cells correspond to the functionally defined Type 3 and Type 2 cells of Tu et al. (Tu et al., 2005), based on the 10-fold higher photosensitivity and higher peak firing rates

of M1 and Type 3 cells over both M2 and Type 2 cells. This correspondence seems likely. A morphological correlate of Type 1 cells is lacking, however. M3 cells are unlikely candidates as they are relatively rare and their light response is like M2 cells and therefore Type 2 cells (Schmidt and Kofuji, 2011). Possibly pre-eye opening M4 and M5 cells correspond to Type 3 cells. As Type 3 cells are not present after eye-opening, they could correspond to cells lost during the decrease in melanopsin immuno-positive cells discussed earlier. A decrease in melanopsin immunopositivity could lead to a change in response characteristics or lose of photosensitivity. Type 2 cells seem to gain in some measures of sensitivity with age, presumably from an increase in melanopsin expression. A previous quantification of rat ipRGC subtype M1 and M2 numbers over development found no changes in M1 cells but a slight increase in M2 cells at an age that can only be explained by increased melanopsin expression (González-Menéndez et al., 2010). M2 cells are known to project to the OPN core (Baver et al., 2008). While work showing the timing of PLR onset at P10 corresponds to the innervation of the PLR shell by M1 projections (McNeill et al., 2011), an increase in M2 (Type 2) sensitivity may also contribute to adult PLR.

The fact that P8 Type 1 cells behave differently from other subtypes suggests it underlies a separate, distinct function. Its lack of adaptation could benefit necessary developmental functions such as spontaneous wave modulation in neonates. Changes to long-term light exposure responses in Types 2 and 3 cells, while present are incremental and in-line with a continuous but less sensitive response in adults.

Previous work by Wong et al. (Wong et al., 2005) demonstrated ipRGC adaptation responses similar to those seen in other photoreceptors. Here we extend that work to the

adaptation of the functional output of ipRGCs instead of direct measurements of photocurrents. This is an important measurement, demonstrating how melanopsin mediated outputs to targets like the SCN and OPN may change with light histories consistent with prolonged daily exposure experienced outside of experimental procedures. Our data demonstrate that functional adaptation in most ipRGCs can be profound and long lasting. Those cells that continued to fire throughout the 1-hr light exposure showed relatively low levels of adaptation, recovering to high values. Interestingly, those cells that continued firing throughout the hour occurred in all cell types and ages except P8 Type 2 cells. Having only a small number of cells of all subtypes that fire continuously with little adaptation, suggests that continued activation of downstream targets may decrease the input requirements of those targets, requiring only minimal input for sustained function. Finally, the work of Wong et al (Wong, 2012) shows that some rat ipRGCs can fire continuously in response to a 10-hr light stimulus and respond dynamically to changes in light intensity over that period. It would be of interest to see if a similar RPE attached preparation could decrease the adaptation of cells seen here, even though direct retinoid supplementation could not. This apparent difference between the studies may instead indicate inherent differences between mouse and rat ipRGCs.

Figure 1

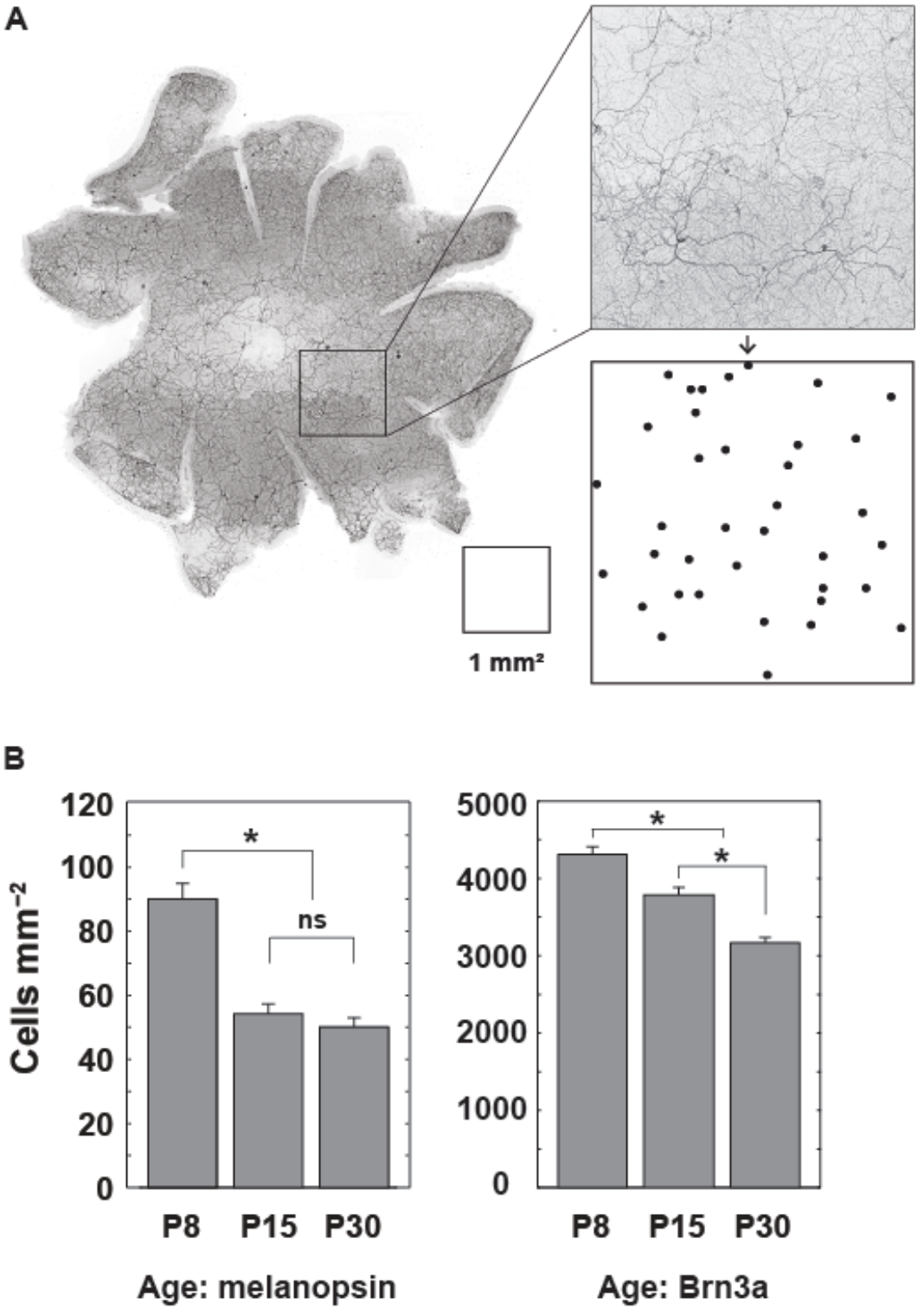
A
1 mm²
B
Cells mm⁻²
120
100
80
60
40
20
0
*
ns
P8
P15
P30
Age: melanopsin
5000
4000
3000
2000
1000
0
*
*
P8
P15
P30
Age: Brn3a

Figure 1

Melanopsin positive cells decrease in density with increasing age. A) Representative melanopsin immuno-staining in P30 retina from which density estimates were made. B) Average densities of melanopsin positive cell or Brn3 positive cells in P8, P15 and P30 (n=20 for each age)

Figure 2

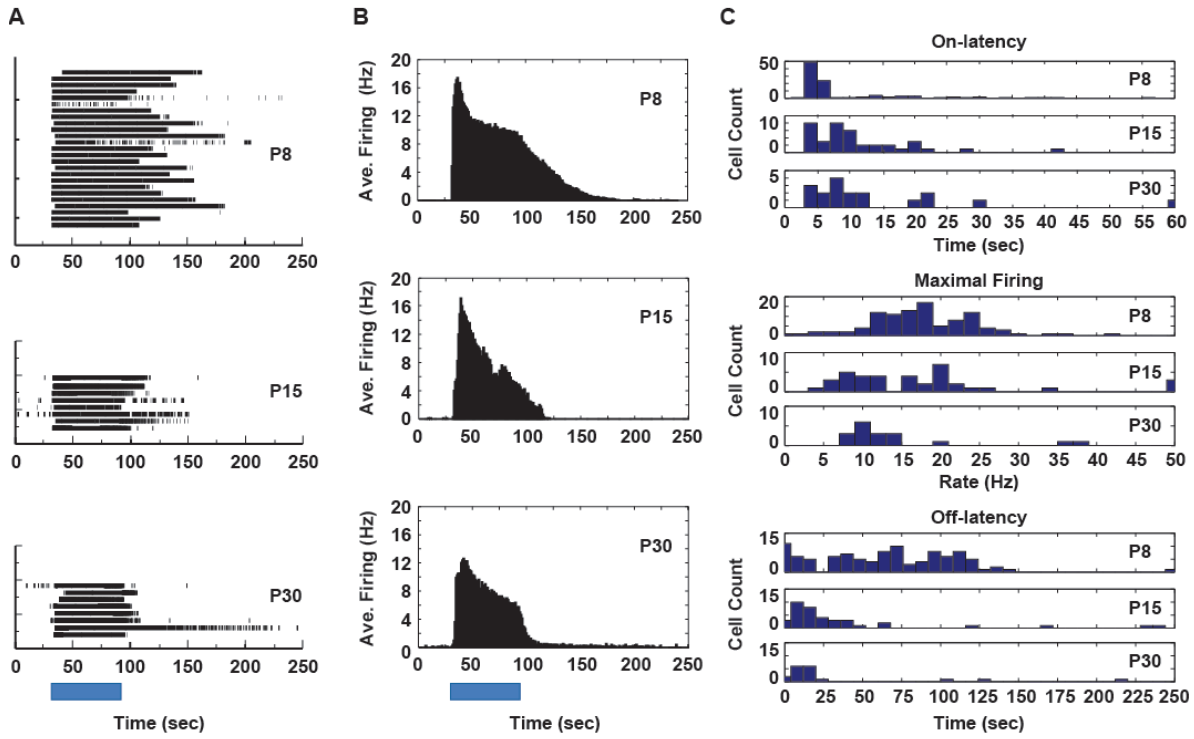

Figure 2

ipRGC become less photosensitive with age. A) Histograms of P8 (n=101), P15 (n=35) and P30 (n=18) light response dynamics including on-latency, maximal firing and off-latency. B) Raster plots of representative ipRGCs from P8 (n=25), P15 (n=8), P30 (n=8). C) Histograms of average ipRGC firing from cells depicted in B.

Figure 3

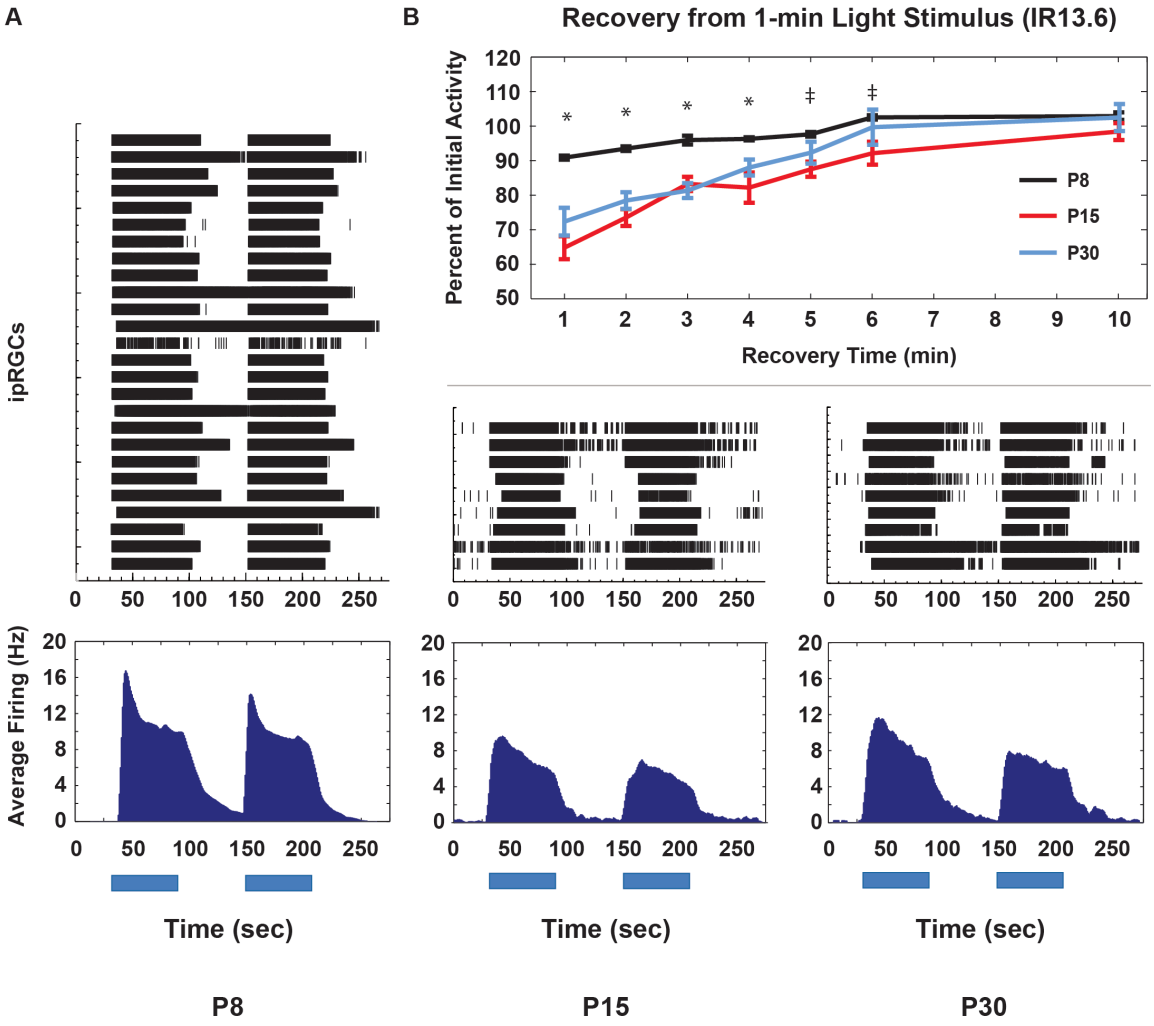

Figure 3

Younger ipRGCs recover more quickly than older ipRGCs. A) Rasters and average histograms of a sample of individual ipRGCs used in time course experiments B)Time courses of P8 (n=74), P15 (n=10 to 15), and P30 (n=6 to 16) ipRGC recovery following a 1-min light exposure. A second 1-min test light was administered at multiple time points between 1 and 10-min. * P8 difference from P15/P30 statistically significant ($P<0.05$, Mixed-model, Bonferronni corrected, followed One Way Anova) ++ P8 difference from P15 statistically significant ($P<0.05$, Mixed-model, Bonferronni corrected, followed One-way Anova).

Figure 4

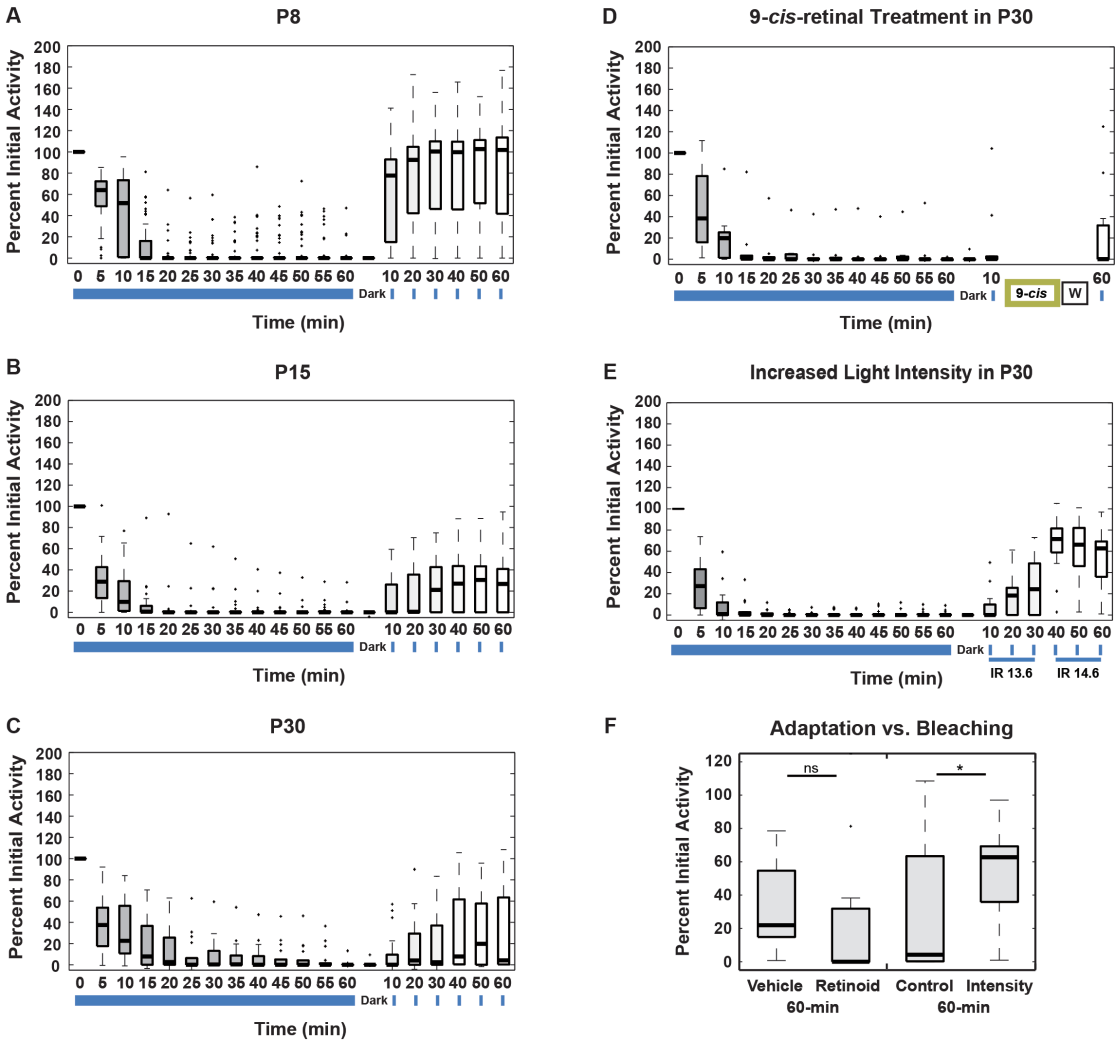

Figure 4

Older ipRGCs exhibit marked adaptation in response to a 1-hr light stimulus. Boxplots of exposure and recovery time courses for A) P8 (n=60), B) P15 (n=23), and C) P30 (n=17). Boxplots of 1-hr exposure followed D) 9-*cis*-retinal treatment (100 µM) or E) a 10-fold higher light intensity during the recovery period. F) Comparison of 9-cis-retinal treatment with vehicle control (1% ethanol in AMES) and the 10-fold higher light level with control from lower light level. * P< 0.05, Rank sum.

Figure 5

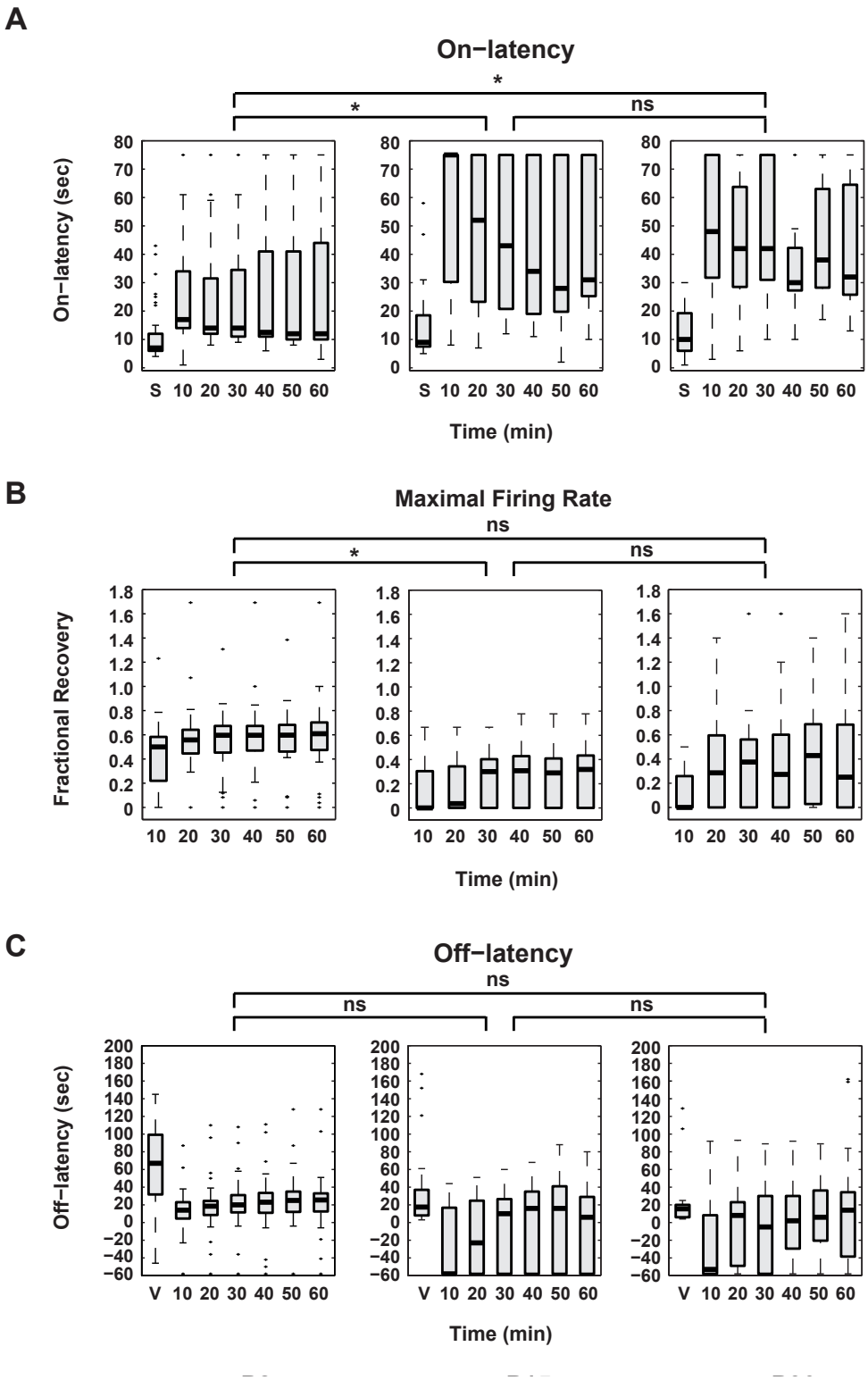
A
On−latency
*
*
ns
On−latency (sec)
S 10 20 30 40 50 60
Time (min)
B
Maximal Firing Rate
ns
*
ns
Fractional Recovery
10 20 30 40 50 60
Time (min)
C
Off−latency
ns
ns
ns
Off−latency (sec)
V 10 20 30 40 50 60
Time (min)

Figure 5

Recovery parameters in P8 (n=60), P15 (n=23), and P30 (n=17) including A) on-latency with on-latency for the same cells from the start of the 1-hr light exposure (S), B) maximal firing fractional recovery of initial 1-hr exposure values, and C) off-latency with the off-latency distribution and median from the 1-min test exposures from Figure 1. No off-latency measurements were made at the beginning of the 1-hr exposure. * $P<0.05$, Mixed-model, Bonferronni corrected, followed Kruskal-Wallis analysis.

Figure 6

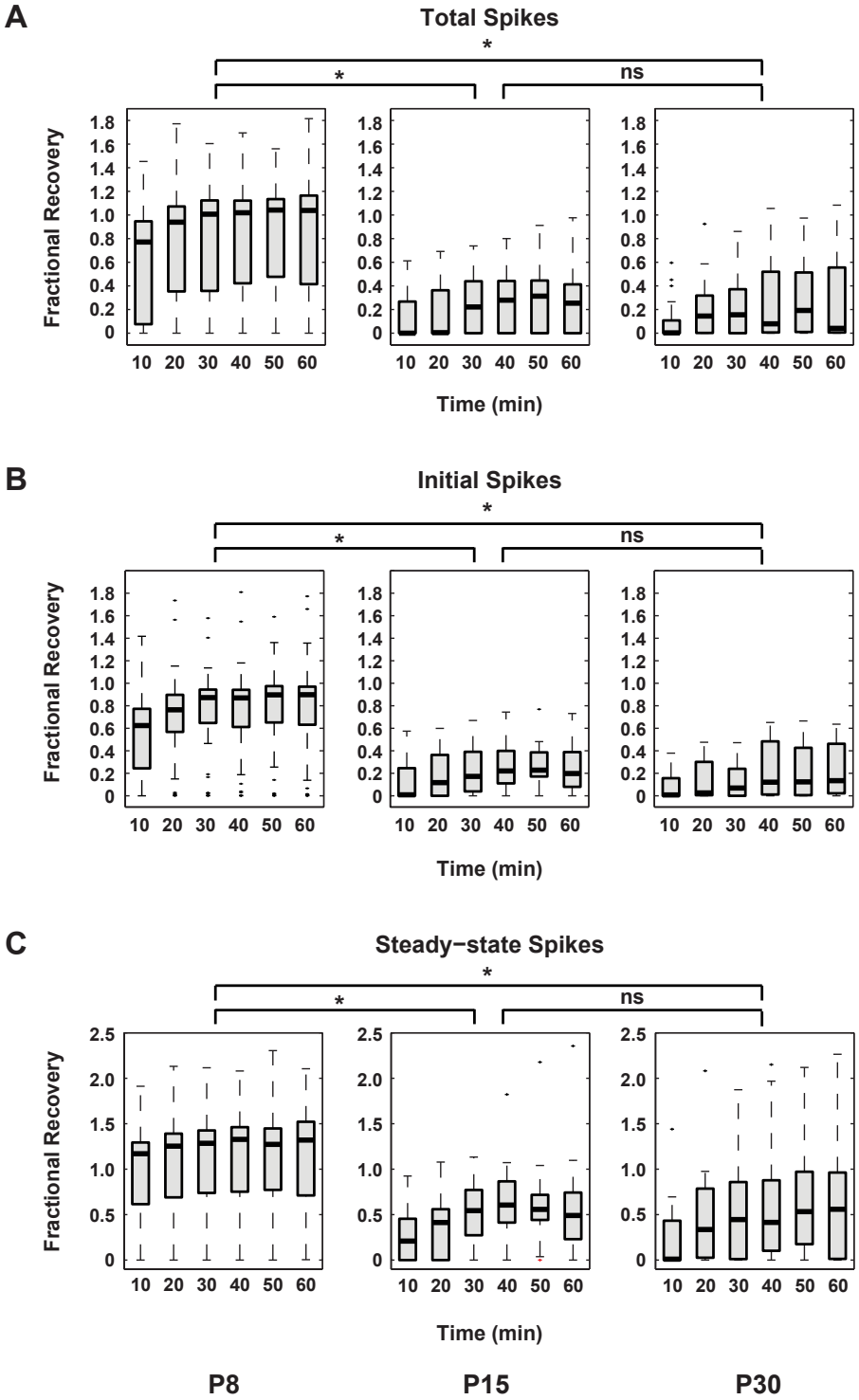
A
Total Spikes
*
*
ns
Fractional Recovery
Time (min)
B
Initial Spikes
*
*
ns
Fractional Recovery
Time (min)
C
Steady−state Spikes
*
*
ns
Fractional Recovery
Time (min)
P8
P15
P30

Figure 6

Recovery characteristics in P8 (n=60), P15 (n=23), and P30 (n=17). A) Total spikes, B) Initial spikes, C) Steady-state spikes. * $P<0.05$, Mixed-model, Bonferronni corrected, followed Kruskal-Wallis analysis.

Figure 7

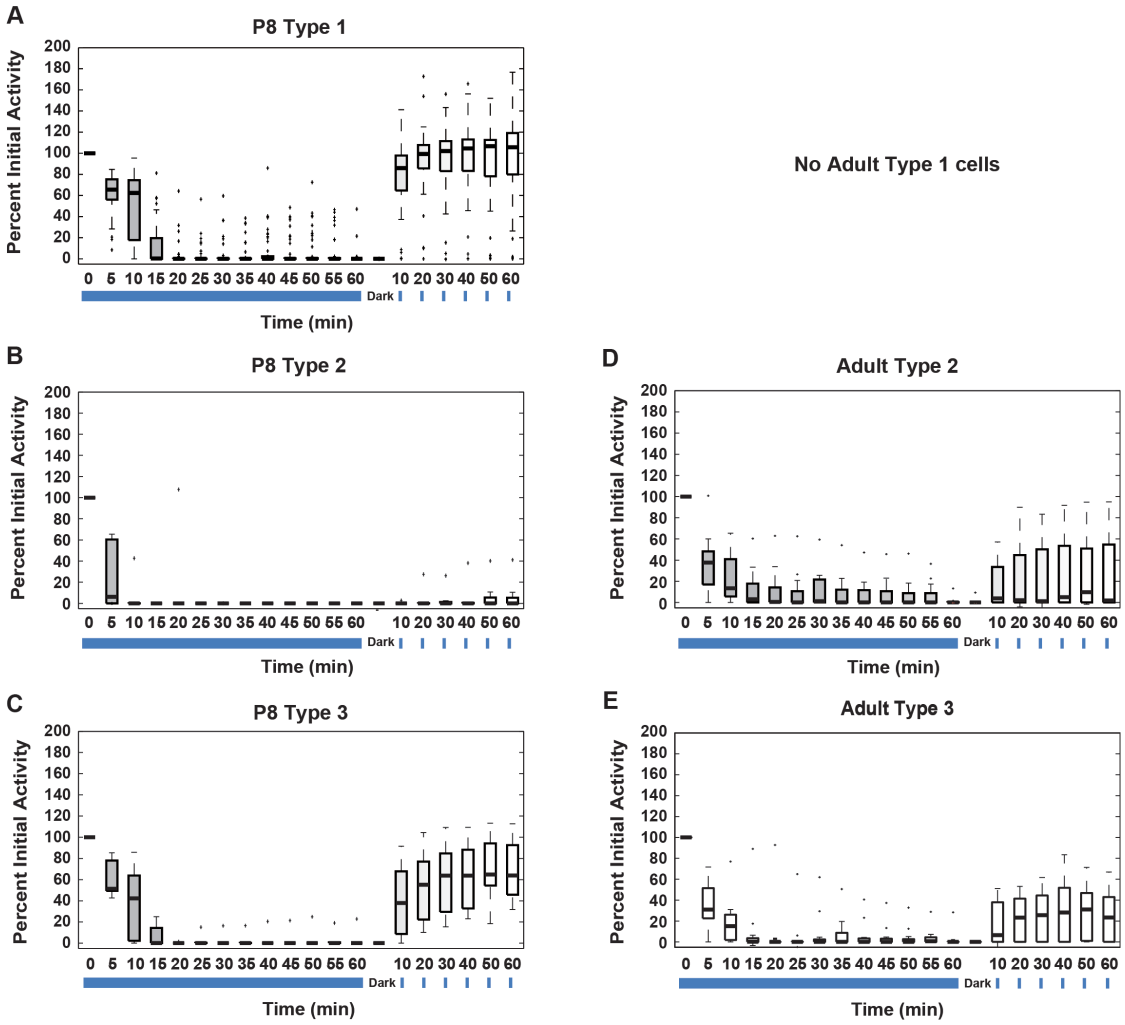

Figure 7

Young ipRGC recovery is dominated by Type 1 cells. Boxplots of exposure and recovery time courses for a subset of cells from the ages in Figure4. A) P8 subtype 1 (n=45), B) P8 subtype 2 (n=8), C) P8 subtype 3 (n=7), D) Adult Type 2 (n=13), E) Adult Type 3 (n=12). Data from P15 and P30 ipRGCs were pooled into and Adult category for analysis.

Figure 8

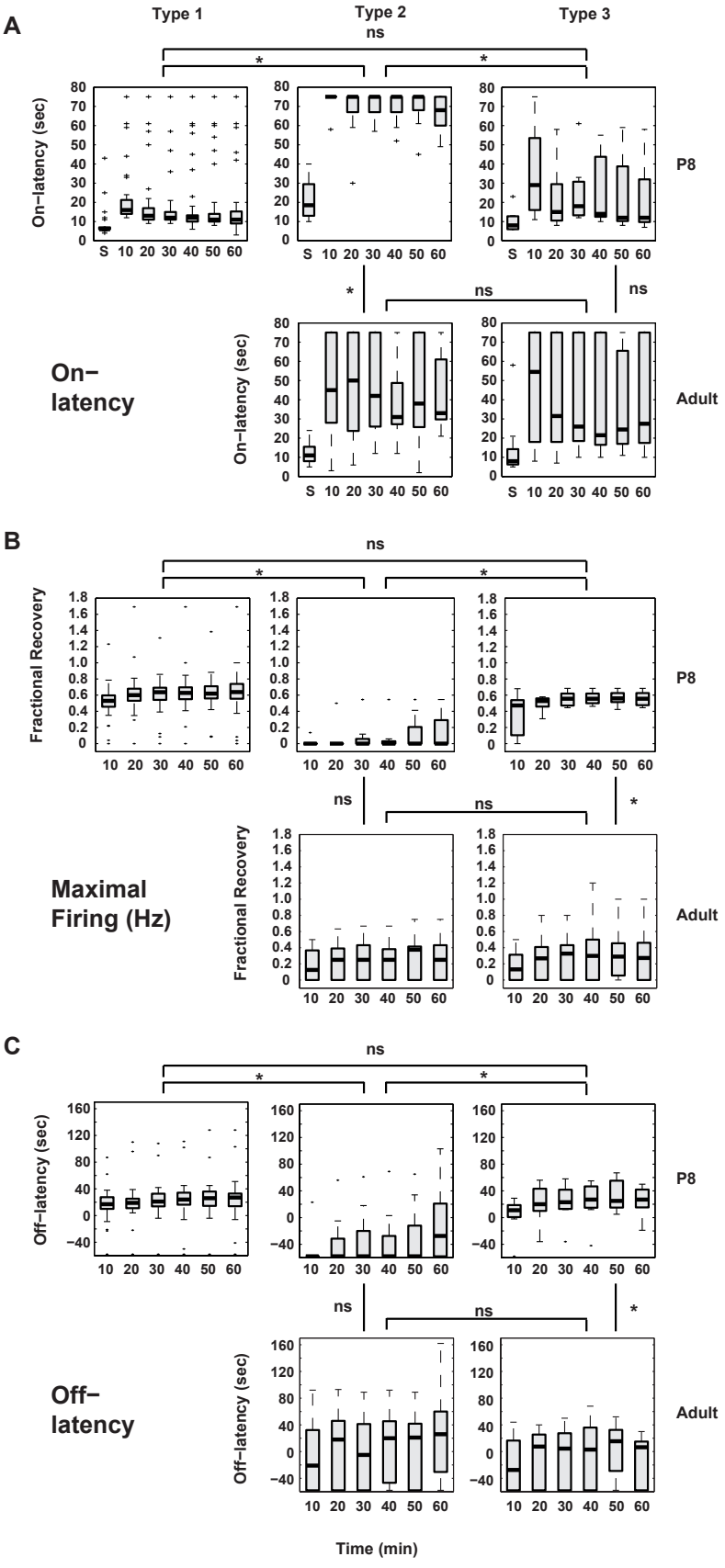
A
Type 1
Type 2
Type 3
ns
*
*
On−latency (sec)
P8
*
ns
ns
On−latency (sec)
Adult
On−
latency
B
ns
*
*
Fractional Recovery
P8
ns
ns
*
Fractional Recovery
Adult
Maximal
Firing (Hz)
C
ns
*
*
Off−latency (sec)
P8
ns
ns
*
Off−latency (sec)
Adult
Off−
latency
S 10 20 30 40 50 60
10 20 30 40 50 60
Time (min)

Figure 8

Boxplots of recovery parameters following 1-hr light exposure in P8 Types 1 (n=45), 2 (n=8) and 3 (n=7) and Adult Types 2 (n=13) and 3 (n=12). A) On-latency with on-latency for the same cells at the beginning of the 1-hr exposure. B) Maximal firing. C) Off-latencies. * $P<0.05$, Mixed-model, Bonferronni corrected, followed by Kruskal-Wallis analysis.

Figure 9

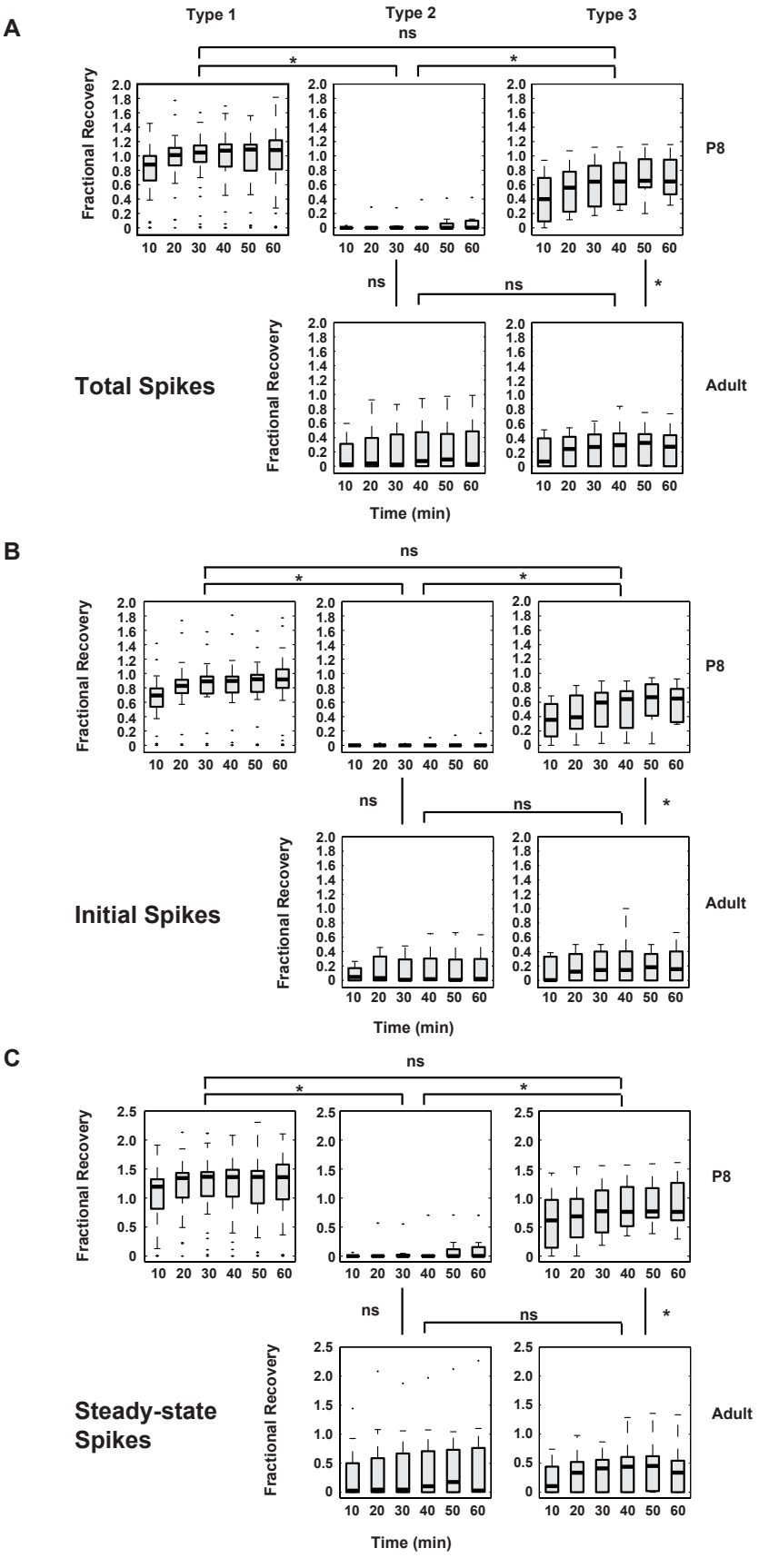
A
Type 1
Type 2
Type 3
ns
*
*
Fractional Recovery
P8
ns
ns
*
Total Spikes
Adult
Time (min)
B
ns
*
*
Fractional Recovery
P8
ns
ns
*
Initial Spikes
Adult
Time (min)
C
ns
*
*
Fractional Recovery
P8
ns
ns
*
Steady-state Spikes
Adult
Time (min)

Figure 9

Boxplots of recovery parameters following 1-hr light exposure in P8 Types 1 (n=45), 2 (n=8) and 3 (n=7) and Adult Types 2 (n=13) and 3 (n=12). A) Total Spikes B) Initial spikes. C) Steady-state spikes. * $P<0.05$, Mixed-model, Bonferronni corrected, followed by Kruskal-Wallis analysis.

Chapter 4: GRK2 regulation of melanopsin activity

Abstract

Phosphorylation is a major mechanism modulate GPCRs. For example, knocking out rhodopsin kinase, GRK1, leads to a much larger single photon response and a 100-fold longer termination time for rhodopsin (Chen et al., 1999). Recent evidence suggests that a related enzyme, GRK2, phosphorylates melanopsin and reduces its activity *in vitro* (Blasic et al., 2012). Using a melanopsin specific GRK2 knockout animal, we show that GRK2 does influence melanopsin response dynamics and termination. The relatively small changes in melanopsin responses in comparison to the large changes in rhodopsin activity in GRK1 knockout animals suggests that other kinases may also control melanopsin mediated activity. Other GRK loss of function alles should be combined with the GRK2 knockout to further determine melanopsin phosphorylation mechanisms.

Introduction

Hallmarks of the ipRGC light response are its long response latencies, sustained firing, and long off-latencies lasting well beyond light termination. Responses so different from rods and cones initially suggested that ipRGCs might not adapt like other photoreceptors. However, Wong et al., (Wong et al., 2005) demonstrated that many rod and cone photoreceptor adaptation responses are present in ipRGCs; including

desensitization under continuous background light, 'resensitization' to flashes of light during the decaying phase of a continuous light response, acceleration of light responses, and recovery from desensitization upon extended dark incubation. More recently Do and Yao (Do and Yau, 2013) have shown that ipRGC responses follow a Weber-Fechner relation (Luo et al., 2008) upon exposure to increasing background light levels as other photoreceptors do.

Adaptation mechanisms underlying these responses in ipRGCs is only minimally understood, given that the second-messenger cascade and subsequent channel activation are not fully demarcated. However, taking adaptation in other opsins as a starting point, regulatory steps can be postulated and tested. Both rhodopsin and the cone-opsin pathways have common mechanisms controlling activity following light activation, including 1) phosphorylation of the c-terminus by G-protein-coupled receptor kinases (GRK1 and GRK7 respectively) followed by arrestin binding to inactivate opsin activity, 2) a G-protein activating protein (GAP) complex to inactivate G_t and decrease PDE activity, and 3) a decrease in calcium feedback loops leading to a) an increase in guanylyl cyclase activity via release of calcium inhibition of the calcium binding guanylate cyclase activating proteins (GCAPs), and b) an increase in opening of the cyclic nucleotide gated ion channel mediating the dark current by increasing its affinity for cGMP (Luo et al., 2008; Yau and Hardie, 2009).

C-terminal phosphorylation is a general mode of GPCR regulation regardless of downstream messenger pathways. Since understanding of the melanopsin second messenger cascade is incomplete, melanopsin phosphorylation is a logical first process to look for changes in light response kinetics indicative of light adaptation. Phosphorylation

of GPCRs is mediated primarily by two families of protein kinases: 1) G-protein-coupled receptor kinases (GRKs) and 2) second messenger activated kinases such as cAMP-dependent kinase (PKA) and protein kinase C (PKC)(Willets et al., 2003). Currently 7 subtypes of GRKs are known, with GRK1 and GRK7 also referred to as rhodopsin kinase and cone-opsin kinase respectively (Iacovelli et al., 1999; Moore et al., 2007). The two most studied GRKs are GRK2 and GRK3, originally known as β-adrenoceptor kinase 1 (β-ARK1) and β-adrenoceptor kinase 2 (β-ARK2). Both are involved in heart development and function (Matkovich et al., 2006; Vinge et al., 2008). A knockout of GRK2 is an embryonically lethal because of heart abnormalities.

Recent work by Blasic et al., (Blasic et al., 2012) has shown 1) that GRK2 and GRK3 can both bind to melanopsin, 2) that GRK2 can regulate melanopsin mediated intracellular calcium changes in HEK293 cells expressing melanopsin, 3) *in vivo* evidence that melanopsin is phosphorylated in response to light and 4) that GRK2 and GRK3 colocalize with melanopsin expression in ipRGCs. Here we expand on this work by testing ipRGC responses in an ipRGC specific GRK2 knockout (KO).

Methods

Animals

All experiments were performed in accordance with Association for Research in Vision and Ophthalmology guidelines for animal studies, under an approved animal study protocol at the University of Washington. Animals were maintained in a 12:12-hr light-dark cycle with *ad libitum* food. Floxed GRK2 animals in a B6.129 background were

purchased from Jackson Laboratory (Bar Harbor, Maine). GRK2 animals were bred with a line of C57BL/6, 129SvJ mixed background mice containing a Cre-recombinase gene knocked into the melanopsin locus (Gift of Samer Hattar). Knockout (KO) animals were genotyped as $Cre^{+/-}$ / $GRK2^{-/-}$ and controls as $Cre^{+/-}$ / $GRK2^{+/+}$. Animals were littermates when possible were progeny of the same set of breeding pairs for repeated experiments.

Preparation of Retina

All procedures were performed under dim red light illumination. Mice were euthanized by CO_2 narcosis and cervical dislocation. Isolated mouse retinas were cut in half, positioned with the vitreal face in contact with a multielectrode array (MEA) (Multi Channel Systems, Reutlingen, Germany) and superperfused (2-3 ml/min) with a bicarbonate-buffered physiologic solution (125 mM NaCl, 2.5 mM KCl, 1 mM $MgCl_2$, 1.25 mM NaH_2PO_4, 20 mM glucose, 26 mM $NaHCO_3$, 2 mM $CaCl_2$, 500 μM glutamine) oxygenated with 95% O_2/5% CO_2 to obtain a pH of 7.4. The temperature of both perfusate and tissue chamber was maintained at 33.0^{o}C. For ipRGC recordings from P8-10 mouse retinas, spontaneous retinal waves (Wong et al., 2000) (as well as any possible input from rod and cone photoreceptors), were suppressed by using glutamatergic [50 μM d(2)-2-amino-5-phosphonopentanoic acid (d-AP5); 20 μM d(-)-2-amino-4-phosphonobutyric acid (d-AP4), 10 μM CNQX] and cholinergic (5 nM epibatidine) inhibitors (Tocris Biosciences, Ellisville, MO). For ipRGC recordings from P30-35

mouse retinas, only glutamatergic blockade was used (200 μM d-AP5, 100 μM d-AP4 and 80 μM CNQX).

Multi-electrode recordings and Light stimulation

Electrophysiological recordings were performed using planar arrays of 60 electrodes (30 μm diameter, 200 μm inter-electrode spacing; Multi Channel Systems, Reutlingen, Germany). Raw electrical signals were amplified, filtered, and digitized through an A/D card (National Instruments, Austin, TX), written to disk and analyzed off-line, as described previously (Holy et al., 2000).

Retinas were stimulated with continuous light with a Xenon light source (Sutter Instruments, Novato, CA) fed through a liquid light guide and diffusing filter (Thorlabs Inc., Newton, NJ). Intensities and wavelengths of light were adjusted via neutral density and narrow band-pass 480 nm interference filters (Thorlabs, Inc., Newton, NJ) and calibrated with a radiometer (Advanced Photonics International, Fairfield, CT). All retinas were successively exposed to 10-sec, 30-sec and 60-sec continuous 480 nm at 3.98×10^{13} photon cm^{-2} s^{-1} (IR 13.6). The 30-sec exposure is not reported here. Retinas were also successively expose to 1, 3, 5, and 10 brief flashes of bright white light (4.6 J m^{-2}) from a commercial camera flash (SunPak) held 30 cm above the MEA preparation. Multiple flashes were 5-sec apart (fastest recharge time of flash). Only the 1 and 5 flash experiments are reported here for brevity.

Several response parameters measured were not normally distributed. Data for those parameters are represented in boxplots. Boxes represent the 25th and 75th percentiles of the data and center-lines are medians. Dashed lines indicate the maximal and minimal data points except for dots indicating outliers (data points more than 2.7 standard deviations away from the mean if data were interpreted to be normal).

Pharmacology

Retinas from wildtype C57BL/6 mice were treated with the GRK2/5/6 inhibitor bisindolylmaleaimide XI hydrochloride (Adipogen, San Diego, CA). Solubility requirements for the inhibitor required that retinas be exposed to a 1% DMSO solution for drug delivery. Retinas were pre-tested for ipRGC light responses with brief light flashes. P8 retinas were tested with 5 flashes and P30 retinas were tested with 1 flash. Retinas were then treated with 1% DMSO in bubbling AMES for 10-min, washed in AMES for 5-min, re-exposed to synaptic blockade for 5-min and tested for ipRGC light responses. Retinas were finally treated with the GRK inhibitor (100-200 μM in bubbling AMES with 1% DMSO as carrier) for 10-min, washed in AMES for 5-min, re-exposed to glutamatergic blockade for 5-min and tested for ipRGC light responses.

Recovery

For recovery experiments, ipRGCs were exposed to 1-min of 480 nm light at 3.98 x 10^{13} photon cm^{-2} s^{-1} (IR 13.6), allowed to recover for 1, 3, 5, or 10 minutes in the dark and retested with a 1-min exposure of the same light. For each recovery time interval, the percent recovery of the number of spikes was calculated.

Results

For analysis, P8 ipRGCs were categorized into those with on-latencies (time from lights on to maximal firing rate) greater than 13-sec (early cells) or less than or equal to 13-sec (late cells) under 60-sec of 480 nm light at 3.98 x 10^{13} photon cm^{-2} s^{-1} (IR 13.6). Categories were suggested by the shape of light responses (Figure 1). It was rationalized that clumping like responses together would decrease "noise" during analysis, revealing small changes caused by the absence of GRK2. These differences were not seen in P30 animals perhaps because of the small sample size when compared to P8 animals or because of the change in photosensitivity seen in chapter 3.

Under 60-sec of light, P8 GRK2 KO ipRGCs looked similar to controls (Figure 2 C and D). Only at 10-sec exposures was an appreciable increase in sustained firing rates and lengthening of termination times seen (Figure 2 A and B). In an attempt to elicit a more pronounced result, cells were exposed to a series of brief flashes of bright white light (4.6 J m^{-2}). A single flash, as with a 60-sec exposure, produced no appreciable difference in responses of controls vs. GRK2 KOs. With 5-flashes, an increase in steady

firing rates and an extension of termination times were found, qualitatively comparable to the response of a 10-sec exposure. One difference between the 10-sec and 5-flash exposures was in the peak firing rate of late category cells (on-latency of ≥13-sec under 1-min 480 nm light at IR 13.6). In the 10-sec exposure experiment, maximal firing rates were 6.5 ± 0.1 Hz and 11.9 ± 0.1 Hz for control late cells and KO late cells, respectively. This difference is absent in the 60-sec and 5-flash exposures. Such a large difference in peak firing rate between the control and KO in the 10-sec exposure may simply reflect the relatively small number of cells. The distribution of control cells may be randomly skewed toward cells of a somewhat lower photosensitivity, accentuated by the short light exposure. This interpretation is supported by the later equalization of peak firing rates during the 60-sec exposure. The flash was of a greater intensity and pushed all cells toward maximal possible firing quickly.

Consistent increases were seen in several firing dynamic parameters predominantly in the 10-sec and 5-flash conditions. All parameters exhibited non-normal behavior in some or all of the conditions including age, as seen in Chapter 3. Therefore, all parameter data has been analyzed non-parametrically. In P8 early cells, the 10-sec and 5-flash decay constant tau (measured from time of peak firing to time of 33% peak firing), off-latencies (time from lights off to end of firing in the case of the a continuous exposure or time from light flash till the end of firing), and total number of spikes increased significantly in GRK2 KO animals over controls (MannWhitney, $P<0.05$, Bonforonni corrected). For 10-sec and 5-flash experiments, median increases in tau were 21-sec and 32-sec, median increases in off-latency were 32-sec and 38.5-sec, and increases in total spikes were 237 and 301, respectively (Figure 4). In P8 late cells, similar increases were observed but

never reached statistical significance (Figure 5), possibly because of the small number of late cells. Oddly, in P8 early cells, on-latencies decreased by 1-sec and 1.5-sec in the 10-sec and 60-sec condition respectively in GRK2 KO vs. controls (MannWhitney, $P<0.05$, Bonforonni corrected)(Figure 4 A). However, these are small changes with unclear implications.

For P30 animals, peak firing was dramatically reduced in the GRK2 KO vs. control under all conditions (Figure 6). This may reflect developmental changes from the long-term absence of GRK2. Differences in peak-firing rates and total spikes were significant under the 60-sec and 5-flash condition only, though similar trends appeared in the other conditions (Figure 7 C). On-latencies and off latencies displayed only small changes (Figure 7 A, B). Interestingly the decay constant for adult GRK2 KO ipRGCs decreased with a distribution stretching far below that of control animals (Figure 7 E) suggesting that the active light response has been shortened with only minor influence on off-latencies specifically.

Drug treatment with a GRK2/5/6 inhibitor did not phenocopy GRK2 KO ipRGC response dynamics in P8 animals. The EC_{50} of bisindolylmaleimide XI for GRK2 inhibition in cell culture is 30 μM (Aiyar et al., 2000). Both of the concentrations used here were well above that (100 and 200 μM). However no major change in responses from those of the 1% DMSO control were observed (Figure 8 A and B). A 1% DMSO solution was the minimal DMSO concentration achievable because of the inhibitor solubility. Interestingly 1% DMSO did increase cell photosensitivity over pre-treatment levels in some cases (Figure 8 B and C). Our lab has noted an increased basal firing of

RGCs when treated with a 0.5% DMSO solution. Higher baseline firing would reflect a more depolarized state of the cells and could explain the increased light response.

Treatment of P30 animals with 100 μM bisindolylmaleimide XI did decrease ipRGC response as in the GRK2 KO. However, tau and off-latencies were decreased far more than in the knockout. This may be a general decrease in light sensitivity from a toxic drug effect. Bisindolylmaleimide XI is known to be a GRK5/6 and protein kinase C inhibitor at 10-fold lower concentrations required for GRK3 inhibition (Aiyar et al., 2000) further confounding interpretation.

In an attempt to explain the dramatic differences in light response recovery at different ages seen in Chapter 3, P30 GRK2 KO animals were tested for recovery from a 1-min 480 nm light at 3.98 x 1013 photons s^{-1} cm^{-2} (IR 13.6). Recovery in GRK2 KO ipRGCs overlapped with wildtype aged matched ipRGCs (data from chapter 3)(Figure 9). GRK2 alone does not appear responsible for age specific changes in ipRGC adaptation mechanisms for 1-min exposures found in chapter 3.

Discussion

Removing GRK2 activity from ipRGCs has limited effect on ipRGC responses *in vivo*. The decay constant, off-latencies, and total spikes increase in P8 ipRGCs as would be expected by removing phosphorylative controls. However, the changes are small. In contrast, knocking out rhodopsin kinase (GRK1) in rods leads to a doubling of the single photon current response and an extension of termination time by several hundred-fold (Chen et al., 1999). Using rhodopsin as a model system suggests that GRK2 is not the

only kinase regulating melanopsin activity. In the work of Blasic et al., (Blasic et al., 2012), both GRK2 and GRK3 bound to melanopsin in immunoprecipitation assays. However, only knocking down GRK2 expression with siRNA altered light induced, melanopsin-mediated intracellular calcium increases in the heterologous expression system used. This group also found, in single cell RT-PCR of ipRGCs, that GRK2 was present in all ipRGCs while GRK3 was found in only half of cells. Despite this, GRK3 regulation cannot be ruled out. Evidence of GRK3 knockdown in their data is not of an optimum quality. The fact that GRK3 is not found in all ipRGCs may reflect differential regulation in different ipRGC subtypes but does not eliminate it as a candidate kinase for melanopsin phosphorylation. In GRK2 KO animals, up-regulation of GRK3 may compensate for the absence GRK2, especially in ipRGCs in which GRK3 expression was not found by Blasic et al., (Blasic et al., 2012). Compensatory mechanisms are not unlikely as a non-targeted GRK2 knockout is embryonically lethal because of altered development in adrenergic regulation of heart tissue (GRK2 is also known as adrenergic receptor kinase, beta 1).

Two hypotheses may explain the P8 GRK2 knockout data. GRK2 could be one of several GRKs coordinating melanopsin phosphorylation. Removing GRK2 may prevent phosphorylation of specific serine/threonine residues on the melanopsin C-terminus leading to changes in kinetics. Such differential phosphorylation by different GRK subtypes in other systems leads to differential receptor-arrestin localization within cells (Moore et al., 2007). In cultured heart myocytes expressing peptide inhibitors of either GRK2 or GRK3, distinct subsets of receptors were modified depending upon the dominant GRK activity present in the cell (Vinge et al., 2007). Instead of such specific

regulation, other GRKs found in ipRGCs, such as GRK3, may phosphorylate the same sites on melanopsin but with lower efficiency, leading to a slower melanopsin inactivation. Further exploration would require a combination of the GRK2 KO with at least a GRK3 KO. A combination of knockout animals and pharmacological intervention could also be tried. The value of the later approach is doubtful given the paucity of GRK specific inhibitors and the pharmacological data reported here. The only reported inhibitor of GRK3 is a small peptide, the delivery of which to specific cells in knockout animals would not be trivial.

The lack of a specific pharmacological GRK2 inhibitor does leave unanswered whether or not changes in ipRGC kinetics seen here are a direct consequence of GRK2 KO or a coincidental compensatory change not directly related to melanopsin phosphorylation. Given that the effects of the GRK2 KO are consistent with the hypothesis that GRK2 specifically modulates melanopsin, qualitatively if not quantitatively, the lack of drug effect is more suspect. No example of bisindolylmaleimide XI use outside of cell culture exists in the literature. The concentration needed to alter GRK2 activity in tissue is therefore unknown. Drug penetration into the retina did not seem to be of primary issue, as what looked like a toxic effect on the light response was seen in P30 retinas. This indicates that the drug was able to reach ipRGCs. It is unclear if this toxic effect was because of other more potent specific effects of bisindolylmaleimide XI such as protein kinase C inhibition or non-specific effects directly on the light response or cell health. Recovery of light responses after bisindolylmaleimide XI treatment was not specifically tested; but, when a second light stimulus was delivered 30 minutes after the one reported here, no increase in the

light response was seen. Given the question over pharmacological intervention, the GRK2 KO data have been discussed at face value.

An alternative explanation is suggested by the role of opsin phosphorylation in rhabdomeric photoreceptors. There, phosphorylation itself does not appear necessary to inactivate opsin activity. Removal of C-terminal phosphorylation sites in Drosophila rhodopsin does not prevent the binding of the arrestin required for deactivation, Arr2, but does prevent the binding of the arrestin required for receptor internalization via clatharin coated-pits, Arr1 (Hardie and Postma, 2008). Termination of rhodopsin signaling by Arr2 is further enhanced by the influx of calcium into the cell (Liu et al., 2008)(Liu et al., 2009). Since melanopsin is phylogenetically classified as a rhabdomeric opsin (Yau and Hardie, 2009), it is possible that termination of melanopsin signaling is not predominately regulated by phosphorylation events. Recently Do and Yao (Do and Yau, 2013) demonstrated Ca^{2+} modulation of peak light induced current and response termination time. Even in the absence of Ca^{2+} strong response relaxation persisted indicating other mechanisms are involved. Again, experiments utilizing double or triple GRK knockouts would be necessary to differentiate between a cilliary or rhabdomeric opsin inactivation.

Figure 1

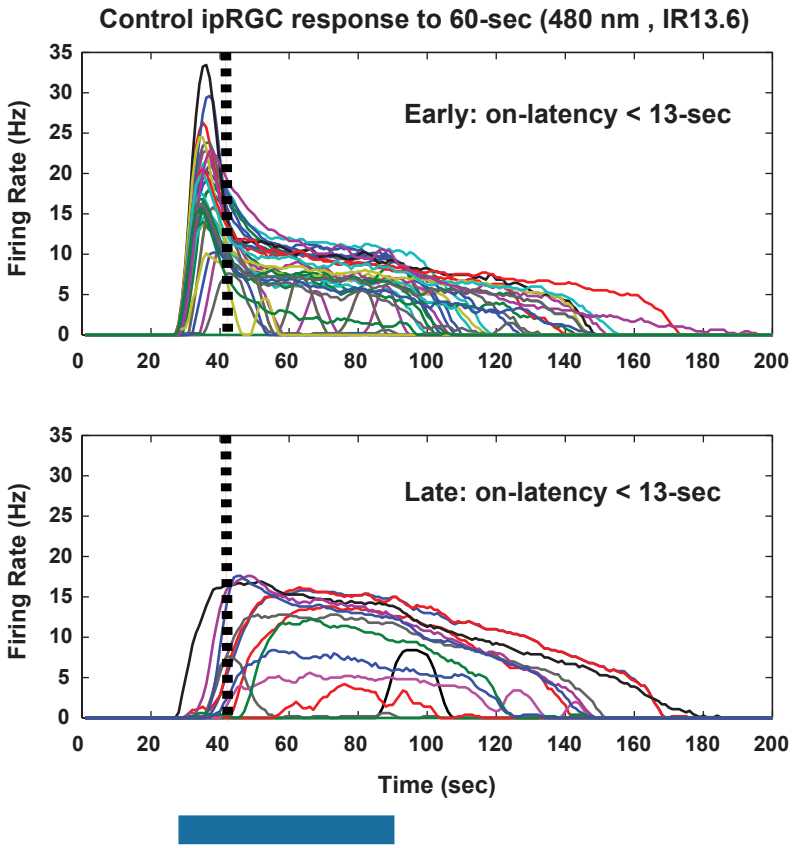

Figure 1

Light response from control ipRGCs under 60-sec of 480 nm at 3.98 x 10^{13} photons s^{-1} cm^{-2} (IR 13.6). Top panel shows cells with early peak response times (<13-sec). Bottom panel depicts longer, late peak response times (≥13-sec). Light begins at 30-sec and ends at 90-sec. Dashed line marks 13 seconds from line onset. Each trace represents a single cell. Line color is added for clarity.

Figure 2

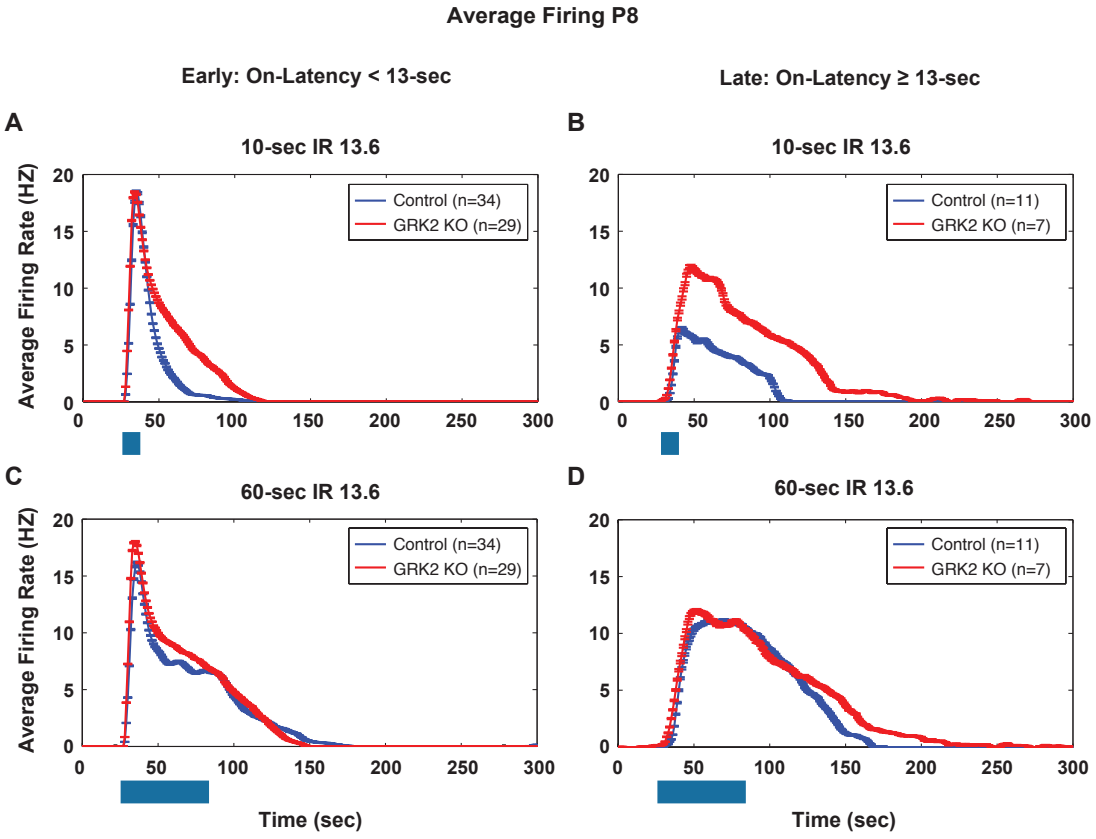

Figure 2

P8 ipRGC average firing with SEM in response to continuous light exposure. Firing for early control (n=34) and GRK2$^{-/-}$ (n=29) cells in response to A) 10-sec and C) 60-sec light. Firing for late control (n=11) and GRK2$^{-/-}$ (n=7) cells in response to B) 10-sec light and D) 60-sec light. All light was 480 nm at IR 13.6. The apparent dashed lines at the beginning of responses are SEM bars at each second during the fast rise in firing.

Figure 3

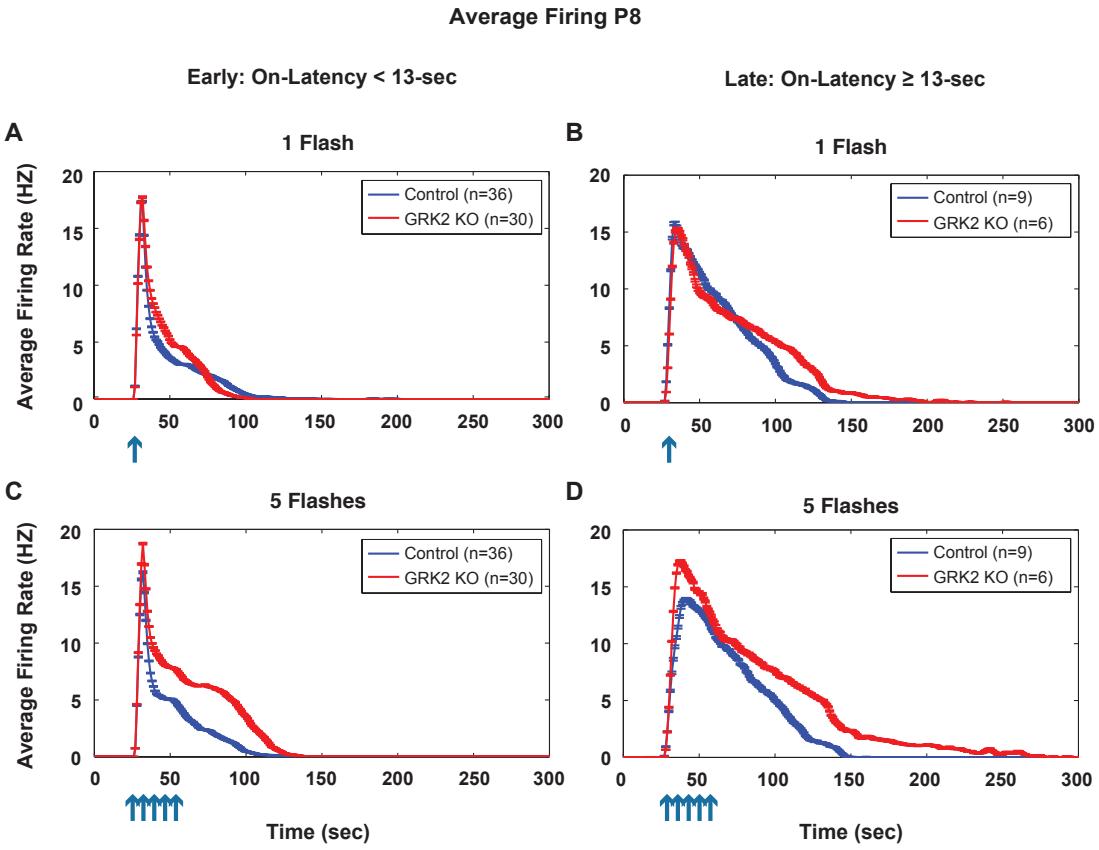

Figure 3

P8 ipRGC average firing with SEM in response to flashes of light. A flash is represented by an arrow. Firing for P8 early control (n=36) and GRK2$^{-/-}$ (n=30) cells in response to A) 1-flash and C) 5-flashes. Average firing with SEM for late control (n=9) and GRK2$^{-/-}$ (n=6) cells in response to B) 1-flash and D) 5-flashes. All flashes were bright white light from a camera flash. The apparent dashed lines at the beginning of responses are SEM bars at each second during the fast rise in firing.

Figure 4

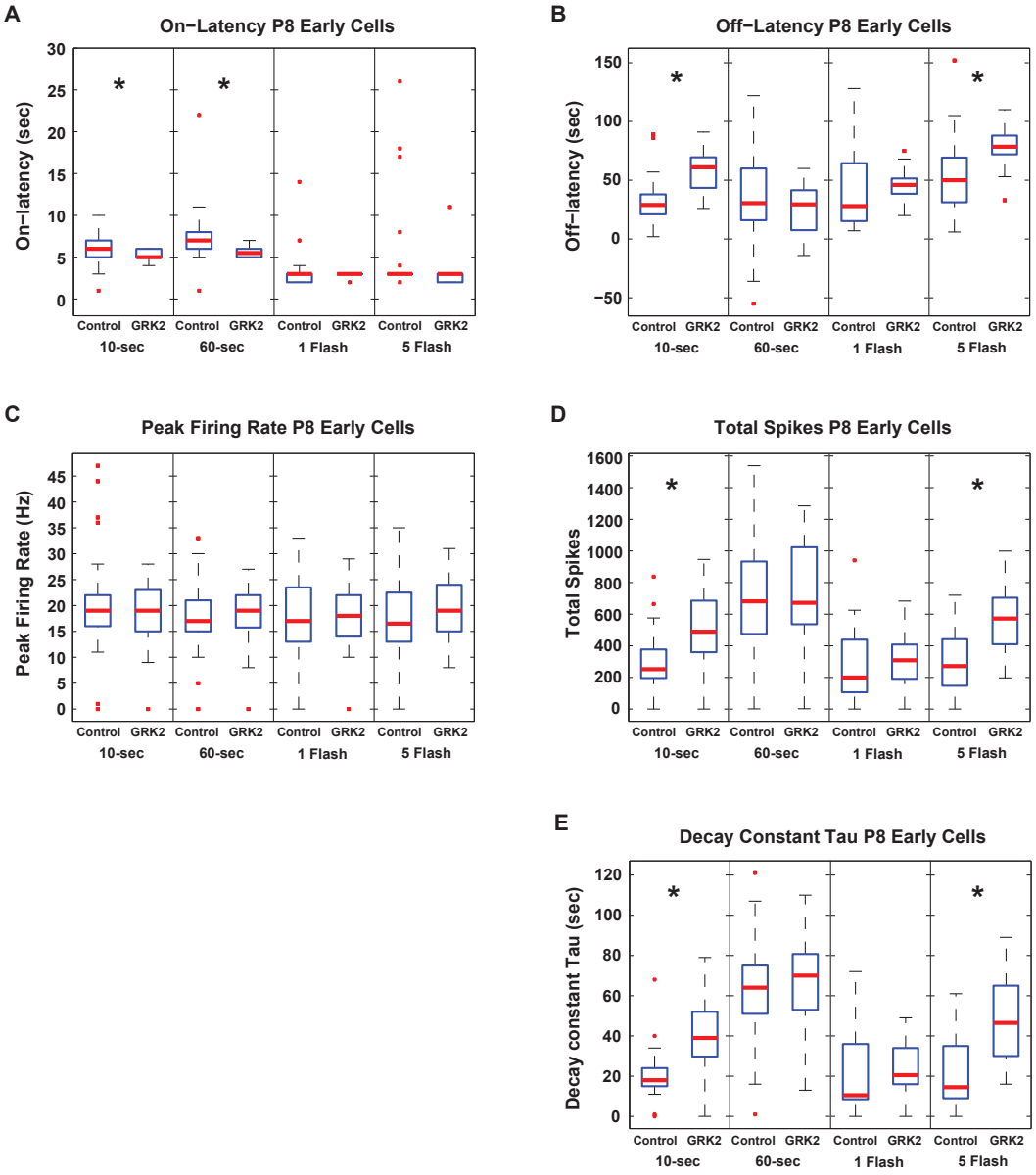

Figure 4

Boxplots of response parameters for P8 early cells from Figure 2. Parameters include A) On-latency, B) Off-latency, C) Peak firing, D) Total spikes, D) Decay constant tau. * MannWhitney, P<0.05, Bonforonni corrected for 4 comparisons per panel).

Figure 5

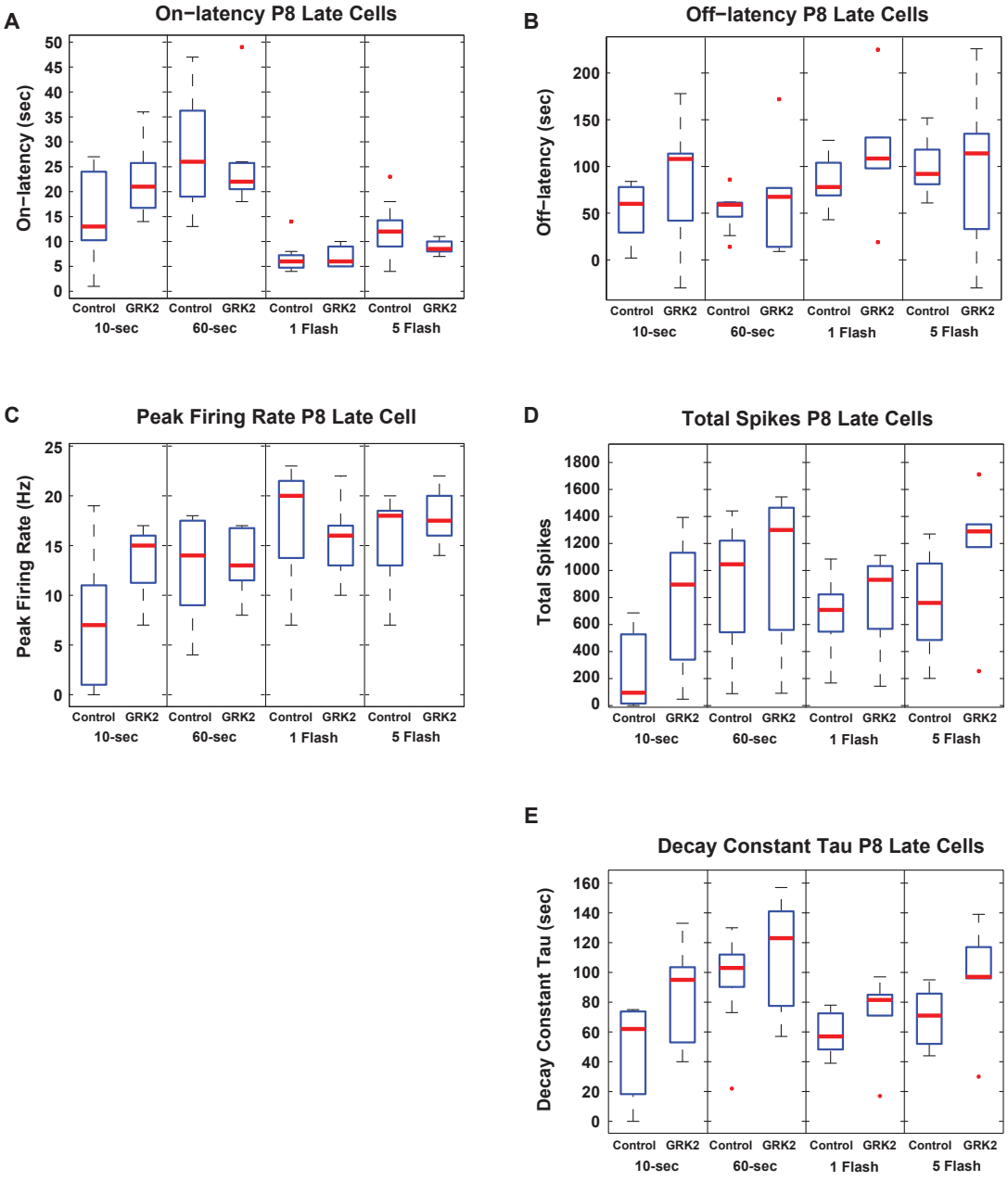

Figure 5

Boxplots of response parameters for P8 late cells from Figure 3. Parameters include A) On-latency, B)Off-latency , C) Peak firing, D) Total spikes, D) Decay constant tau. * MannWhitney, P<0.05, Bonforonni corrected for 4 comparisons per panel

Figure 6

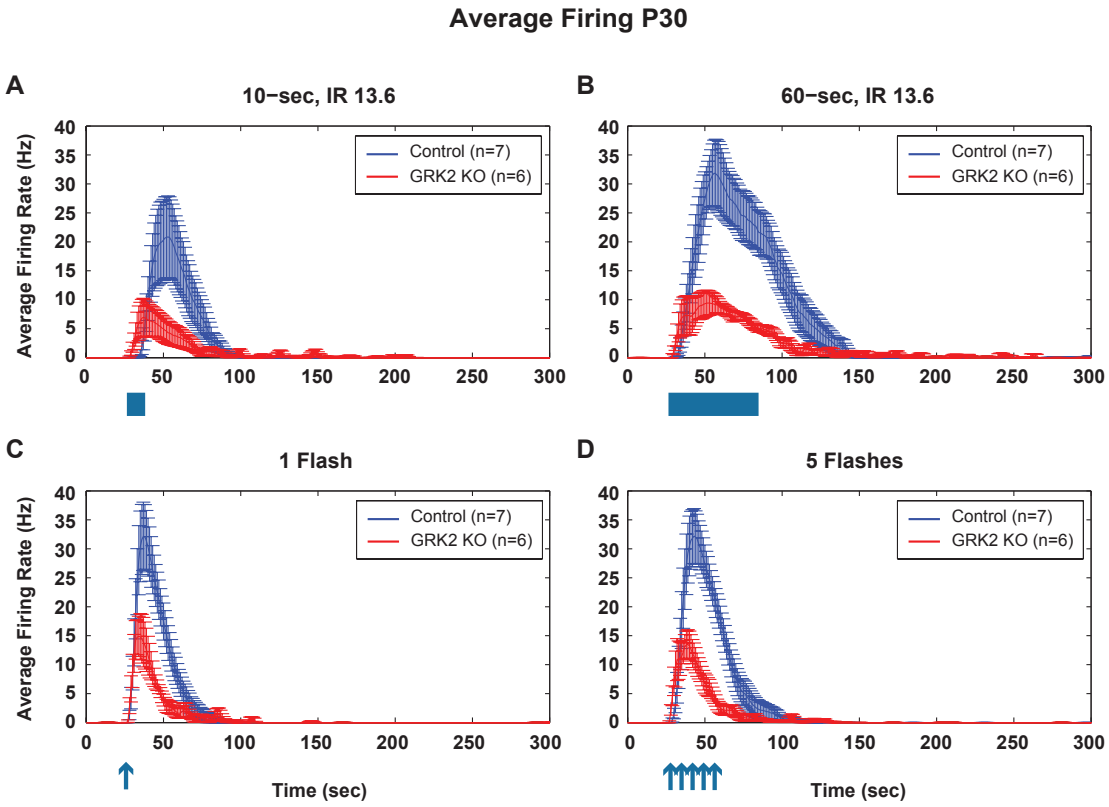

Figure 6

P30 ipRGC average firing with SEM in response to flashes of light. A flash is represented by an arrow. Firing for control (n=7) and GRK2$^{-/-}$ (n=6) cells in response to A) 10-sec light, C) 60-sec light, B) 1-flash and D) 5-flashes. All flashes were bright white light from a camera flash. All continuous light was 480 nm at IR 13.6. The apparent dashed lines at the beginning of responses are SEM bars at each second during the fast rise in firing.

Figure 7

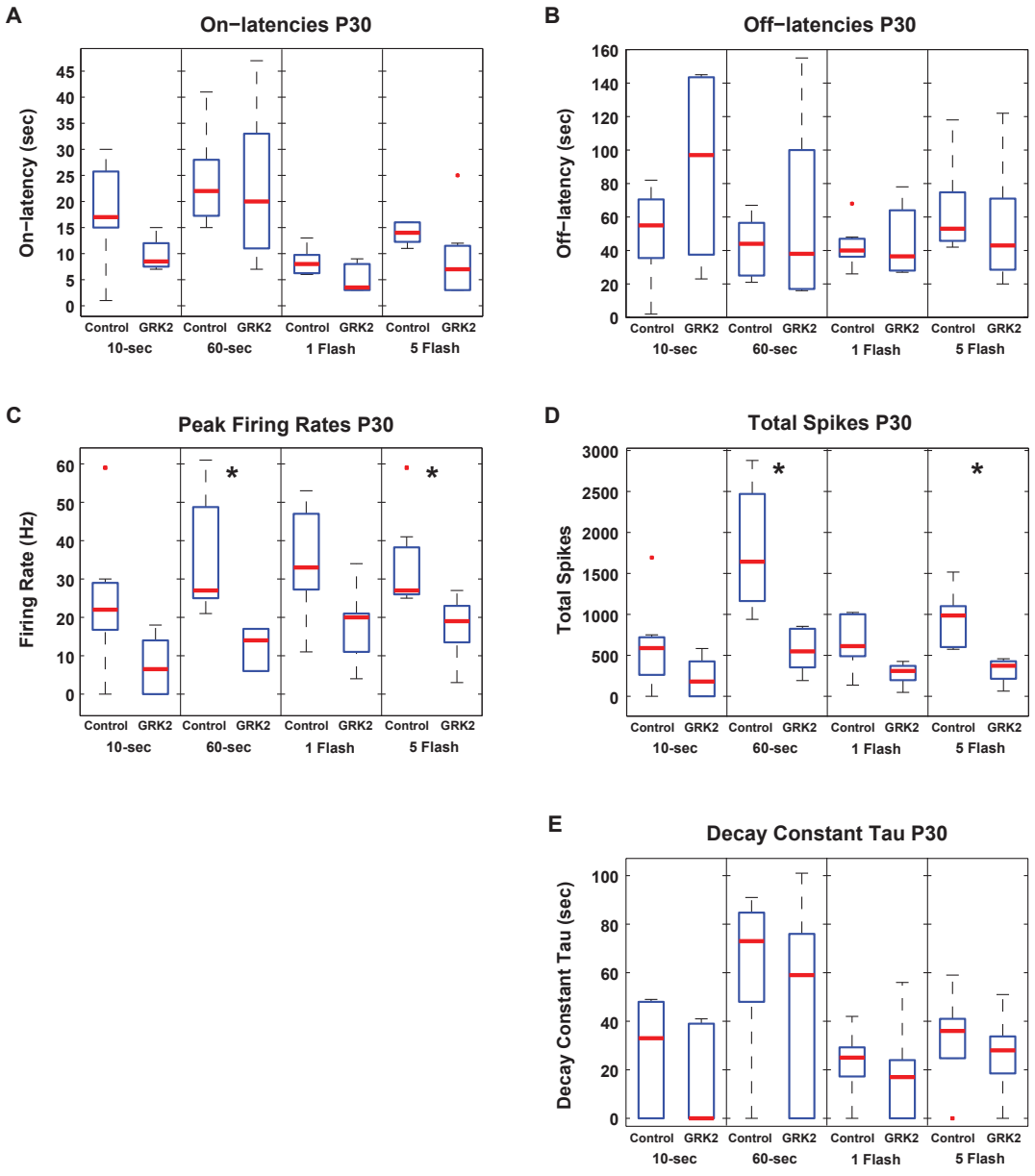

Figure 7

Boxplots of response parameters for P30vcells from Figure 6. Parameters include A) On-latency, B)Off-latency , C) Peak firing, D) Total spikes, D) Decay constant tau. * MannWhitney, P<0.05, Bonforonni corrected for 4 comparisons per panel)

Figure 8

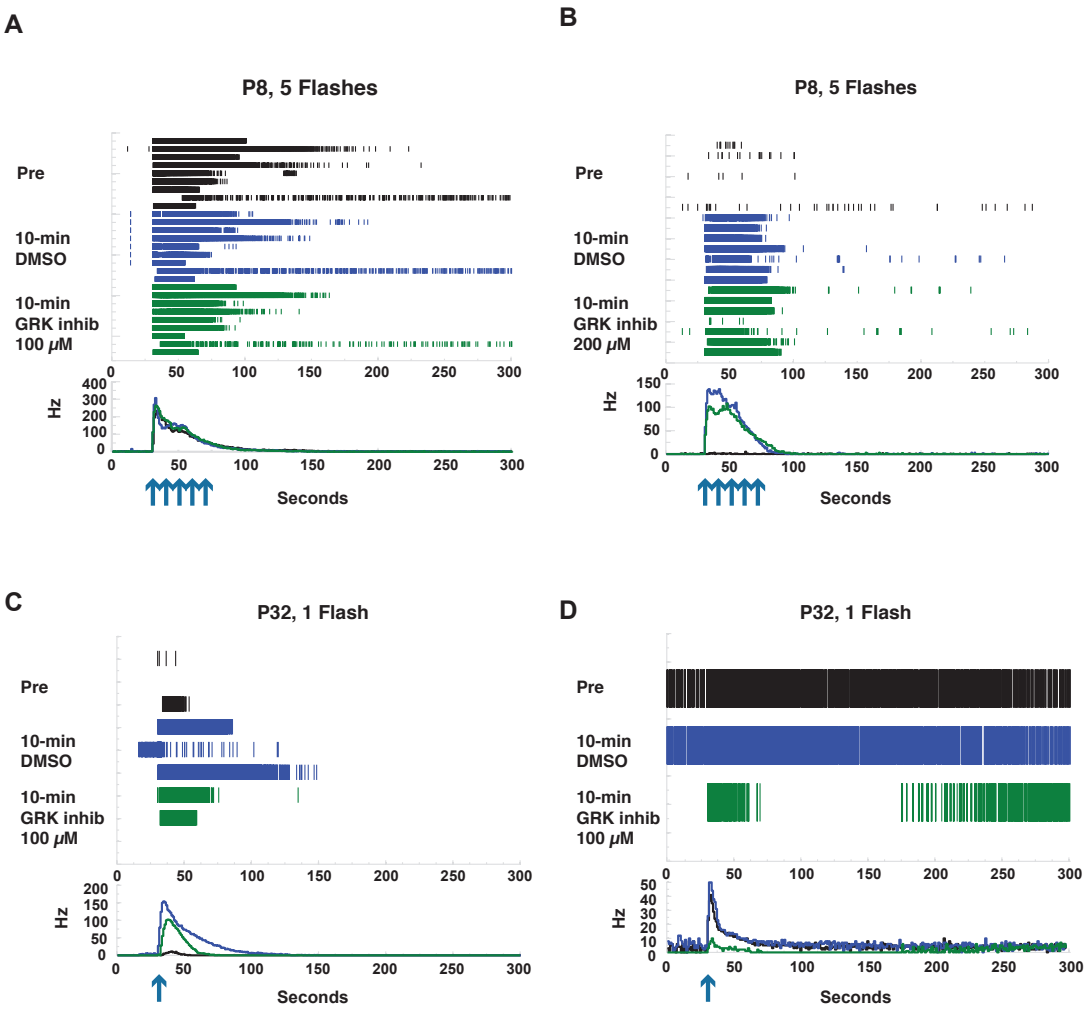

Figure 8

Treatment of ipRGCs with the GRK2/5/6 inhibitor bisindolylmaleimide XI. Light response measurements were made pre-treatment, post-DMSO carrier control treatement, and post-inhibitor treatment. Raster plots of A) 9 P8 ipRGCs treated with 100 μM inhibitor, B) 7 P8 ipRGCs treated with 200 μM inhibitor, C) 3 P30 ipRGCs treated with 100 μM inhibitor, D)1 P30 ipRGCs treated with 100 μM inhibitor. Arrows indicate flashes of white light.

Figure 9

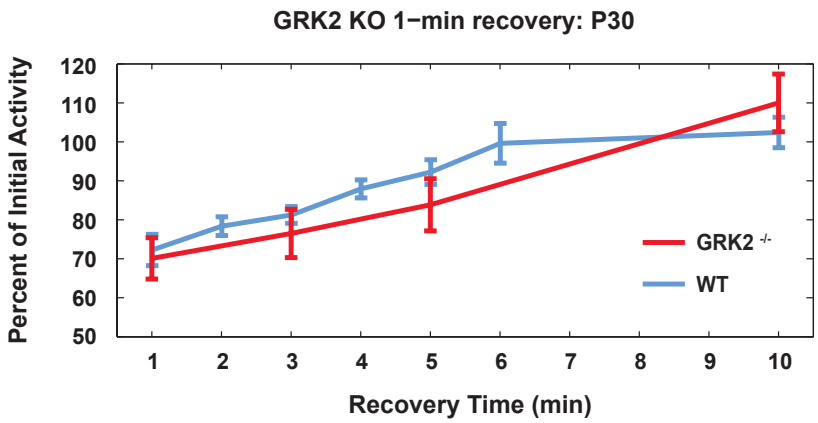

Figure 9

Time course of P30 wildtype (n=6 to 16) and P30 GRK2-/- (n=7) ipRGC recovery following a 1-min light exposure. A second 1-min test light was administered at multiple time points between 1 and 10-min.

Chapter 5: Conclusions and Future Directions

Introduction

Several aspects of melanopsin and ipRGC function have been addressed in this work, including the melanopsin photocycle, ipRGC adaptation, and mechanisms of melanopsin adaptation. This work has advanced our understanding of melanopsin function by extending previous *in vitro* work into whole retina. Overall, I found that of melanopsin is a 'tenacious" photopigment, resistant to bleaching under many conditions. Indeed, to UV bleach ipRGCs to a level below the 35% of initial activity found in Chapter 1 resulted in an unacceptably high retinal mortality rate. Retinas from animals whose eyes had recently opened could not withstand the amount of UV needed to obtain even the 35% of baseline firing. How this level of light induced firing is maintained at all in the absence of pigmented epithelium or any measurable retinoid is unclear. This is one of many unanswered questions remaining from the work presented here. The following sections address some of those questions and propose experiments to answer them.

The photocycle

From Chapter 2, the most fundamental finding is that melanopsin is a bistable pigment requiring binding of 11-*cis*-retinal to form an active photopigment *in vivo*. This is in-line with melanopsin's phylogenetic position being closer to the rhabdomeric opsins of squid and octopus than to mammalian rhodopsin and cone opsin (Provencio et al.,

1998). One of the continuing controversies concerning melanopsin's putative bistability has been a lack in ipRGCs of a prolonged depolarizing after-potential (PDA) in response to a strong activating wavelength pulse of light that can be reversed with a second, red shifted inactivating wavelength pulse (Hardie and Postma, 2007). Because of work in Drosophila rhabdomeric photoreceptors, in which the PDA was defined, it has become a common assumption that a PDA is a hallmark of bistable pigments. However, fly rhodopsin is a special case in which the peaks of the forward activating action spectrum and the inactivating reversal action spectrum are separated by nearly 100 nm. Most bistable pigments have much smaller separation between the forward and reversal wavelengths. In fact in squid rhodopsin (λ_{max} 493 nm), phylogenetically closer to melanopsin than fly rhodopsin, the reversal wavelength is only 7 nm red shifted from the activating wavelength. A separate reversal wavelength can only be seen clearly in preparations of isolated squid rhodopsin in a pH 9.7 buffer (alkaline metarhodopsin), in which case the reversal wavelength becomes blue shifted from 500 nm to 380 nm (Hubbard and St George, 1958). No other example of a PDA in a photoreceptor outside of Drosophila is noted in the literature. This fact led me to propose the model of bistability in which the melanopsin forward and reversal wavelengths were separated by approximately 10 nm. This was later confirmed *in vitro* last year to be 9 nm (Matsuyama et al., 2012).

One of the most mysterious questions about melanopsin's photocycle is what is its original source of chromophore. Several studies have shown that ipRGCs are photoactive from birth (Hannibal and Fahrenkrug, 2004; Tu et al., 2005; Schmidt et al., 2008). Cell types surrounding ipRGCs that have differentiated at this point include other

RGCs and amacrine cells (Young, 1985; Cepko et al., 1996; Voinescu et al., 2009). Any of these cells could potentially have retinoid synthetic capacity, including ipRGCs. Antibody staining of retinas for retinoids, including retinaldehyde or which it should be possible theoretically to raise antibodies), or retinal binding proteins accompanied by RT-PCR of RNA from RT-PCR of developing retinas for core retinal processing proteins would be a useful first step to confirm or refute this. For example, RPE65, critical for RPE photocycle function, is found as early as E18 in whole Retina RNA and increases several fold over early post-natal development (Manès et al., 1998). RPE65 itself is not involved in the photocycle of melanopsin because ipRGC activity is unaffected by knocking out RPE65 (Tu et al., 2006) although other recycling proteins may be involved and may be expressed early in development. Additionally, RT-PCR on immune-panned ipRGCs for retinaldehyde processing proteins would be of value. Melanopsin expression has been found as early as E10 (Tarttelin et al., 2003; Fahrenkrug et al., 2004). Since bistable pigments tend to be unstable outside of the rhabdomal membrane in the absence of chromophore (Hubbard and St George, 1958; Seki et al., 1980), and growing up large quantities of melanopsin in cell culture systems requires the early addition of chromophore to produce properly folded protein (Matsuyama et al., 2012), chromophore production may begin concurrent with melanopsin expression. Most parsimonously this would take place in developing ipRGCs.

Related to the origin of initial chromophore is the question of where fresh chromophore for newly synthesized melanopsin comes from throughout the life of the animal. These sources need not be the same. A first step to answer this question is to continue probing for retinal processing proteins via RT-PCR and immunostaining as

proposed for discovering the initial source of chromophore. A second possibility to discover if ipRGCs themselves have processing machinery is to enrich fractions of dissociated retina with ipRGCs that do not contain melanopsin, the only known retinoid binding protein in ipRGCs. Two approaches could be used. The first would using a fluorescent marker either knocked directly into the melanopsin locus or one that is floxed and combined with a Cre recombinase knocked into the melanopsin locus. Both versions would be bred to produce homozygotic animals. Cell fractions from dissociated retinas could be enriched by FACS if the fluorescent marker is bright enough (preferably a newly constructed tdTomato mouse line). Alternatively a synthetic transmembrane protein with a unique cell surface epitope for which a high affinity antibody has been produced could take the place of the fluorescent marker above. These cells could be immuno-panned for the synthetic epitope. The enriched fraction of non-melanopsin ipRGCs would then be incubated in cell culture with precursor retinoids like all-*trans*-retinal for extended times in both light and dark. Cultures would then be analyzed by HPLC and spectroscopy for the type of retinoid isomers present. A limit of this approach is that a large number of cells would be needed.

One last approach to address this question is to look for altered ipRGC activity in animals with knock-outs for various retinoid processing and binding proteins as they become available. Independence of the melanopsin from the RPE photocycle was determined this way (Tu et al., 2006). I tested a mouse knockout of the enzyme carotenoid-15,15'-monooxygenase (BMCO1) which cleaves beta-carotene into two molecules of all-*trans*-retinaldehyde (Hessel et al., 2007; von Lintig et al., 2010). This enzyme is expressed in many tissues including the RPE (Yan et al., 2001). However, no

change in ipRGC function was seen.

If other early-differentiated cells do contain retinoid synthetic capacity it may need be only miniscule because of what appears to be a very high binding affinity of melanopsin for its chromophore. Two lines of evidence support a high affinity. First, UV bleached ipRGCs recover from 0% activity to around 35% of initial activity over the course of the hour following UV treatment shown in Chapter 2. This happens in the absence of any measurable retinoids in the retina. Possibly the cells are "stunned" and unable to fire action potentials after UV treatment. This could be caused by UV damage to cell proteins and other components. In this case, ipRGCs may recover spiking ability separate from melanopsin activity. This was not tested directly in Chapter 2. Determining this could be done by the addition of potassium chloride to cells immediately after UV treatment and/or by voltage-clamp measurement of melanopsin photocurrents after UV treatment. If it is the case that cells are "stunned", then it is likely melanopsin protects its chromophore from UV destruction and that the 35% activity reflects the survival of 35% of melanopsin-protected chromophore. Alternatively, recovery may reflect melanopsin's scavenging of any remaining retinoid via a high binding affinity. A second line of evidence for high affinity come from the work of Lin et al (2008)(Lin et al., 2008) who essentially turned regular RGCs into ipRGCs with injection of an adeno-associated virus carrying melanopsin into the eyes of living retinal degenerate mice (rd/rd). These animals were able to recover some behavioral measure of light sensitivity and a nearly full pupillary light response. Direct recording of infected cells, labeled with eGFP, showed robust melanopsin mediated light responses. All of this occurred without the addition of any retinoid. This raises the possibility that all RGCs produce minute

amounts of 11-cis-retinal that melanopsin is able to scavenge upon ectopic expression, or that all RGCs have access to an external source of chromophore when needed. The former is more likely.

There is an adjunct to the answer of from where a continuing source of chromophore comes. Perhaps, adult ipRGCs receive new chromophore through their synaptic-like connection with Müller glial cells (Viney et al., 2007). While I've demonstrated that ipRGCs do not use the Müller glial photocycle product 11-*cis*-retinol, Müller glia contain cellular retinaldehyde binding protein (CRLBP) that is capable of binding both 11-*cis*-retinol and 11-*cis*-retinal (Bunt-Milam and Saari, 1983; Saari and Crabb, 2005). In the RPE, CRLBP is bound almost exclusively to 11-*cis*-retinal. In the neural retina, i.e., in Müller glia, CRLBP binds both 11-*cis*-retinal and 11-*cis*-retinol. The 11-*cis*-retinal presumably originating in RPE. Possibly a small amount of 11-*cis*-retinal traverses the Müller cells and arrives at ipRGCs as needed. The work of Wong (2013)(Wong, 2012) suggests this is true under extended, high intensity light. To test this, I propose recording from ipRGCs in CRLBP knock-out animals to monitor both normal function and function under prolonged, high intensity light conditions similar to those found in Chapter 2.

One last question I will address concerns what appears to be dark relaxation of melanopsin. After a 1-min 480 nm light at IR13.6 (3.98×10^{13} photons cm^{-2} s^{-1}), one need wait only 5 to 6 minutes in the dark before full recovery is seen in P8 animals (Chapter 3). Evidence for dark relaxation, or dark recovery, was seen in spectrophotometric measurements of purified amphioxus melanopsin (Terakita et al., 2008). Dark relaxation is also a common mechanism for photopigment regeneration, if slower than direct photoreversal regeneration, in bacterial and archeabacterial opsins

(Chow et. al., 2011). Evidence also exists for dark regeneration of squid and octopus rhodopsin with a half-life of approximately 4 minutes. The process is thought to begin with one of the photointermediates of metarhodopsin (Kito et al., 1971; Suzuki, 1972). It is unfortunate that the recent work by Matsuyama et al., (2012) determining the mouse melanopsin reversal wavelength did not address this issue. Repeating those experiments including a dark incubation period would be worthwhile. There is one major caveat to repeating those experiments. Instability of the recombinant melanopsin grown in cell culture may have rendered the experiment fruitless but unreported by Matsuyama et al. (2012).

With a dark regeneration mechanism, recovery times from the 1-min light exposure in Chapter 3 may reflect dark regeneration. If this is the case, differences between young and old animals may reflect lower melanopsin levels in older animals that require a larger proportion of regeneration before full spiking recovers. Young animals, with higher expression levels, may have "spare" molecules of melanopsin, which are not needed to fully activate cell firing. A smaller proportion of melanopsin need be regenerated in young animals if this were the case, leading to faster recovery times. Continuing the work to define integration times to short, strong flashes of light started with Peter Detwiler and extending that to longer times to produce photon-response and photon-recovery models may help answer this question by measuring photocurrents directly over the course of recovery and comparing those directly with spiking activity

ipRGC ontology

From Chapter 3 the major finding is the unique recovery behavior of P8 Type 1 cells. Why these cells are so resilient to light exposure must speak to their function in the developing retina. Increased relative photosensitivity in neonatal animals is understandable and advantageous given the decreased photon flux reaching the retina under closed eyelids. Fast recovery by Type 1 cells would be a useful characteristic if they are primarily responsible for lengthening spontaneous waves in developing retina. If the cells responsible easily adapted, defects in segregation of retinothalamic projections segregation would result, as seen in the work of Renna et al., (2012), leading to defects in the retinotopic map becoming a common problem and decreasing overall survival fitness. Fast recovery could also be of paramount importance for keeping neonatal pups safe in the nest. Adaptation could lead to a decrease in negative phototaxis, increasing the likelihood of neonates wondering toward open, lit areas where they are easy prey. It is unlikely Type 1 cells would be responsible for the aforementioned functions solely since young Type 3 cells also adapt less dramatically than older Type 3 cells. However Type 1 cells may be paramount in the reliability of these functions.

Results of a prolonged recovery, or dark adaptation, from Chapter 3 agree with the results of Wong et al., (2005) but are more extreme as they exposed ipRGCs to briefer 1-5 minute light exposures. Finding a relationship between time of recovery and photon exposure to relate the two results would require additional study. It is possible to follow the 1-hr exposure of Chapter 3 with a longer recovery time, possibly up to two hours. With MEA experiments of more than 4-hr duration, retinal mortality increases however. Perfusion flow rate could be increased to the 7-min of Wong (2013) to extend the viable

time on the MEA. Alternatively, 1-hr exposure at a selection of lower light levels would allow greater experimental flexibility. Preliminary data of IR 12.6 (3.98×10^{12} photons cm^{-2} s^{-1}) does show higher recovery levels than at IR 13.6 (3.98×10^{13} photons cm^{-2} s^{-1}). Approaching threshold light levels, though, is problematic, as the shape of ipRGC responses are different with on-latencies reaching 1-min over a 1-min light stimulus. Direct comparison of many parameters from IR 11.6 exposures (3.98×10^{11} photons cm^{-2} s^{-1}) with those from higher light levels proved impossible and alternative measurement strategies would need to be devised. Developing a photon-flux-adaptation model would be useful for future experimental design but also in shedding light on other intensity-time relationships such as the inverse photon-flux to light length requirement for photoentrainment (Takahashi et al., 1984).

The major questions arising from Chapter 3 are 1) what makes P8 Type 1 cells different from other subtypes and 2) what are these cells doing. To begin to answer these questions, Type 1 cells need to be anatomically identified. Mounting work published (Estevez et al., 2012) and unpublished suggests adult alpha-on cells are melanopsin positive, but only with enhanced immunohistochemical techniques. Additionally this can be seen by patch clamp recordings of alpha-on cells under high intensity light with glutamatergic blockade. Our preliminary data has found that a subset of SMI-32 labeled alpha-on cells also stain for melanopsin at P8. At P24 no SMI-32 labeled alpha-on cells showed reliable melanopsin staining using standard techniques. Very likely, these are the cells that disappear between P8 and P15 in Chapter 3. I am currently co-staining P8 retinas with melanopsin and SMI-32 to see if the proportion of co-staining cells is similar to the 30% decrease in melanopsin immunopositive cells between P8 and P15.

Unfortunately there is a lack of known genetic markers specific for alpha-on cells, which could be used to target alpha-on cells expressing melanopsin for deletion using a melanopsin specific Cre-recombinase mouse line. This is true even for markers that are simply expressed in alpha-on cells but not melanopsin cells. Instead, since alpha-on cells are one of the largest retinal ganglion cells (O'Brien et al., 2002; Wong et al., 2012), I propose recording from large fluorescent cells in a melanopsin specific Cre-recombinase, floxed YFP P8 animal using both patching clamp and cell-attached recording. Defining their intensity response curve and recovery from long light exposures would determine if these cells have the same characteristics of P8 Type 1 cells. If P8 Type 1 cells are alpha-on cells, then a series of immunohistochemical and single cell RT-PCR studies should be performed on the co-labeling cells looking for possible differential expression of potential melanopsin activity control components such as GRK2 and GRK3.

Adaptation and desensitization are usually accompanied by receptor phosphorylation. A possible technique to look at differences in melanopsin phosphorylation in P8 Type 1 cells is to use an *in situ* proximity ligation assay (Blasic et al., 2012). In this assay, antibodies for the melanopsin C-terminus and either phosphoserine or phosphotyrosine are incubated with retinas from animals exposed to light just prior to sacrifice and fixation. Secondary antibodies conjugated with oligonucleotide linkers then label primary antibodies. If the antibodies are in close enough proximity, the oligos anneal to form circular DNA that can be amplified and detected with fluorescently labeled oligonucleotides. It would be of great interest to see if there is differential phosphorylation between subtypes in ipRGCs, underpinning recovery differences.

A mysterious finding from Chapter 2 is the apparent sensitization of P8 Type 1 cells only in their steady-state firing following a 1-hr light exposure. This suggests different mechanisms control initial maximal firing and steady-state firing. Voltage clamp recording of photocurrents may help determine if this is a consequent of direct melanopsin activation or of downstream differences in spiking mechanisms. Looking for differences in calcium changes using calcium sensitive dyes in patch-clamp or in whole retinal monitoring of calcium activity (Sekaran et al., 2003) could indicate if the difference is related to TRPC and TRP-like channel activation and inactivation kinetics in the transition from maximal firing to steady-state firing.

GRK2

Phosphorylation is a major mode of GPCR regulation. Starting with mechanisms of melanopsin phosphorylation is likely to extend knowledge about melanopsin kinetics. In using mammalian rhodopsin phosphorylation and the results of knocking out rhodopsin kinase (GRK1) as an example, it was hoped we would have a clear, unambiguous outcome. This was not the case. GRK2 does seem to contribute to the inactivation kinetics of melanopsin, with prolonged response decay constants and off-latencies. A dramatically extended inactivation time nearing the 100-fold increase seen in rhodopsin in the rhodopsin kinase GRK1 knockout was not seen.

Unfortunately, the work here raises more questions than it answers. Because of the possibility of GRK3 activity in melanopsin inactivation, as GRK3 co-immunoprecipitates with melanopsin in addition to GRK2 (Blasic et al., 2012), no strong conclusion can be

made until a GRK2/GRK3 double knock-out animal is made. This would take considerable time, as the GRK3 KO animal is currently cryopreserved and not readily available. Questions about what role phosphorylation may have on melanopsin inactivation may be posed as alternatives.

Once again regulation of melanopsin via phosphorylation centers around the question of whether melanopsin behaves like a ciliary opsin or a rhabdomeric opsin. Ciliary opsins are inactivated by phosphorylation and arrestin binding, while in rhabdomeric opsins phosphorylation has little to do with inactivation by arrestin binding but rather targets the opsin for internalization. Currently it is unknown if melanopsin is internalized. I suggest the use of minute gold particle labeled antibodies for melanopsin for incubation in light expose retina. Preliminary data suggest that fluorophore conjugated melanopsin antibody incubation has no effect on ipRGC light response on the MEA. Antibody access was confirmed with faint labeling present upon fixation of incubated retinas. Fixation and subsequent 3D EM analysis of retinas incubated with the gold-labeled antibody in the presences of varying lengths and intensity of light would demonstrate if melanopsin internalization occurs and if it is a consequent of light exposure. Differences in Type 1 cell responses from other subtypes to prolonged light could be caused by differential internalization of melanopsin that may depend on differential phosphorylation. It is also unknown what the natural half-life of melanopsin is in ipRGCs. The aforementioned experiment could also give rough estimates of this.

A second approach to looking at phosphorylation is to make a transgenic animal producing a melanopsin that is not phosphorylatable at its C-terminus like the construct used in Blasic et al., (2012). Such an animal could help to elucidate the role of

phosphorylation in 1) basic melanopsin kinetics and 2) the role of internalization on long-term adaptation and recovery in response to extended light exposure. Looking at arrestin binding via co-immunoprecipitation in these animals could also help differentiate a cilliary or rhabdomeric behavior for melanopsin.

References

Abrahamson EW, Fager RS, Mason WT (1974) Comparative properties of vertebrate and invertebrate photoreceptors. Experimental eye research 18:51-67.

Aiyar N, Disa J, Dang K, Pronin AN, Benovic JL, Nambi P (2000) Involvement of G protein-coupled receptor kinase-6 in desensitization of CGRP receptors. European journal of pharmacology 403:1-7.

Altimus CM, Güler AD, Villa KL, McNeill DS, Legates TA, Hattar S (2008) Rods-cones and melanopsin detect light and dark to modulate sleep independent of image formation. Proc Natl Acad Sci USA 105:19998-20003.

Altimus CM, Güler AD, Alam NM, Arman AC, Prusky GT, Sampath AP, Hattar S (2010) Rod photoreceptors drive circadian photoentrainment across a wide range of light intensities. Nat Neurosci 13:1107-1112.

Badea TC, Cahill H, Ecker J, Hattar S, Nathans J (2009) Distinct roles of transcription factors brn3a and brn3b in controlling the development, morphology, and function of retinal ganglion cells. Neuron 61:852-864.

Bakall B, Marmorstein LY, Hoppe G, Peachey NS, Wadelius C, Marmorstein AD (2003) Expression and localization of bestrophin during normal mouse development. Invest Ophthalmol Vis Sci 44:3622-3628.

Baver SB, Pickard GE, Sollars PJ, Pickard GE (2008) Two types of melanopsin retinal ganglion cell differentially innervate the hypothalamic suprachiasmatic nucleus and the olivary pretectal nucleus. Eur J Neurosci 27:1763-1770.

Bellingham J, Whitmore D, Philp AR, Wells DJ, Foster RG (2002) Zebrafish melanopsin: isolation, tissue localisation and phylogenetic position. Brain Res Mol Brain Res 107:128-136.

Bellingham J, Chaurasia SS, Melyan Z, Liu C, Cameron MA, Tarttelin EE, Iuvone PM, Hankins MW, Tosini G, Lucas RJ (2006) Evolution of melanopsin photoreceptors: discovery and characterization of a new melanopsin in nonmammalian vertebrates. PLoS Biol 4:e254.

Benca RM, Gilliland MA, Obermeyer WH (1998) Effects of lighting conditions on sleep and wakefulness in albino Lewis and pigmented Brown Norway rats. Sleep 21:451-460.

Berson DM (2003) Strange vision: ganglion cells as circadian photoreceptors. Trends Neurosci 26:314-320.

Berson DM, Dunn FA, Takao M (2002) Phototransduction by retinal ganglion cells that set the circadian clock. Science 295:1070-1073.

Berson DM, Castrucci AM, Provencio I (2010) Morphology and mosaics of melanopsin-expressing retinal ganglion cell types in mice. The Journal of comparative neurology 518:2405-2422.

Blasic JR, Brown RL, Robinson PR (2012) Light-dependent phosphorylation of the carboxy tail of mouse melanopsin. Cellular and Molecular Life Sciences 69:10.

Bowmaker JK, Loew ER (1976) The action of hydroxylamine on visual pigments in the intact retina of the frog (Rana temporaria). Vision Res 16:811-818.

Brin KP, Ripps H (1977) Rhodopsin photoproducts and rod sensitivity in the skate retina. The Journal of general physiology 69:97-120.

Brown TM, Wynne J, Piggins HD, Lucas RJ (2011) Multiple hypothalamic cell populations encoding distinct visual information. J Physiol 589:1173-1194.

Brown TM, Gias C, Hatori M, Keding SR, Semo M, Coffey PJ, Gigg J, Piggins HD, Panda S, Lucas RJ (2010) Melanopsin contributions to irradiance coding in the thalamo-cortical visual system. PLoS Biol 8:e1000558.

Bunt-Milam AH, Saari JC (1983) Immunocytochemical localization of two retinoid-binding proteins in vertebrate retina. J Cell Biol 97:703-712.

Cepko CL, Austin CP, Yang X, Alexiades M, Ezzeddine D (1996) Cell fate determination in the vertebrate retina. Proc Natl Acad Sci U S A 93:589-595.

Chen CK, Burns ME, Spencer M, Niemi GA, Chen J, Hurley JB, Baylor DA, Simon MI (1999) Abnormal photoresponses and light-induced apoptosis in rods lacking rhodopsin kinase. Proceedings of the National Academy of Sciences of the United States of America 96:3718-3722.

Chen SK, Badea TC, Hattar S (2011) Photoentrainment and pupillary light reflex are mediated by distinct populations of ipRGCs. Nature 476:92-95.

Chen SK, Chew KS, McNeill DS, Keeley PW, Ecker JL, Mao BQ, Pahlberg J, Kim B, Lee SC, Fox MA, Guido W, Wong KY, Sampath AP, Reese BE, Kuruvilla R, Hattar S (2013) Apoptosis regulates ipRGC spacing necessary for rods and cones to drive circadian photoentrainment. Neuron 77:503-515.

Chow BY, Han X, Bernstein JG, Monahan PE, Boyden ES (2011) Light-Activated Ion Pumps and Channels for Temporally Precise Optical Control of Activity in Genetically Targeted Neurons. Neuromethods 55:99-132.

Coombs JL, Van Der List D, Chalupa LM (2007) Morphological properties of mouse retinal ganglion cells during postnatal development. The Journal of comparative neurology 503:803-814.

Dartnall HJ (1968) The photosensitivities of visual pigments in the presence of hydroxylamine. Vision research 8:339-358.

Delwig A, Logan AM, Copenhagen DR, Ahn AH (2012) Light evokes melanopsin-dependent vocalization and neural activation associated with aversive experience in neonatal mice. PloS one 7:e43787.

Do MT, Yau KW (2010) Intrinsically photosensitive retinal ganglion cells. Physiol Rev 90:1547-1581.

Do MT, Yau KW (2013) Adaptation to steady light by intrinsically photosensitive retinal ganglion cells. Proc Natl Acad Sci U S A 110:7470-7475.

Do MTH, Kang SH, Xue T, Zhong H, Liao H-W, Bergles DE, Yau K-W (2009) Photon capture and signalling by melanopsin retinal ganglion cells. Nature 457:281-287.

Dollet A, Albrecht U, Cooper HM, Dkhissi-Benyahya O (2010) Cones are required for normal temporal responses to light of phase shifts and clock gene expression. Chronobiol Int 27:768-781.

Doyle SE, Castrucci AM, McCall M, Provencio I, Menaker M (2006) Nonvisual light responses in the Rpe65 knockout mouse: rod loss restores sensitivity to the melanopsin system. Proc Natl Acad Sci USA 103:10432-10437.

Ebihara S, Tsuji K (1980) Entrainment of the circadian activity rhythm to the light cycle: effective light intensity for a Zeitgeber in the retinal degenerate C3H mouse and the normal C57BL mouse. Physiological Behavior 24:523-527.

Ecker JL, Dumitrescu ON, Wong KY, Alam NM, Chen SK, LeGates T, Renna JM, Prusky GT, Berson DM, Hattar S (2010) Melanopsin-expressing retinal ganglion-cell photoreceptors: cellular diversity and role in pattern vision. Neuron 67:49-60.

Estevez ME, Fogerson PM, Ilardi MC, Borghuis BG, Chan E, Weng S, Auferkorte ON, Demb JB, Berson DM (2012) Form and function of the M4 cell, an intrinsically photosensitive retinal ganglion cell type contributing to geniculocortical vision. J Neurosci 32:13608-13620.

Fahrenkrug J, Nielsen HS, Hannibal J (2004) Expression of melanopsin during development of the rat retina. Neuroreport 15:781-784.

Fisher LJ (1979) Development of synaptic arrays in the inner plexiform layer of neonatal mouse retina. The Journal of comparative neurology 187:359-372.

Freedman MS, Lucas RJ, Soni B, von Schantz M, Muñoz M, David-Gray Z, Foster R (1999) Regulation of mammalian circadian behavior by non-rod, non-cone, ocular photoreceptors. Science 284:502-504.

Fu Y, Zhong H, Wang MH, Luo DG, Liao HW, Maeda H, Hattar S, Frishman LJ, Yau KW (2005) Intrinsically photosensitive retinal ganglion cells detect light with a vitamin A-based photopigment, melanopsin. Proc Natl Acad Sci U S A 102:10339-10344.

Garwin GG, Saari JC (2000) High-performance liquid chromatography analysis of visual cycle retinoids. Methods in enzymology 316:11.

Gomez MP, Angueyra JM, Nasi E (2009) Light-transduction in melanopsin-expressing photoreceptors of Amphioxus. Proc Natl Acad Sci U S A 106:9081-9086.

González-Menéndez I, Contreras F, García-Fernández JM, Cernuda-Cernuda R (2011) Perinatal development of melanopsin expression in the mouse retina. Brain Res 1419:12-18.

González-Menéndez I, Contreras F, Cernuda-Cernuda R, Provencio I, García-Fernández JM (2010) Postnatal development and functional adaptations of the melanopsin photoreceptive system in the albino mouse retina. Invest Ophthalmol Vis Sci 51:4840-4847.

Gooley JJ, Lu J, Chou TC, Scammell TE, Saper CB (2001) Melanopsin in cells of origin of the retinohypothalamic tract. Nat Neurosci 4:1165.

Graham D, Wong K, Shapiro P, Frederick C, Pattabiraman K, Berson D (2008) Melanopsin Ganglion Cells Use a Membrane-associated Rhabdomeric Phototransduction Cascade. J Neurophysiol.

Guler AD, Altimus CM, Ecker JL, Hattar S (2007) Multiple photoreceptors contribute to nonimage-forming visual functions predominantly through melanopsin-containing retinal ganglion cells. Cold Spring Harb Symp Quant Biol 72:509-515.

Göz D, Studholme K, Lappi DA, Rollag MD, Provencio I, Morin LP (2008) Targeted destruction of photosensitive retinal ganglion cells with a saporin conjugate alters the effects of light on mouse circadian rhythms. PLoS ONE 3:e3153.

Güler AD, Ecker JL, Lall GS, Haq S, Altimus CM, Liao H-W, Barnard AR, Cahill H, Badea TC, Zhao H, Hankins MW, Berson DM, Lucas RJ, Yau K-W, Hattar S (2008) Melanopsin cells are the principal conduits for rod-cone input to non-image-forming vision. Nature 453:102-105.

Hannibal J, Fahrenkrug J (2004) Melanopsin containing retinal ganglion cells are light responsive from birth. Neuroreport 15:2317-2320.

Hardie RC (2011) A brief history of trp: commentary and personal perspective. Pflugers Arch 461:493-498.

Hardie RC, Raghu P (2001) Visual transduction in Drosophila. Nature 413:186-193.

Hardie RC, Postma M (2007) Phototransduction in Microvillar Photoreceptors of Drosophila and Other Invertebrates. The Senses 1:55.

Hardie RC, Postma M, eds (2008) Phototransduction in Microvillar Photoreceptors of Drosophila and Other Invertebrates. San Diego, CA: Academic Press.

Hargrave PA, McDowell JH (1992) Rhodopsin and phototransduction: a model system for G protein-linked receptors. FASEB J 6:2323-2331.

Hartwick ATE, Bramley JR, Yu J, Stevens KT, Allen CN, Baldridge WH, Sollars PJ, Pickard GE (2007) Light-evoked calcium responses of isolated melanopsin-expressing retinal ganglion cells. J Neurosci 27:13468-13480.

Hatori M, Le H, Vollmers C, Keding SR, Tanaka N, Schmedt C, Jegla T, Panda S (2008) Inducible ablation of melanopsin-expressing retinal ganglion cells reveals their central role in non-image forming visual responses. PLoS ONE 3:e2451.

Hattar S, Liao HW, Takao M, Berson DM, Yau KW (2002) Melanopsin-containing retinal ganglion cells: architecture, projections, and intrinsic photosensitivity. Science 295:1065-1070.

Hattar S, Kumar M, Park A, Tong P, Tung J, Yau K-W, Berson DM (2006) Central projections of melanopsin-expressing retinal ganglion cells in the mouse. J Comp Neurol 497:326-349.

Hattar S, Lucas RJ, Mrosovsky N, Thompson S, Douglas RH, Hankins MW, Lem J, Biel M, Hofmann F, Foster RG, Yau KW (2003) Melanopsin and rod-cone photoreceptive systems account for all major accessory visual functions in mice. Nature 424:76-81.

Hessel S, Eichinger A, Isken A, Amengual J, Hunzelmann S, Hoeller U, Elste V, Hunziker W, Goralczyk R, Oberhauser V, von Lintig J, Wyss A (2007) CMO1 deficiency abolishes vitamin A production from beta-carotene and alters lipid metabolism in mice. J Biol Chem 282:33553-33561.

Hillman P, Hochstein S, Minke B (1983) Transduction in invertebrate photoreceptors: role of pigment bistability. Physiol Rev 63:668-772.

Holy TE, Dulac C, Meister M (2000) Responses of vomeronasal neurons to natural stimuli. Science 289:1569-1572.

Hu C, Hill DD, Wong KY (2013) Intrinsic physiological properties of the five types of mouse ganglion-cell photoreceptors. J Neurophysiol 109:1876-1889.

Hubbard R, St George RC (1958) The rhodopsin system of the squid. The Journal of General Physiology 41:27.

Hughes S, Watson TS, Foster RG, Peirson SN, Hankins MW (2013) Nonuniform distribution and spectral tuning of photosensitive retinal ganglion cells of the mouse retina. Curr Biol 23:1696-1701.

Iacovelli L, Sallese M, Mariggiò S, de Blasi A (1999) Regulation of G-protein-coupled receptor kinase subtypes by calcium sensor proteins. FASEB J 13:1-8.

Johnson J, Wu V, Donovan M, Majumdar S, Renteria RC, Porco T, Van Gelder RN, Copenhagen DR (2010) Melanopsin-dependent light avoidance in neonatal mice. Proceedings of the National Academy of Sciences of the United States of America 107:17374-17378.

Keeler CE (1927) Iris movements in blind mice. American Journal of Physiology:6.

Kirkby LA, Feller MB (2013) Intrinsically photosensitive ganglion cells contribute to plasticity in retinal wave circuits. Proc Natl Acad Sci U S A 110:12090-12095.

Kiser PD, Golczak M, Maeda A, Palczewski K (2011) Key enzymes of the retinoid (visual) cycle in vertebrate retina. Biochimica et biophysica acta.

Kito Y, Suzuki T, Sugahara M (1971) Dark process of photoregeneration in squid. Zoological Magazine: The Zoological Society of Japan:4.

Koutalos Y, Ebrey TG, Tsuda M, Odashima K, Lien T, Park MH, Shimizu N, Derguini F, Nakanishi K, Gilson HR, et al. (1989) Regeneration of bovine and octopus opsins in situ with natural and artificial retinals. Biochemistry 28:2732-2739.

Koyanagi M, Terakita A (2008) Gq-coupled rhodopsin subfamily composed of invertebrate visual pigment and melanopsin. Photochem Photobiol 84:1024-1030.

Koyanagi M, Kubokawa K, Tsukamoto H, Shichida Y, Terakita A (2005) Cephalochordate melanopsin: evolutionary linkage between invertebrate visual cells and vertebrate photosensitive retinal ganglion cells. Curr Biol 15:1065-1069.

Kuksa V, Imanishi Y, Batten M, Palczewski K, Moise AR (2003) Retinoid cycle in the vertebrate retina: experimental approaches and mechanisms of isomerization. Vision Res 43:2959-2981.

Laemle LK, Ottenweller JE (1998) Daily patterns of running wheel activity in male anophthalmic mice. Physiol Behav 64:165-171.

Lall GS, Revell VL, Momiji H, Al Enezi J, Altimus CM, Güler AD, Aguilar C, Cameron MA, Allender S, Hankins MW, Lucas RJ (2010) Distinct contributions of rod, cone, and melanopsin photoreceptors to encoding irradiance. Neuron 66:417-428.

Leibrock CS, Lamb TD (1997) Effect of hydroxylamine on photon-like events during dark adaptation in toad rod photoreceptors. The Journal of Physiology 501 (Pt 1):97-109.

Lin B, Koizumi A, Tanaka N, Panda S, Masland RH (2008) Restoration of visual function in retinal degeneration mice by ectopic expression of melanopsin. Proc Natl Acad Sci USA 105:16009-16014.

Liu CH, Satoh AK, Postma M, Huang J, Ready DF, Hardie RC (2008) Ca2+-dependent metarhodopsin inactivation mediated by calmodulin and NINAC myosin III. Neuron 59:778-789.

Lucas RJ, Hattar S, Takao M, Berson DM, Foster RG, Yau KW (2003) Diminished pupillary light reflex at high irradiances in melanopsin-knockout mice. Science 299:245-247.

Luo DG, Kefalov V, Yau KW (2008) Phototransduction in Rods and Cones. The Senses: A Comprehensive Reference 1:32.

Lupi D, Oster H, Thompson S, Foster RG (2008) The acute light-induction of sleep is mediated by OPN4-based photoreception. Nat Neurosci 11:1068-1073.

Manès G, Leducq R, Kucharczak J, Pagès A, Schmitt-Bernard CF, Hamel CP (1998) Rat messenger RNA for the retinal pigment epithelium-specific protein RPE65 gradually accumulates in two weeks from late embryonic days. FEBS Lett 423:133-137.

Matkovich SJ, Diwan A, Klanke JL, Hammer DJ, Marreez Y, Odley AM, Brunskill EW, Koch WJ, Schwartz RJ, Dorn GW (2006) Cardiac-specific ablation of G-protein receptor kinase 2 redefines its roles in heart development and beta-adrenergic signaling. Circ Res 99:996-1003.

Matsuyama T, Yamashita T, Imamoto Y, Shichida Y (2012) Photochemical properties of mammalian melanopsin. Biochemistry 51:5454-5462.

Mawad K, Van Gelder RN (2008) Absence of long-wavelength photic potentiation of murine intrinsically photosensitive retinal ganglion cell firing in vitro. J Biol Rhythms 23:387-391.

McNeill DS, Sheely CJ, Ecker JL, Badea TC, Morhardt D, Guido W, Hattar S (2011) Development of melanopsin-based irradiance detecting circuitry. Neural development 6:8.

Melyan Z, Tarttelin EE, Bellingham J, Lucas RJ, Hankins MW (2005) Addition of human melanopsin renders mammalian cells photoresponsive. Nature 433:741-745.

Moore CA, Milano SK, Benovic JL (2007) Regulation of receptor trafficking by GRKs and arrestins. Annual review of physiology 69:451-482.

Mrosovsky N, Hattar S (2003) Impaired masking responses to light in melanopsin-knockout mice. Chronobiol Int 20:989-999.

Murakami M, Kouyama T (2008) Crystal structure of squid rhodopsin. Nature 453:363-367.

Mure LS, Rieux C, Hattar S, Cooper HM (2007) Melanopsin-dependent nonvisual responses: evidence for photopigment bistability in vivo. J Biol Rhythms 22:411-424.

Muñoz Llamosas M, Huerta JJ, Cernuda-Cernuda R, García-Fernández JM (2000) Ontogeny of a photic response in the retina and suprachiasmatic nucleus in the mouse. Brain Res Dev Brain Res 120:1-6.

Nemargut JP, Wang GY (2009) Inhibition of nitric oxide synthase desensitizes retinal ganglion cells to light by diminishing their excitatory synaptic currents under light adaptation. Vision Res 49:2936-2947.

Newman LA, Walker MT, Brown RL, Cronin TW, Robinson PR (2003) Melanopsin forms a functional short-wavelength photopigment. Biochemistry 42:12734-12738.

Nickle B, Robinson PR (2007) The opsins of the vertebrate retina: insights from structural, biochemical, and evolutionary studies. Cell Mol Life Sci 64:2917-2932.

O'Brien BJ, Isayama T, Richardson R, Berson DM (2002) Intrinsic physiological properties of cat retinal ganglion cells. J Physiol 538:787-802.

Ozaki K, Hara R, Hara T, Kakitani T (1983) Squid retinochrome. Configurational changes of the retinal chromophore. Biophysical Journal 44:127-137.

Oztürk N, Song SH, Ozgür S, Selby CP, Morrison L, Partch C, Zhong D, Sancar A (2007) Structure and function of animal cryptochromes. Cold Spring Harb Symp Quant Biol 72:119-131.

Palczewski K (2006) G protein-coupled receptor rhodopsin. Annual review of biochemistry 75:743-767.

Palczewski K, Kumasaka T, Hori T, Behnke CA, Motoshima H, Fox BA, Le Trong I, Teller DC, Okada T, Stenkamp RE, Yamamoto M, Miyano M (2000) Crystal structure of rhodopsin: A G protein-coupled receptor. Science 289:739-745.

Panda S, Nayak SK, Campo B, Walker JR, Hogenesch JB, Jegla T (2005) Illumination of the melanopsin signaling pathway. Science 307:600-604.

Panda S, Sato TK, Castrucci AM, Rollag MD, DeGrip WJ, Hogenesch JB, Provencio I, Kay SA (2002) Melanopsin (Opn4) requirement for normal light-induced circadian phase shifting. Science 298:2213-2216.

Panda S, Provencio I, Tu DC, Pires SS, Rollag MD, Castrucci AM, Pletcher MT, Sato TK, Wiltshire T, Andahazy M, Kay SA, Van Gelder RN, Hogenesch JB (2003) Melanopsin is required for non-image-forming photic responses in blind mice. Science 301:525-527.

Peirson S, Foster RG (2006) Melanopsin: another way of signaling light. Neuron 49:331-339.

Pepperberg D (1992) Hydroxylamine-dependent inhibition of rhodopsin phosphorylation in the isolated retina. Experimental eye research 54:369-376.

Pepperberg DR, Morrison DF, O&apos, Brien PJ (1995) Depalmitoylation of rhodopsin with hydroxylamine. Methods in Enzymology 250:348-361.

Perez-Leighton CE, Schmidt TM, Abramowitz J, Birnbaumer L, Kofuji P (2011) Intrinsic phototransduction persists in melanopsin-expressing ganglion cells lacking diacylglycerol-sensitive TRPC subunits. Eur J Neurosci 33:856-867.

Provencio I, Rollag MD, Castrucci AM (2002) Photoreceptive net in the mammalian retina. This mesh of cells may explain how some blind mice can still tell day from night. Nature 415:493.

Provencio I, Jiang G, De Grip WJ, Hayes WP, Rollag MD (1998) Melanopsin: An opsin in melanophores, brain, and eye. Proc Natl Acad Sci USA 95:340-345.

Provencio I, Rodriguez IR, Jiang G, Hayes WP, Moreira EF, Rollag MD (2000) A novel human opsin in the inner retina. J Neurosci 20:600-605.

Qiu X, Kumbalasiri T, Carlson SM, Wong KY, Krishna V, Provencio I, Berson DM (2005) Induction of photosensitivity by heterologous expression of melanopsin. Nature 433:745-749.

Quina LA, Pak W, Lanier J, Banwait P, Gratwick K, Liu Y, Velasquez T, O'Leary DD, Goulding M, Turner EE (2005) Brn3a-expressing retinal ganglion cells project

specifically to thalamocortical and collicular visual pathways. J Neurosci 25:11595-11604.

Rao S, Chun C, Fan J, Kofron JM, Yang MB, Hegde RS, Ferrara N, Copenhagen DR, Lang RA (2013) A direct and melanopsin-dependent fetal light response regulates mouse eye development. Nature 494:243-246.

Ratto GM, Robinson DW, Yan B, McNaughton PA (1991) Development of the light response in neonatal mammalian rods. Nature 351:654-657.

Renna JM, Weng S, Berson DM (2011) Light acts through melanopsin to alter retinal waves and segregation of retinogeniculate afferents. Nature neuroscience 14:827-829.

Robles LJ, Camacho JL, Torres SC, Flores A, Fariss RN, Matsumoto B (1995) Retinoid cycling proteins redistribute in light-/dark-adapted octopus retinas. J Comp Neurol 358:605-614.

Roecklein KA, Rohan KJ, Duncan WC, Rollag MD, Rosenthal NE, Lipsky RH, Provencio I (2009) A missense variant (P10L) of the melanopsin (OPN4) gene in seasonal affective disorder. J Affect Disord 114:279-285.

Ruby NF, Brennan TJ, Xie X, Cao V, Franken P, Heller HC, O'Hara BF (2002) Role of melanopsin in circadian responses to light. Science 298:2211-2213.

Ruggiero L, Allen CN, Lane Brown R, Robinson DW (2009) The development of melanopsin-containing retinal ganglion cells in mice with early retinal degeneration. Eur J Neurosci 29:359-367.

Saari JC, Crabb JW (2005) Focus on molecules: cellular retinaldehyde-binding protein (CRALBP). Exp Eye Res 81:245-246.

Schmidt TM, Kofuji P (2009) Functional and morphological differences among intrinsically photosensitive retinal ganglion cells. J Neurosci 29:476-482.

Schmidt TM, Kofuji P (2011) Structure and function of bistratified intrinsically photosensitive retinal ganglion cells in the mouse. J Comp Neurol 519:1492-1504.

Schmidt TM, Taniguchi K, Kofuji P (2008) Intrinsic and extrinsic light responses in melanopsin-expressing ganglion cells during mouse development. Journal of neurophysiology 100:371-384.

Sekaran S, Foster RG, Lucas RJ, Hankins MW (2003) Calcium imaging reveals a network of intrinsically light-sensitive inner-retinal neurons. Curr Biol 13:1290-1298.

Sekaran S, Lupi D, Jones SL, Sheely CJ, Hattar S, Yau KW, Lucas RJ, Foster RG, Hankins MW (2005) Melanopsin-dependent photoreception provides earliest light detection in the mammalian retina. Current biology : CB 15:1099-1107.

Seki T (1984) Metaretinochrome in membranes as an effective donor of 11-cis retinal for the synthesis of squid rhodopsin. J Gen Physiol 84:49-62.

Seki T, Hara R, Hara T (1980) Dark regeneration of squid rhodopsin and isorhodopsin. Vision Res 20:79-82.

Sernagor E, Eglen SJ, Wong RO (2001) Development of retinal ganglion cell structure and function. Progress in retinal and eye research 20:139-174.

Sexton T, Buhr E, Van Gelder RN (2012a) Melanopsin and mechanisms of non-visual ocular photoreception. The Journal of biological chemistry 287:1649-1656.

Sexton TJ, Golczak M, Palczewski K, Van Gelder RN (2012b) Melanopsin is highly resistant to light and chemical bleaching in vivo. The Journal of biological chemistry 287:20888-20897.

Shi M, Kumar SR, Motajo O, Kretschmer F, Mu X, Badea TC (2013) Genetic Interactions between Brn3 Transcription Factors in Retinal Ganglion Cell Type Specification. PLoS One 8:e76347.

Stecher H, Palczewski K (2000) Multienzyme analysis of visual cycle. Methods Enzymol 316:330-344.

Suzuki T (1972) An intermediate in the photoregeneration of squid rhodopsin. Biochim Biophys Acta 275:10.

Takahashi JS, DeCoursey PJ, Bauman L, Menaker M (1984) Spectral sensitivity of a novel photoreceptive system mediating entrainment of mammalian circadian rhythms. Nature 308:186-188.

Tarttelin EE, Bellingham J, Bibb LC, Foster RG, Hankins MW, Gregory-Evans K, Gregory-Evans CY, Wells DJ, Lucas RJ (2003) Expression of opsin genes early in ocular development of humans and mice. Exp Eye Res 76:393-396.

Terakita A, Tsukamoto H, Koyanagi M, Sugahara M, Yamashita T, Shichida Y (2008) Expression and comparative characterization of Gq-coupled invertebrate visual pigments and melanopsin. J Neurochem 105:883-890.

Thompson CL, Blaner WS, Van Gelder RN, Lai K, Quadro L, Colantuoni V, Gottesman ME, Sancar A (2001) Preservation of light signaling to the suprachiasmatic nucleus in vitamin A-deficient mice. Proc Natl Acad Sci U S A 98:11708-11713.

Thompson CL, Selby CP, Van Gelder RN, Blaner WS, Lee J, Quadro L, Lai K, Gottesman ME, Sancar A (2004) Effect of vitamin A depletion on nonvisual phototransduction pathways in cryptochromeless mice. J Biol Rhythms 19:504-517.

Tian N, Copenhagen DR (2003) Visual stimulation is required for refinement of ON and OFF pathways in postnatal retina. Neuron 39:85-96.

Tsai JW, Hannibal J, Hagiwara G, Colas D, Ruppert E, Ruby NF, Heller HC, Franken P, Bourgin P (2009) Melanopsin as a sleep modulator: circadian gating of the direct effects of light on sleep and altered sleep homeostasis in Opn4(-/-) mice. PLoS Biol 7:e1000125.

Tu DC, Batten ML, Palczewski K, Van Gelder RN (2004) Nonvisual photoreception in the chick iris. Science 306:129-131.

Tu DC, Zhang D, Demas J, Slutsky EB, Provencio I, Holy TE, Van Gelder RN (2005) Physiologic diversity and development of intrinsically photosensitive retinal ganglion cells. Neuron 48:987-999.

Tu DC, Owens LA, Anderson L, Golczak M, Doyle SE, McCall M, Menaker M, Palczewski K, Van Gelder RN (2006) Inner retinal photoreception independent of the visual retinoid cycle. Proc Natl Acad Sci USA 103:10426-10431.

Van Gelder RN (2003) Making (a) sense of non-visual ocular photoreception. Trends Neurosci 26:458-461.

Viney TJ, Balint K, Hillier D, Siegert S, Boldogkoi Z, Enquist LW, Meister M, Cepko CL, Roska B (2007) Local retinal circuits of melanopsin-containing ganglion cells identified by transsynaptic viral tracing. Curr Biol 17:981-988.

Vinge LE, Andressen KW, Attramadal T, Andersen G, Ahmed MS, Peppel K, Koch WJ, Freedman NJ, Levy FO, Skomedal T, Osnes JB, Attramadal H (2007) Substrate specificities of g protein-coupled receptor kinase-2 and -3 at cardiac myocyte receptors provide basis for distinct roles in regulation of myocardial function. Mol Pharmacol 72:582-591.

Vinge LE, von Lueder TG, Aasum E, Qvigstad E, Gravning JA, How OJ, Edvardsen T, Bjørnerheim R, Ahmed MS, Mikkelsen BW, Oie E, Attramadal T, Skomedal T, Smiseth OA, Koch WJ, Larsen TS, Attramadal H (2008) Cardiac-restricted expression of the carboxyl-terminal fragment of GRK3 Uncovers Distinct Functions of GRK3 in regulation of cardiac contractility and growth: GRK3 controls cardiac alpha1-adrenergic receptor responsiveness. J Biol Chem 283:10601-10610.

Voinescu PE, Emanuela P, Kay JN, Sanes JR (2009) Birthdays of retinal amacrine cell subtypes are systematically related to their molecular identity and soma position. J Comp Neurol 517:737-750.

von Lintig J, Kiser PD, Golczak M, Palczewski K (2010) The biochemical and structural basis for trans-to-cis isomerization of retinoids in the chemistry of vision. Trends Biochem Sci 35:400-410.

Vought BW, Salcedo E, Chadwell LV, Britt SG, Birge RR, Knox BE (2000) Characterization of the primary photointermediates of Drosophila rhodopsin. Biochemistry 39:14128-14137.

Wald G, Brown PK (1950) The Synthesis of Rhodopsin from Retinene(1). Proceedings of the National Academy of Sciences of the United States of America 36:84-92.

Wald G, Brown PK, Smith PH (1955) Iodopsin. J Gen Physiol 38:623-681.

Walker MT, Brown RL, Cronin TW, Robinson PR (2008) Photochemistry of retinal chromophore in mouse melanopsin. Proc Natl Acad Sci USA 105:8861-8865.

Wang J-S, Kefalov V (2009) An Alternative Pathway Mediates the Mouse and Human Cone Visual Cycle. Curr Biol 19:1-5.

Wang J-S, Estevez ME, Cornwall MC, Kefalov V (2009) Intra-retinal visual cycle required for rapid and complete cone dark adaptation. Nat Neurosci 12:295-302.

Wang JS, Kefalov VJ (2011) The cone-specific visual cycle. Progress in retinal and eye research 30:115-128.

Wang X, Wang T, Jiao Y, von Lintig J, Montell C (2010) Requirement for an enzymatic visual cycle in Drosophila. Curr Biol 20:93-102.

Warren EJ, Allen CN, Brown RL, Robinson DW (2006) The light-activated signaling pathway in SCN-projecting rat retinal ganglion cells. Eur J Neurosci 23:2477-2487.

Wee R, Castrucci AM, Provencio I, Gan L, Van Gelder RN (2002) Loss of photic entrainment and altered free-running circadian rhythms in math5-/- mice. J Neurosci 22:10427-10433.

Willets JM, Challiss RA, Nahorski SR (2003) Non-visual GRKs: are we seeing the whole picture? Trends Pharmacol Sci 24:626-633.

Williams RW, Strom RC, Zhou G, Yan Z (1998) Genetic dissection of retinal development. Seminars in cell & developmental biology 9:249-255.

Wong KY (2012) A retinal ganglion cell that can signal irradiance continuously for 10 hours. The Journal of neuroscience : the official journal of the Society for Neuroscience 32:11478-11485.

Wong KY, Dunn FA, Berson DM (2005) Photoreceptor adaptation in intrinsically photosensitive retinal ganglion cells. Neuron 48:1001-1010.

Wong RC, Cloherty SL, Ibbotson MR, O'Brien BJ (2012) Intrinsic physiological properties of rat retinal ganglion cells with a comparative analysis. J Neurophysiol 108:2008-2023.

Wong WT, Myhr KL, Miller ED, Wong RO (2000) Developmental changes in the neurotransmitter regulation of correlated spontaneous retinal activity. The Journal of neuroscience : the official journal of the Society for Neuroscience 20:351-360.

Xue T, Do MT, Riccio A, Jiang Z, Hsieh J, Wang HC, Merbs SL, Welsbie DS, Yoshioka T, Weissgerber P, Stolz S, Flockerzi V, Freichel M, Simon MI, Clapham DE, Yau KW (2011) Melanopsin signalling in mammalian iris and retina. Nature 479:67-73.

Yan W, Jang GF, Haeseleer F, Esumi N, Chang J, Kerrigan M, Campochiaro M, Campochiaro P, Palczewski K, Zack DJ (2001) Cloning and characterization of a human beta,beta-carotene-15,15'-dioxygenase that is highly expressed in the retinal pigment epithelium. Genomics 72:193-202.

Yau KW, Hardie RC (2009) Phototransduction motifs and variations. Cell 139:246-264.

Ye H, Daoud-El Baba M, Peng RW, Fussenegger M (2011) A synthetic optogenetic transcription device enhances blood-glucose homeostasis in mice. Science 332:1565-1568.

Young RW (1985) Cell differentiation in the retina of the mouse. Anat Rec 212:199-205.

Zhu Y, Tu DC, Denner D, Shane T, Fitzgerald CM, Van Gelder RN (2007) Melanopsin-dependent persistence and photopotentiation of murine pupillary light responses. Investigative Ophthalmology & Visual Science 48:1268-1275.